

Meta-modelling of carbon fluxes from crop and grassland multi-model outputs

Roland Hollós^{1,2,3}, Nándor Zrinyi^{2,4}, Zoltán Barcza^{2,3}, Gianni Bellocchi⁵, Renáta Sándor¹, János Ruff⁶, Nándor Fodor^{1,7}

¹ Centre for Agricultural Research HUN-REN, Agricultural Institute, Martonvásár, 2462, Hungary

² Eötvös Loránd University, Department of Meteorology, Budapest, 1117, Hungary

³ Czech Academy of Sciences, Global Change Research Institute, Brno, 603 00, Czech Republic

⁴ Eötvös Loránd University, Doctoral School of Earth Sciences, Budapest, 1117, Hungary

⁵ INRAE, VetAgro Sup, Unité Mixte de Recherche sur l'Ecosystème Prairial (UREP), Clermont-Ferrand, 63000, France

⁶ University of Pécs, Institute of Mathematics and Informatics, Pécs, 7624, Hungary

⁷ University of Debrecen, Faculty of Agricultural and Food Sciences and Environmental Management, Debrecen, 4032, Hungary

* Correspondence to: Nándor Fodor (fodor.nandor@atk.hu)

Abstract. We evaluated ~~four-five~~ stacking-based meta-models - Multiple Linear Regression, Random Forest, XGBoost, ~~and also Random Forest and XGBoost~~ with environmental covariates (~~RF+ and XGB+, respectively~~) - against the multi-model median (MMM) and best individual process-based models for gross primary production (GPP), ecosystem respiration (RECO) and net ecosystem exchange (NEE) at two cropland and two grassland sites. ~~We tested two validation strategies for GPP and RECO (70%/30% training/validation approach and the time-aware leave-one-year-out (LOYO) method), and three strategies for NEE (70%/30%, complete LOYO and independent validation using the meta-model based RECO-GPP).~~ All meta-models were associated with improved RMSE, bias and correlation. ~~Based on the LOYO validation strategy, average correlation increase was ~2% for GPP (0.2-4.4%), 9% for RECO (5-13.6%) and 8% for NEE (0.5-12.5%). In case of the independent validation strategy correlation increase was ~40% for NEE (24.5-64%) with explained variance gains of ~10-38.5% over MMM, largest for RECO in croplands and smallest for NEE in grasslands.~~ Bias was nearly eliminated except at one cropland site. ~~SHapley Additive exPlanations (SHAP) analysis of XGB+~~ showed that diverse individual models, not always the top performers, contributed most, and that temperature - especially for RECO in croplands and NEE in grasslands - was the dominant environmental driver, while precipitation had minor effects. These findings highlight the predictive and diagnostic advantages of ~~meta-modeling stacking-based~~ approaches over ~~equal weight~~ MMM, with potential applications across agroecosystem, Earth system and environmental model ensembles.

1 Introduction

Biogeochemical processes are central to agricultural planning, underpinning concepts such as “climate-smart agriculture”, “low-carbon agriculture” and “greenhouse gas-mitigating farming practices” within narratives/storylines (e.g. Thornton et al., 2018; Hou and Hou, 2019; Anuga et al., 2020). As governments and societies reshape economies, particularly in the context of decarbonisation (e.g. Sroufe and Watts, 2022), biogeochemical modelling has emerged as an essential tool to support agricultural policies (Bellocchi, 2023). These models simulate the complex interactions between agriculture and ecosystem services, such as C sequestration,

biodiversity conservation and water quality regulation, thereby empowering policymakers to integrate ecosystem value into agricultural decision-making and land-use strategies (e.g. Lambin and Meyfroidt, 2011). Moreover, by
45 simulating a wide variety of ecosystem processes, the models facilitate the assessment of agricultural emissions and mitigation strategies, forming a scientific basis for climate policy and agricultural resilience (Li et al., 2006; Valin et al., 2013; Sándor et al., 2018; Lembaid et al., 2021, 2022; Gascuel-Odoux et al., 2022).

Many state-of-the-art biogeochemical models have a long development history with some of them spanning 50 years (Hidy et al., 2022). Still, inherent uncertainties in model structures, parameterisations and assumptions pose
50 challenges for reliable predictions under diverse environmental and management conditions (e.g. Riccio et al., 2007; Bellocchi et al., 2010; Therond et al., 2011; Harrison et al., 2012; Brilli et al., 2017; Bilotto et al., 2021). This calls for improved mathematical tools and innovative solutions to strengthen the trust in the models.

Ensemble modelling has gained prominence as a robust method to address these uncertainties in biogeochemical models (e.g. Challinor et al., 2013; Snow et al., 2014; Calanca et al., 2016; Jones et al., 2017; Knutti et al., 2019).
55 Each model adopts unique assumptions about processes like soil nutrient cycling, photosynthesis, allocation and crop phenology, leading to significant variability in predictions under similar scenarios. Such structural uncertainties (e.g. divergent representations of water stress or heat tolerance), ~~and~~ also with parameter uncertainty can lead to inconsistent predictions. Ensemble approaches mitigate these discrepancies by synthesising outputs from multiple models, compensating biases and highlighting consistent trends (e.g. Bassu et al., 2014; Rosenzweig et al., 2014;
60 Kollas et al., 2015; Li et al., 2015; Ruane et al., 2016, 2017; Sándor et al., 2017, 2020; Ehrhardt et al., 2018; Wallach et al., 2018). This increases the reliability of predictions and reduces the risks associated with over-reliance on individual models.

Although ensemble techniques are proven to improve modelling accuracy and increase the trust in biogeochemical models, problems still exist. For example, the ensemble models are hard to explain, and currently only the simplest
65 methods (averaging or median calculation; Sándor et al., 2016) are the most widely used for ecosystem models. These simple model combination algorithms usually have many implicit presumptions that models often cannot meet (for example, same-equal variance and independence). In the field of machine learning (ML), which generates models directly from data, instead of following physical, biological and biogeochemical principles, much more developed techniques exist, which can be potentially exploited to improve the predictive power of the ensemble
70 output. These ML-based techniques usually have less and ~~also~~ more explicitly stated conditions (Scowen et al., 2023).

As an advanced, potentially promising approach, ML based meta-modelling extends the concept of ensemble technique by synthesising outputs even across multiple calibration scenarios. Recent advancements in ML offer innovative tools to refine data-intensive modelling in Earth sciences (e.g. Li et al., 2015; Jackson et al., 2017; Keskin
75 et al., 2019; Reichstein et al., 2019; Bai et al., 2021; Chandel et al., 2024; Wang et al., 2024). By using ensemble learning – a subset of ML methods – predictive frameworks can integrate diverse model outputs with improved accuracy and interpretability (e.g. Hansen and Salamon, 1990; Opitz and Maclin, 1999; Dietterich, 2000; Hagedorn et al., 2005; Palmer, 2019). Stacking, as a flexible ensemble learning technique, combines outputs from heterogeneous models into a *meta-model*, assigning weights to highlight their relative importance (e.g. Breiman, 1996; Van der
80 Laan et al., 2007; Sagi and Rokach, 2018). This approach has potential for biogeochemical modelling, offering simplicity and adaptability with Multiple Linear Regression (e.g. Kutner et al., 2005), and enhanced prediction accuracy through decision-tree-based methods like Random Forest (e.g. Breiman, 2001a,b; Liaw and Wiener, 2002)

and XGBoost (e.g. Chen and Guestrin, 2016). ~~In Despite of the potential of in stacking methods, up to the knowledge of the authors, it they whaves not yet been used so far as a stacking ensemble method., but iinstead, some papersprevious studies have used them for predicting the outputs directly from the driving input data directly.~~

The integration of diverse environmental drivers with sophisticated analytical methods is central to advancing predictive modelling in environmental science. For instance, Hengl et al. (2017) demonstrated that spatial predictions of soil properties improved significantly when large stacks of remote-sensing and environmental covariates were incorporated into ensemble machine-learning frameworks. This approach is further supported by research such as Luo et al. (2009), who found that high-frequency driver data reduces parameter equifinality in ecosystem data assimilation, and Pappas et al. (2014), who developed efficient methods for gap-filling hydrometeorological observations. More recently, Sándor et al. (2023) showed that analysing residual correlations among crop and grassland model ensembles can reveal structural model deficiencies and improve simulation of C-N fluxes when combined with ensemble averaging. Collectively, these studies highlight the substantial value of leveraging diverse variables, advanced techniques, and residual-based ensemble diagnostics to build more robust and accurate predictive models. Building on these advancements, the present study introduces a meta-modelling framework that integrates biogeochemical model outputs and environmental variables, guided by residual correlation insights, to address structural model error and enhance predictive performance.

This study aims to improve the predictive accuracy of biogeochemical flux calculations, particularly C fluxes, in diverse agricultural systems (crop rotations and grassland systems). Building on an already established multi-model framework, a novel ~~calibration~~ methodology is used to develop a meta-model that balances scientific rigour and practical feasibility. The results of this meta-model are compared with the multi-model ensemble median and other meta-models to demonstrate the improvement, interpretability and reliability of ensemble predictions (~~where multi-model median is considered as the baseline~~). This dual focus aims to improve methodologies for sustainable crop and grassland management and to inform agricultural policy to better address the challenges of climate resilience and sustainability.

~~The novelty of these study lies in the interpretability of the multi-model system and itshe linkage with environmental factors to improve the performance of the method. Additionally, the application of multiple meta-modelling approaches providing that is an abstract framework tfo provide improved modelling exercises, further supplementorted withby SHapley Additive exPlanations (SHAP) fto ensure interpretability.~~

2 Materials and methods

2.1 Meta-modelling framework

The methods employed in this study arise from the contemporary landscape of crop and grassland modelling, specifically focusing on ensemble modelling. We adopt and extend the concept of meta-modelling by comparing it to the multi-model median (MMM) ~~baseline~~ estimator (e.g. Sándor et al., 2018).

While the term *meta-modelling* can be conveyed ambiguously, some clarification is needed. Widely used in mathematics, computer science and engineering, a meta-model is understood as a model of one or more models. Here, we define it as the use of model outputs from a multi-model ensemble - for ~~one-two~~ particular methods

120 supplemented by environmental variables - as inputs to a higher-level statistical model. Unlike traditional surrogate
models that approximate the structure of a process-based model, our meta-model approach complements, rather than
replaces, process-based models by exploiting the information embedded in multiple model outputs. The enhanced
predictive power and the resulting trust in model outcomes are particularly valuable for informing policy decisions.
This method goes beyond Bayesian model averaging, non-democratic model selection and some machine learning
125 based output combination techniques, allowing for more flexibility in capturing nonlinear relationships.

~~The foundation of the method is the so-called “No Free Lunch” (NFL) theorem (Wolpert and Macready, 2005),
which formally states that when evaluating performance over the entire space of possible tasks (assuming a uniform
distribution), all machine learning models achieve the same average result. This implies that no single algorithm is
universally superior. Crucially, however, real world problems deviate from this uniform distribution, displaying
130 inherent structure and regularities that models with well-suited inductive biases can effectively exploit.~~

Here ~~We~~ adopt *stacked generalization* (called simply as *stacking* hereinafter), as an ensemble method wherein a
meta-model integrates predictions generated by multiple base models. Thus, throughout the study, *stacking*
~~means~~ refers to an ensemble learning technique, in which the multi-model framework is used to construct a new
estimation for the target variables. This method relies on the observation that diverse models inherently capture
135 different aspects of real-world systems like the plant-soil system. Consequently, training a meta-model to optimally
integrate these varied predictions allows stacking to leverage the individual strengths of the base models, ultimately
leading to improved generalisation across various tasks focusing on the plant-soil systems.

Linear models are the most prevalent meta-models in ensemble learning, largely due to their simplicity,
computational efficiency, and ease of interpretation. Their additive structure makes it straightforward to quantify
140 the relative influence of individual models within an ensemble, which is particularly valuable for diagnostic
purposes. Notably, a precursor to formal meta-modelling can be seen in the Granger–Ramanathan averaging method
(Granger and Ramanathan, 1984; Nand et al., 2025), which introduced the idea of optimally weighting model outputs
through constrained linear regression. This approach laid the foundation for modern stacking techniques by
demonstrating how combining forecasts in a regression framework could systematically improve predictive
145 accuracy.

However, when base models exhibit substantial structural differences and higher structural errors, the relationship
between predicted and observed outcomes may no longer be well-approximated by a linear model. In such scenarios,
simple linear approaches like the Granger–Ramanathan averaging may prove insufficient. Furthermore, the often-
implicit assumption of conditional independence among base-model predictions in linear meta-modelling is
150 frequently violated, rendering multiple linear regression a suboptimal choice.

To address this limitation, ensemble-based machine-learning meta-models offer a compelling alternative. These
models can effectively capture complex, non-linear relationships and do not rely on the conditional independence
of base-model predictions. Random Forests, for example, have been among the earliest and most effective ensemble
methods used as meta-models, particularly in contexts where linear approaches underperform (Zhao and Cheng,
155 2022).

While effective, Random Forests can be computationally demanding during both training and inference. They also
tend to overfit the training data, potentially compromising generalization on independent data. XGBoost offers
greater flexibility, often delivering superior predictive accuracy with generally lower computational requirements.
However, XGBoost typically requires extensive hyperparameter tuning to achieve optimal performance.

160 A key limitation of all these approaches is their static nature: the functional relationship learned between the base-models' outputs and the target variable remains fixed. This static feature limits the long-term usability of meta-models, as evolving environmental conditions can shift the relevance of different structural components within the base-models. Consequently, the optimal meta-model may vary over time, necessitating continuous retraining to maintain accuracy, which represents a major drawback.

165 With advancements in machine learning, today we can significantly extend the approach described above. By incorporating differentiating environmental factors — such as temperature or precipitation — as additional features, the meta-model can learn not only the functional relationship between the base-model outputs and the measurements, but also how this relationship varies with environmental conditions.

170 This approach is only possible with flexible meta-models. Simpler models, such as generalized linear models, rely on assumptions like conditional independence and uncorrelated features — assumptions that are often violated when additional environmental factors are introduced. As a result, these simpler models may struggle to capture the conditional dependencies required for enhanced predictive performance.

Such an *environment-aware meta-modelling* framework (i.e. XGBoost or Random Forest with additional meteorological drivers) improves both predictive accuracy and interpretability by revealing the specific conditions under which different models succeed or fail. Examining this-these meta-models allows researchers and modellers to understand their model's limitations in varying contexts. This knowledge guides further model development and facilitates the selection of the most appropriate model for given circumstances, promoting valuable synergy between modelling approaches.

175 ~~In order to~~To establish a clear terminological framework, here we summarize the most important key components of the study. Base models are these are the individual process-based ecosystem models (e.g. DNDC or APSIM; Sándor et al., 2024) that generate the initial flux estimates. Baseline (MMM) is the Multi-Model Median, that is defined as the unweighted central tendency of the base model outputs and used as the benchmark for evaluating all subsequent meta-models. Stacking (Meta-Modelling framework) is this refers to the ensemble-learning framework in which the outputs of the base models aserve used as predictors for a second-level learner. Meta-models are These are the (ML) algorithms that implement this stacking framework.

2.2 Source of the model ensemble

The model ensemble is based on data from international initiatives, primarily the Agricultural Model Intercomparison and Improvement Project (<https://agmip.org>) and the Integrative Research Group of the Global Research Alliance on agricultural GHGs (<https://globalresearchalliance.org/research/integrative>). These exercises have shown that ensembles of process-based biogeochemical models can reliably estimate agricultural productivity, as well as C and N emissions (and stocks) of agricultural systems (Ehrhardt et al., 2018; Sándor et al., 2018, 2020, 2024). These studies, mostly funded by national agencies, also contribute to the assessment of C storage potential (e.g. Farina et al., 2021), aligning with the '4 per mille Soils for Food Security and Climate' initiative established at the 2015 United Nations Climate Change Conference (COP21) by the French Ministry of Agriculture (<https://www.4p1000.org>).

195 Here, we refer to a multi-model scheme, using daily model outputs as inputs for the meta-models. ~~The multi-modelling exercise discussed here is not the primary content but serves as the foundational basis for the subsequent~~

~~meta-modelling exercise.~~ We are revisiting salient elements from previously published studies to build the framework for our meta-modelling analysis. Specifically, we delve into comparisons with the multi-model median from the study by Sándor et al. (2020) on C fluxes, which, in turn, was based on the protocol of Ehrhardt et al. (2018).

Table 1: C-flux outputs provided by different models (Sándor et al., 2024), denoted by symbols such as ✓ (present) and NA (not available). Models are marked as M01–M26, and they are kept anonymous as in the Sándor et al. (2020) study. In cropland sites, we had gross primary production (GPP) from six models, net ecosystem exchange (NEE) from seven models and ecosystem respiration (RECO) from 15 models. At grassland sites, we had GPP from 10 models, NEE from 10 models and RECO from 12 models.

Model type	Crop models												Grassland models								Both systems					
Model id	M01	M02	M04	M09	M12	M13	M18	M19	M20	M25	M26	M03	M06	M16	M21	M22	M23	M24	M28	M05	M07	M08	M14			
Outputs	GPP	✓	NA	NA	✓	NA	NA	NA	✓	NA	NA	NA	NA	✓	✓	✓	✓	✓	✓	✓	✓	✓	✓	✓	NA	✓
	RECO	✓	✓	✓	✓	✓	✓	✓	✓	NA	✓	✓	✓	✓	✓	✓	✓	✓	✓	✓	✓	✓	✓	✓	✓	✓
	NEE	✓	NA	NA	✓	NA	NA	NA	✓	✓	NA	NA	NA	✓	✓	✓	✓	✓	✓	✓	✓	✓	✓	✓	NA	✓

We use daily outputs from 23 crop and grassland simulation models/versions (Table 1; for details see Sándor et al., 2020; 2024). Model names (M01–M28) were anonymised for consistency, with M11 excluded due to missing C fluxes. These models were applied to four long-term field sites: two grazed grasslands (G3, G4) and two croplands (C1, C2) across the UK, France (two sites) and Canada (Table 2). ~~In the original Sándor et al. (2020) paper, there was included one additional cropland site in (India), that was about this site was re-excluded from the present study due to its relatively poor temporal coverage and because of the observations data, and also due to the fact that observations were made using a different methodology, which led to resulting in the absence of GPP and RECO estimates. at that site (the All other sites used relied on the eddy-covariance technique,) ensuring methodological consistency.~~

Table 2: Cropland and grassland sites, and temporal coverage of available data used for the analysis. Different crop rotations were used in the cropland sites, including cereals (spring and winter wheat [W], triticale [T], maize [M] and rice [R]), legumes (soybean [S]), rapeseeds (canola and mustard [C]), borages (phacelia, P) and fallow intercropping periods [I].

Sites, country (latitude, longitude, altitude)	Years of available data (simulation period)	Land use	Annual mean temperature (°C)	Annual mean precipitation (mm)
C1: Ottawa, Canada (45.29, -75.77, 94 m a.s.l.)	2007-2012	W/S/C/M/W/C	7.2±0.9	936±121
C2: Grignon, France (48.85, 1.95, 125 m a.s.l.)	2008-2012	C/M/W/T/P/M /W/I	10.9±0.7	571±35
G3: Laqueuille, France (45.64, 2.74, 1040 m a.s.l.)	2003-2012	Permanent grassland (cattle grazing)	13.7±0.4	910±96
G4: Easter Bush, United Kingdom-UK (55.52, -3.33, 190 m a.s.l.)	2002-2010	Permanent grassland (ewe grazing)	7.8±0.8	1078±205

225 High quality data covering climate, soil, agricultural practices and C fluxes were gathered from Sándor et al. (2024).
Observations at these sites include ~~eddy covariance and chamber~~ measurements of net ecosystem CO₂ exchange
(NEE) data, further divided into two main fluxes- (e.g. Reichstein et al., 2005; Raj et al., 2016): gross primary
production (GPP), representing photosynthetic production from atmospheric CO₂, and total ecosystem respiration
(RECO), encompassing the total C respired by plants, soil organisms and, in the case of grasslands, grazing animals.
230 Initialisation and calibration procedures aligned models with vegetation, soil and atmospheric fluxes from the study
sites, following the protocol described in Ehrhardt et al. (2018). This comprehensive exercise involved a multi-stage
approach, granting modellers access to increasingly detailed data for running and evaluating their models,
progressing from uncalibrated to fully calibrated simulations. In summary, the calibration included five ascending
levels, incorporating additional data for refinement: blind test (S1), utilising only site specific weather and
235 management data for the simulation periods; initialisation (S2), incorporating additional historical climate and
management data, extending to years preceding simulation periods, along with regional productivity for initialisation
purposes; partial calibration (S3), including biomass production and phenology data; intermediate calibration (S4),
integrating soil temperature, soil water content and mineral N data; full calibration (S5), using N₂O emissions, NEE,
GPP, RECO and soil organic C and N data.
240 For the purposes of this study, emphasis was placed on the outputs from the partial calibration stage (S3) stage. S3
involves calibration using plant data exclusively, which enhances the practical implementability of models for end
users and beneficiaries. This approach recognises the importance of ensuring models are not only scientifically
robust but also practically useful. Its validity is supported by findings that additional calibration stages beyond S3
yielded only modest improvements (Sándor et al., 2023).

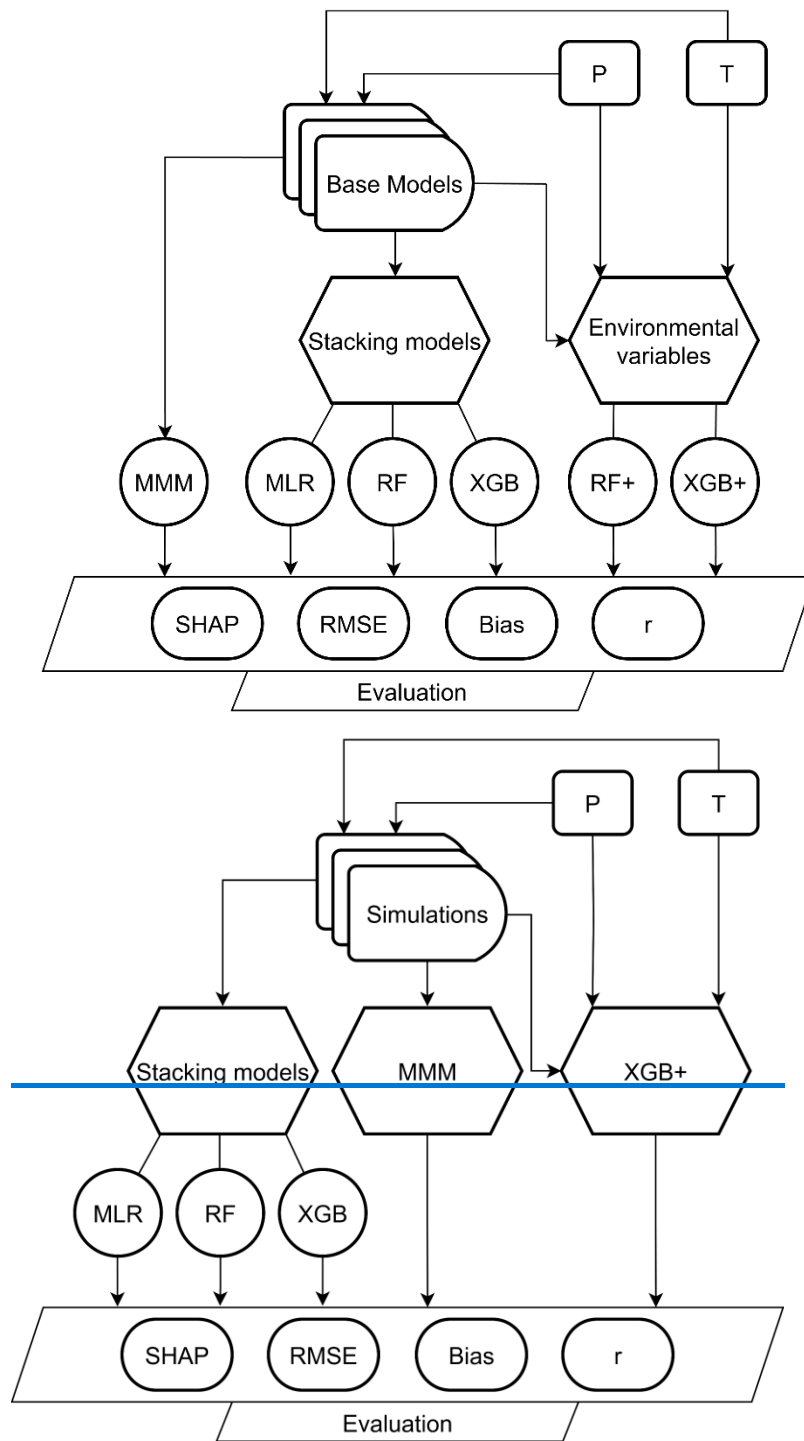
245 **2.3 Meta-modelling approaches and validation strategies**

The meta-model construction was done at the daily time resolution for GPP, RECO and NEE. Two main approaches
were tested in this study for the meta-model construction. The first one focuses on the classic stacking ensemble
method (referred here as CSEM), where the meta-models were constructed using multiple linear regression (MLR),
random forest (RF) method, and XGBoost (XGB) using the model outputs described in Section 2.2. The second
250 approach, that is introduced in this study as a *novel method* (the environment-aware meta-modelling method), uses
the same stacking methods but extends the input dataset so that besides the individual, process-based model outputs,
we use two additional environmental factors (daily mean temperature and precipitation) to predict the final outcome
(i.e. the meta-model). This approach (i.e. inclusion of the meteorological drivers) is referred to here as extended
generic stacking ensemble method (XGB+ and RF+). The inclusion of only temperature and precipitation is
255 grounded in their central roles as primary climatic drivers of terrestrial C fluxes. Temperature governs essential
biological processes such as photosynthesis and respiration (Lloyd and Taylor, 1994; Xu and Baldocchi, 2004),
while precipitation affects soil moisture and plant water stress, both critical for GPP and RECO (Reichstein et al.,
2005; Schwalm et al., 2010). Extensive research has shown that fluctuations in these two variables explain much of
the interannual and seasonal variability in ecosystem C exchange (Jung et al., 2007; Beer et al., 2010). Moreover,
260 temperature and precipitation are consistently measured across sites, widely available and commonly integrated into
ecological and climate models. Their inclusion enhances predictive performance without adding complexity or
compromising generalisability (e.g. Hijmans et al., 2005). Supporting this approach, Dorman et al. (2013) advocate

for the use of core climatic variables over an excess of redundant predictors to maintain model robustness and transferability.

265 Two meta-model validation strategies were used in the study for both main approaches described above. First, All
meta-models were constructed using 70% of the observations for training, and with the remaining 30% was used for
validation. Additionally, we also constructed meta-models using the complete leave-one-year-out (LOYO)
approach. In which this method the observations from a one complete year were omitted and during the model
training was done with the remaining data, and the omitted year was subsequently used for validation. All years were
270 omitted consecutively, and the validation results based on the omitted years were averaged and provided the basis
for the evaluation of the strategy. This alternative method strategy was test included since the carbon flux time series
are autocorrelated, and thus time-aware validation methods like LOYO can provide additional insight into the model
applicability of the methods. The 70%/30% validation split strategy (referred as 70/30 hereinafter) provide evaluates
within-regime flux reconstruction performance, while LOYO assesses the model's ability to
275 generalization and extrapolation beyond the conditions represented in the training test of the meta-models. In the
study the LOYO based methods are presented mainly given the fact that they are more generalizable. Statistical
analysis is also provided for the 70%/30% split for comparability.

For the MLR method we used the *lm* function of base R. The RF method (*randomForest* package from CRAN; Liaw and Wiener, 2002) was used with 1000 trees. For each tree the number of predictors were 1/3 of the number of input
280 data streams (GPP, RECO, NEE and meteorological drivers if applicable) in order to prevent overfitting. The subset
of predictors was used randomly. The minimum size of the terminal nodes was five. We have split the
dataset into training and testing dataset randomly, using 70% and 30% of the data for training and validation,
respectively was done randomly, using the built-in random number generator function of base R, without specifying
the seed. For each particular site, the same site-specific random number sequence was used across the different all
285 meta-model trainings. (between sites the random number while sequences differed between sites due the
different varying lengths of their time series. The XGB method was implemented using the *XGBoost* package from
CRAN (Chen and Guestrin, 2016). For hyper-parameter optimization we used grid-search (in other words systematic
search) technique for XGBoost. Figure 1 shows the overview of the stacking methods used in the study.



290

295

Figure 1: Schematic illustration of the applied stacking ensemble learning methodology. The workflow combines outputs from multiple simulations (base models) with multi-model median (MMM) and stacking models (MLR, RF, XGB). The XGB+ and RF+ models are an extended version that incorporates additional input features: temperature (T) and precipitation (P). The performance of these models and the ensembles are evaluated using four metrics: SHAP (for interpretability), RMSE (root mean square error), Bias and the Pearson correlation coefficient (r). The final output is the site-level carbon flux, which is the same variable type as the initial model outputs.

300 ~~To facilitate the interpretation of the linear meta-model, we examined the normalised feature weights, which provide a direct measure of the relative importance of predictors in a linear framework. For the non-linear ensemble models (RF and XGBoost),~~ feature contributions were quantified using SHAP_ ~~(SHapley Additive exPlanations)~~ values (Shapley, 1953; Lundberg and Lee, 2017). SHAP values are grounded in cooperative game theory, representing the ~~mean-expected~~ marginal contribution of a feature across all possible feature coalitions. This formulation provides a theoretically consistent and locally accurate decomposition of model predictions, enabling a granular understanding of feature effects. In contrast to traditional importance measures such as the mean decrease in impurity (often referred to as the Gini importance; Breiman, 2001a,b), SHAP values address several critical limitations. The Gini metric, while computationally efficient, is known to exhibit biases toward features with a higher number of categories or greater variance (Strobl et al., 2007). Moreover, it does not provide insight into the directionality or context-dependent contribution of features to individual predictions. SHAP overcomes these limitations by providing additive, model-agnostic attributions that remain consistent across different models and capture complex, non-linear interactions between features (Lundberg et al., 2020). These properties make SHAP particularly well-suited for interpreting ensemble methods like RF and gradient-boosted decision trees, where feature interactions and non-linearities are prominent.

All evaluations were performed separately for each study site, and for the studied carbon fluxes (GPP, RECO, NEE). No cross-site meta-model was developed in this study, ~~which meanings that allsite-specific temporal training and validation were~~ ~~as performed on a site-specific temporal basis.~~ To assess how well models approximated site-level observations, we compared each meta-model and the MMM using three common performance metrics (Richter et al., 2012) across 26 site-stage-output combinations: the root mean square error (RMSE), ~~the squared of the~~ Pearson's correlation coefficient (R^2_r), and the bias.

320 The results are organized according to the carbon flux type. First GPP is discussed, as it represents plant photosynthesis and is the most important driver of the plant production and yield. Most likely GPP is the process that is the simplest to simulate by process-based models. ~~†This is †because to the fact that~~ the mechanism of photosynthesis is well-discovered, and practically it is separated from other autotrophic or heterotrophic processes (since this is the only flux that comes into the ecosystem). GPP is a relatively large flux (compared e.g. to NEE or net biome production), so model optimization is perhaps simpler and more interpretable. ~~Of course~~ GPP can be biased for some cases due to improper representation of phenology, and lack of model optimization.

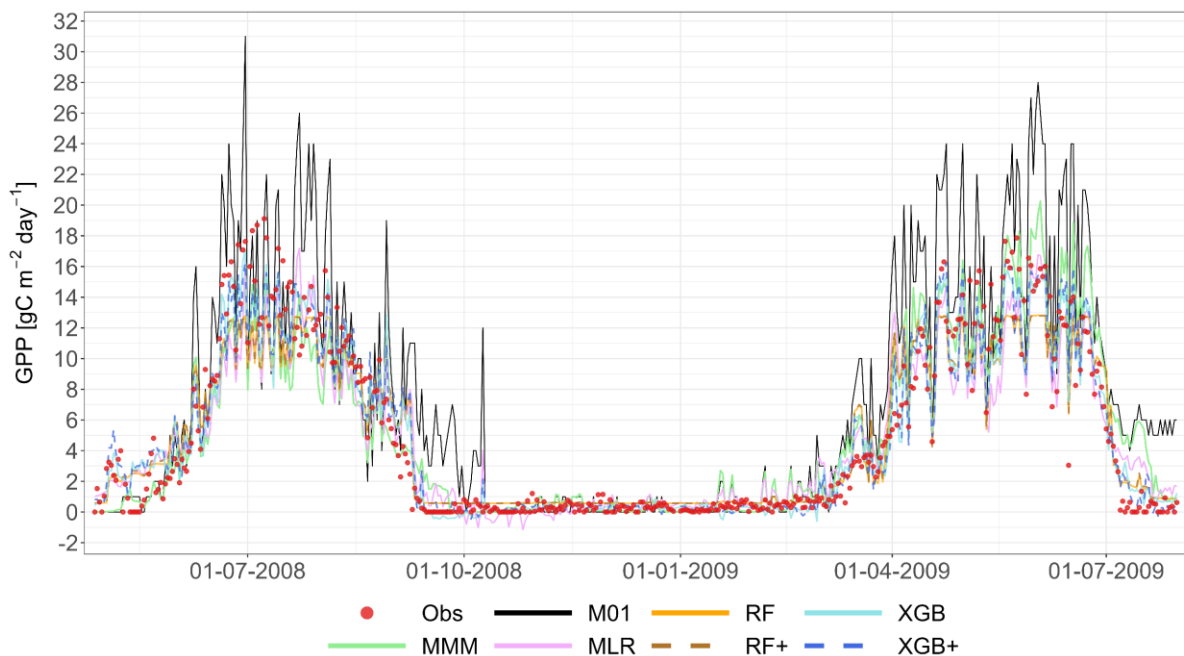
RECO follows the discussion that is typically harder to simulate than GPP. ~~†This is †because to the fact that~~ RECO is the sum of autotrophic and heterotrophic respiration, where both components have their own intrinsic uncertainties. For example, heterotrophic respiration is typically problematic due to the complexity of the decomposition processes in the soil including the rhizosphere and the presence, complexity and activity of the microbial/fungal life forms. RECO can be erroneously simulated if one of the two major components are misrepresented (or even worse if, due to the compensation of errors, RECO looks good due to wrong reasons). Nevertheless, RECO is still a larger carbon flux, so its representation can be expected to be relatively well-adjusted. Finally, we present NEE related results. This flux is probably the hardest to simulate, since it is the sensitive balance between RECO and GPP (by definition, $NEE=RECO-GPP$). Capturing the magnitude and variability of NEE requires the proper representation of plant phenology (start and end of season), and accurate representation of GPP and RECO. If the meta-model captures NEE with greater precision than the more traditional model ensembles, this represents a significant accomplishment.

340 Although ~~As NEE is defined as RECO-GPP, the meta-model based in this study~~ NEE is not calculated ~~as RECO-~~
~~GPP with this definition~~ but rather it is modelled independently from GPP and RECO (due to methodological
reasons). ~~This might introduce some inconsistency, but the aim was to check the ability of the~~
~~metamodelling approaches for any given variable, independent of other observations. In order to~~ To address this issue,
345 we also calculated NEE using the meta-model based GPP and RECO, thus providing consistent results. This
~~independent calculation is used as another level of validation for the LOYO based model construction. It is important~~
to note that ~~S~~successful and unbiased simulation of NEE is a major step forward supporting e.g. atmospheric
inversions or any other bottom-up carbon flux estimations.

3. Results

3.1. GPP

350 Fig. 2 shows a representative example of the observed and simulated time series of GPP at the Grignon cropland
site (C2) for the 2008-2009 growing seasons (maize and after that winter wheat), and for two consecutive years
~~(2004-2005)~~ at the Easter Bush permanent grassland site (G4) ~~(2004-2005)~~. All meta-modelling approaches are
plotted ~~based on the LOYO validation strategy~~ alongside the best-performing individual model (M01 for Grignon
and M22 for Easter Bush). Appendix A contains the complete simulated dataset for all sites, and for all years, ~~and~~
355 ~~also for the 70/30 validation strategy.~~



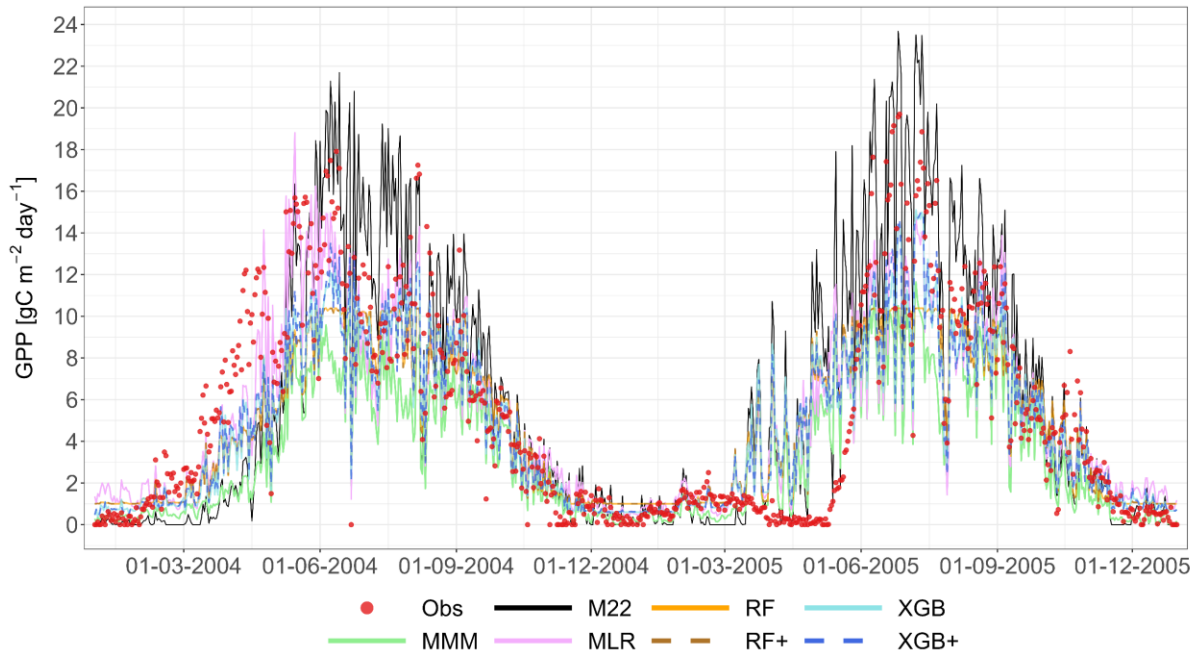


Figure 2: Performance of the multi-model median (MMM, green), the constructed meta-models and the best-performing individual models for simulating GPP based on the LOYO strategy. The top panel shows results for the Grignon cropland site (C2), which includes maize and winter wheat. The bottom panel shows two years of data for the Easter Bush grassland site (G4). Observations are marked by red dots. The meta-models include Multiple Linear Regression (MLR, purple hatched light blue), Random Forest (RF, hatched orange), XGBoost (XGB, light blue hatched purple), Random Forest+ (RF+, hatched brown) and XGBoost+ (XGB+, hatched dark blue). The best-performing individual models (M01 at C2, M22 at G4) are shown in black. Dates are provided in the format of dd-mm-yyyy.

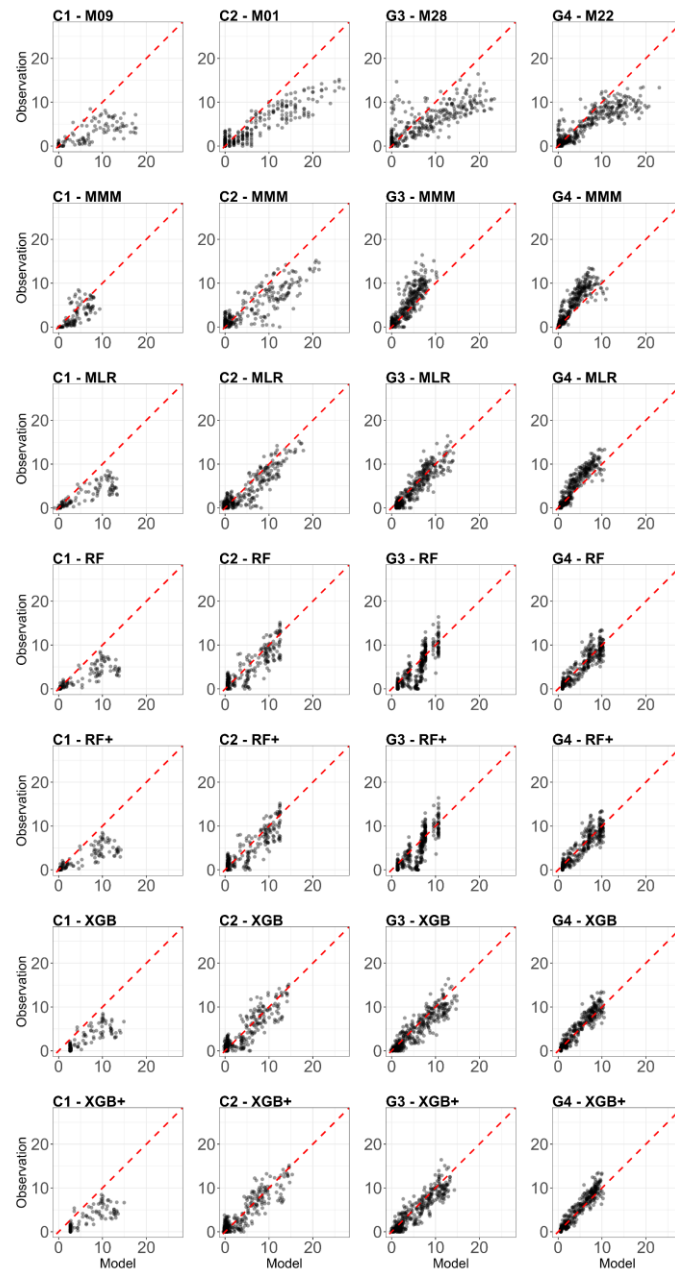
The plots indicate a relatively large scatter in model results compared to observations, especially for croplands. Notably, the best-performing individual model for the cropland time series exhibited considerable biases, generally overestimating GPP. In contrast, all meta-model approaches indicate reduced bias. To provide objective quality indicators, further quantitative analysis was performed.

Fig. 3 compares observed and modelled GPP for all four experimental sites and all meta-model construction methods used in the study the LOYO strategy, including the MMM. The figure includes a scatterplot showing the performance of the best individual model, selected based on its RMSE score. RMSE was chosen as the primary selection metric because it correlates well with other performance metrics (Kobayashi and Salam, 2000; Robeson and Willmott, 2023). The figure was constructed using all data from the sites, using one validation year selected based on the performance of the XGB+ method not only training data.

The figure Fig. 3 shows a gradual improvement in performance from top to bottom, indicated by increases in R^2 and tighter alignment of data points along the 1:1 line. At every site, MMM outperforms the best individual model in terms of explained variance. For sites C2-C1, C2 and G3, and to some extent for G4 as well, MMM already corrects much of the bias seen in the individual simulations.

At site C1, improvements across MLR, RF, RF+, XGB and XGB+ do not always correspond to continuous increases in R^2 , but the alignment of the observation-model data pairs improves relative to the 1:1 line is associated with the restricted temporal coverage of the dataset (in LOYO strategy half of the dataset was retained). For C2, explained

variance steadily increases with a marked improvement upon introduction of RF. Similar trends are observed ~~at~~ the ~~or the~~ grassland sites G3 and G4, where ~~the~~ longer time series was available providing ~~yield~~ a larger number of data points and led to more pronounced improvement. Overall, across all sites, explained variance increases by ~~~20%~~ ~20% for the best performing metamodels (RF, XGB and XGB+).



390 **Figure 3:** Comparison of the best individual model, the constructed meta-models and the traditional Multi-Model
 391 Median with the observations for all sites (from left to right C1, C2, G3 and G4) and for the entire time series for
 392 GPP based on the LOYO strategy. From top to bottom: best individual model ~~with ID,~~ MMM, MLR, RF, RF+,
 393 XGB and XGB+. All units are in $\text{g C m}^{-2} \text{ day}^{-1}$. Red dashed line represents the 1:1 relationship.

394 Table 3 presents ~~model~~-statistical measures for all sites and modelling approaches evaluated, alongside the best-
 395 performing individual model, using data only from the validation subset.

Table 3: Statistical evaluation of the best performing individual model, the multi-model median (MMM) and the applied meta-models (MLR, RF, RF+, XGB and XGB+) with respect to three performance metrics for GPP: root mean square error (RMSE), bias and Pearson's correlation coefficient (r). Only validation data were used for the calculation of the statistics. RMSE and BIAS are provided in g C m⁻² day⁻¹ units. The table present performance metrics for the 70/30 and the LOYO strategy as well.

Site	Metric	best individual model	MMM	MLR	RF		XGB	XGB+
C1	RMSE	3.65	3.03	2.41	1.98		1.93	2.05
	BIAS	1.52	-0.61	-0.56	-0.51		-0.19	-0.28
	r	0.799	0.864	0.889	0.929		0.922	0.914
C2	RMSE	4.22	2.88	2.55	1.93		1.92	1.90
	BIAS	1.02	-0.05	0.16	0.1		0.12	0.15
	r	0.776	0.790	0.817	0.899		0.901	0.902
G3	RMSE	4.48	2.96	2.12	1.79		1.80	1.78
	BIAS	1.22	-1.6	0.02	0.03		0.06	0.05
	r	0.774	0.793	0.855	0.899		0.897	0.901
G4	RMSE	3.02	2.96	2.37	1.84		1.80	1.82
	BIAS	0.11	-1.36	0.04	0.02		0.02	0.03
	r	0.754	0.809	0.844	0.911		0.914	0.912

Site	Metric	best individual base model	MMM	MLR	RF	RF+	XGB	XGB+
C1	RMSE 70/30	3.65	3.03	2.41	1.98	1.95	1.93	2.05
	RMSE LOYO	3.90	2.88	4.57	4.68	4.72	4.53	4.56
	BIAS 70/30	1.52	-0.61	-0.56	-0.51	0.22	-0.19	-0.28
	BIAS LOYO	1.94	-0.04	-0.25	-0.11	-0.07	0.79	0.81
	r 70/30	0.799	0.864	0.889	0.929	0.888	0.922	0.914
r LOYO	0.862	0.795	0.877	0.867	0.863	0.835	0.837	
C2	RMSE 70/30	4.22	2.88	2.55	1.93	2.09	1.92	1.90
	RMSE LOYO	4.14	2.86	2.62	2.71	2.72	2.80	2.81
	BIAS 70/30	1.02	-0.05	0.16	0.1	0.18	0.12	0.15
	BIAS LOYO	1.15	-0.03	0.02	0.16	0.17	0.09	0.00
	r 70/30	0.776	0.790	0.817	0.899	0.886	0.901	0.902
r LOYO	0.839	0.850	0.852	0.828	0.828	0.825	0.818	
G3	RMSE 70/30	4.48	2.96	2.12	1.79	2.28	1.80	1.78
	RMSE LOYO	3.47	2.87	2.26	2.55	2.55	2.31	2.30

	<u>BIAS 70/30</u>	<u>1.22</u>	<u>-1.6</u>	<u>0.02</u>	<u>0.03</u>	<u>0.19</u>	<u>0.06</u>	<u>0.05</u>
	<u>BIAS LOYO</u>	<u>-1.74</u>	<u>-1.60</u>	<u>-0.03</u>	<u>-0.07</u>	<u>-0.07</u>	<u>-0.01</u>	<u>-0.01</u>
	<u>r 70/30</u>	<u>0.774</u>	<u>0.793</u>	<u>0.855</u>	<u>0.899</u>	<u>0.833</u>	<u>0.897</u>	<u>0.901</u>
	<u>r LOYO</u>	<u>0.724</u>	<u>0.825</u>	<u>0.862</u>	<u>0.806</u>	<u>0.805</u>	<u>0.861</u>	<u>0.861</u>
G4	<u>RMSE 70/30</u>	<u>3.02</u>	<u>2.96</u>	<u>2.37</u>	<u>1.84</u>	<u>2.51</u>	<u>1.80</u>	<u>1.82</u>
	<u>RMSE LOYO</u>	<u>2.80</u>	<u>2.95</u>	<u>2.81</u>	<u>2.64</u>	<u>2.63</u>	<u>2.67</u>	<u>2.71</u>
	<u>BIAS 70/30</u>	<u>0.11</u>	<u>-1.36</u>	<u>0.04</u>	<u>0.02</u>	<u>0.00</u>	<u>0.02</u>	<u>0.03</u>
	<u>BIAS LOYO</u>	<u>0.06</u>	<u>-1.37</u>	<u>-0.23</u>	<u>-0.03</u>	<u>-0.03</u>	<u>-0.07</u>	<u>-0.08</u>
	<u>r 70/30</u>	<u>0.754</u>	<u>0.809</u>	<u>0.844</u>	<u>0.911</u>	<u>0.824</u>	<u>0.914</u>	<u>0.912</u>
	<u>r LOYO</u>	<u>0.820</u>	<u>0.835</u>	<u>0.828</u>	<u>0.851</u>	<u>0.851</u>	<u>0.843</u>	<u>0.837</u>

405

The table highlights the improved performance of meta-models relative to both the best individual model and the MMM, which was previously published in Sándor et al. (2020). Notably, moving to more advanced meta-models results in a substantial reduction in both RMSE and absolute bias, which is more emphasized in case of the 70/30 validation strategy. For the G4 site RMSE reduction was marginal for LOYO, while for C1 RMSE increased as we moved to more advanced methods (again, this is attributed to the limited validation data and differing crop types). For the two grassland sites, the meta-models provide almost bias-free estimations, while for the crop sites the bias remains low but does not approach zero. In addition, the correlation coefficient explained variance typically increased by a maximum of 0.11 about 10% for the best-performing meta-model compared with the MMM (and but only 6% at C1). In case of within-regime validation (70/30)

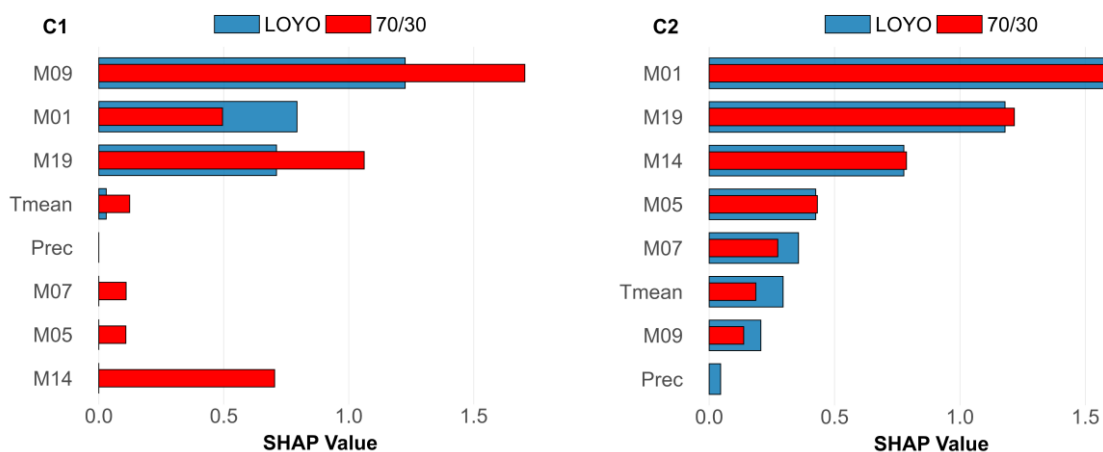
410

415

Given the novelty of the XGB+ approach method and its occasional superior better performance over all other approaches, here we analyse its functioning using SHAP values of the input data streams (individual models, plus temperature and precipitation) for both validation strategies. SHAP value analysis (Fig. 4) shows that certain models (e.g. M09, M19, M01, M14 in case of 70/30 LOYO, while M09, M19, M14 and M01 in case of 70/30 at C1; M01, M19 and M14 using LOYO and 70/30 as well at C2; M16, M24, M14 and M05 using LOYO and 70/30 as well at G3; M22, M16, M06, M22 in case of LOYO, while M22, M16 and M06 in case of 70/30, M16 at G4) dominate contributions to GPP prediction across sites. Temperature is also identified as a notable predictor, especially at sites C1 and C2 (at C2 and G3 for both validation strategies). Precipitation consistently exhibits minimal impact on GPP prediction across all sites, with smaller contributions only at C1 and G4.

420

425



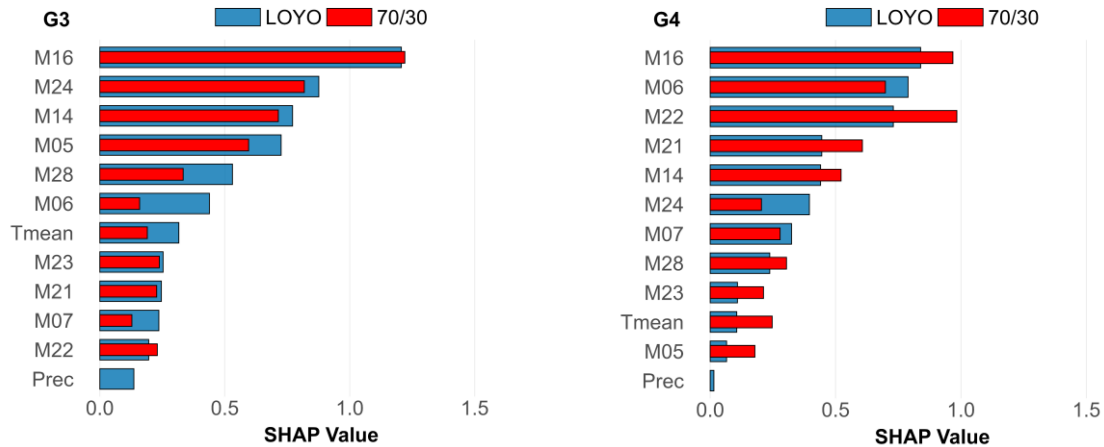


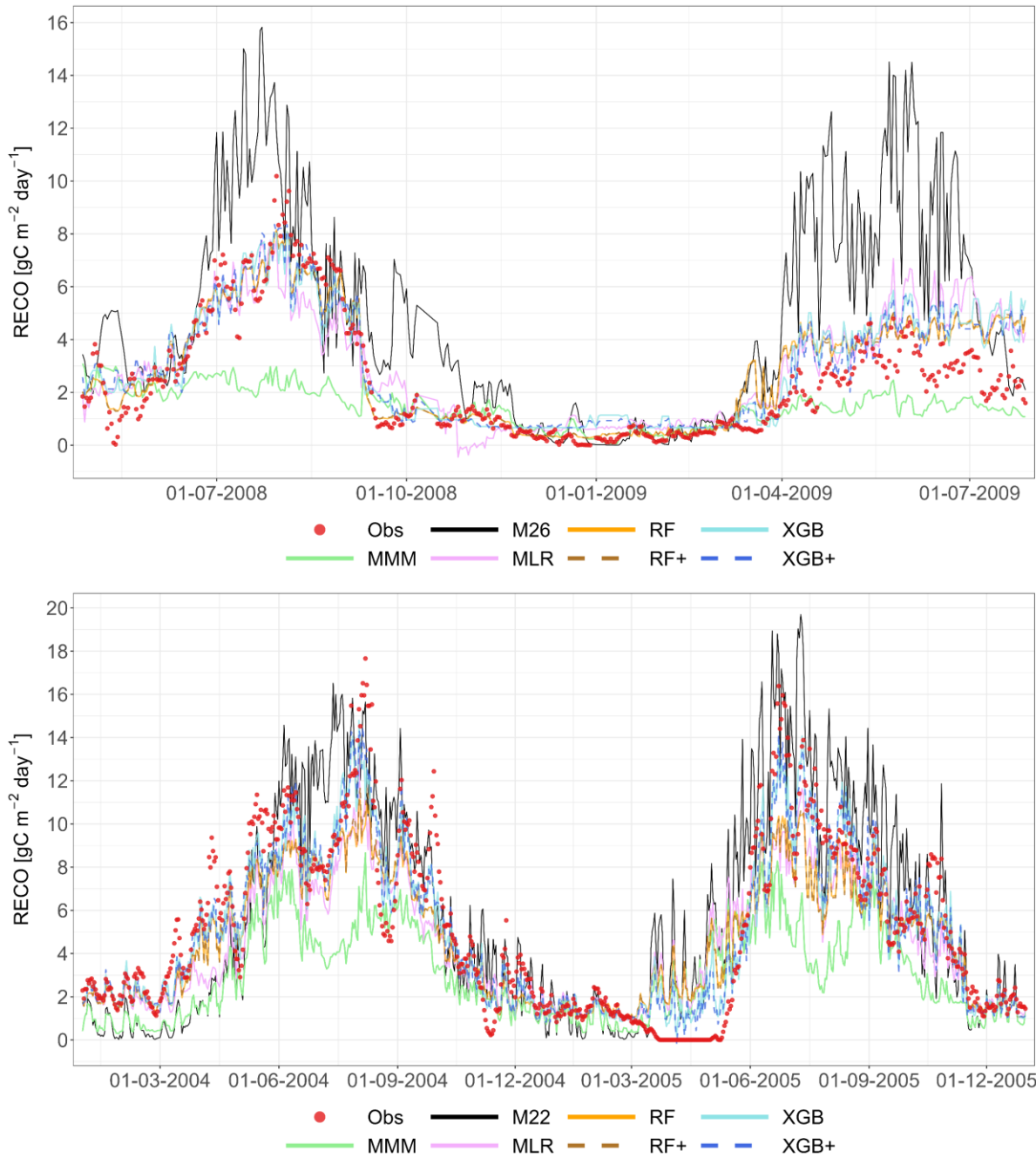
Figure 4: The SHAP values of the XGB+ meta-model for GPP based on the 70/30 strategy (red) and the LOYO strategy (blue). Larger values mean stronger contribution to the resulting GPP. [a\) C1 site;](#) [b\) C2 site;](#) [c\) G3 site;](#) [d\) G4 site.](#) Tmean stands for daily mean temperature, and Prec is daily precipitation.

430 3.2 RECO

Fig. 5 presents a two-year comparison of simulated and observed RECO for Grignon (C2) and Easter Bush (G4), [again based on the LOYO strategy.](#) The graphs display the results of the meta-models, the MMM and the best-performing individual models (M26 and M22). Appendix A contains the complete simulated dataset for all sites, and for all years, [as well as for the 70/30 strategy.](#)

435 At both sites, the MMM consistently underestimates respiration, ~~particularly during peak periods.~~ This bias is especially pronounced at G4, where the MMM produces [a negative peak sharp decline of RECO](#) around June-July, resulting in a poor fit to the observations. In contrast, the meta-models and the best individual model successfully follow the positive peak of the measured values at this site. ~~The meta-models at G4 typically exhibited a negative bias during the observation peaks.~~ Regarding the individual models, the best-performing model at C2 (M26) overestimates both maize and winter wheat respiration. At G4, the best individual model (M22) greatly overestimates the maximum values for both years, ~~though its performance is still better than the MMM.~~ This visual

440 analysis suggests that the MMM does not clearly outperform M22 or M26.



445

Figure 5: Performance of the multi-model median (MMM, green), the constructed meta-models and the best-performing individual models for simulating RECO (LOYO strategy). The top panel shows results for the Grignon cropland site (C2), which includes maize and winter wheat. The bottom panel shows two years of data for the Easter Bush grassland site (G4). Observations are marked by red circles. The meta-models include Multiple Linear Regression (MLR, purple), Random Forest (RF, orange), XGBoost (XGB, light blue), Random Forest+ (RF+, hatched brown) and XGBoost+ (XGB+, hatched dark blue). ~~The meta-models include Multiple Linear Regression (MLR, hatched light blue), Random Forest (RF, hatched orange), RF+ (brown), XGBoost (XGB, hatched purple), and XGBoost+ (XGB+, blue).~~ The best-performing individual models (M01 at C2, M22 at G4) are shown in black. Dates are provided in the format of dd-mm-yyyy.

450

455

A more quantitative analysis can be performed by inspecting Fig. 6, which presents scatterplots comparing simulated and observed RECO. The figures were constructed using one validation year selected based on the performance of the XGB+ method. The MLR consistently provides a “middle-ground” performance, with good performance at G4. The scatter plots in Fig. 6 distinctly illustrate that the MMM has a ~~strong~~ negative bias, which means that it consistently underestimates the observed RECO. This bias is eliminated even by the simplest meta-model (MLR), and as more sophisticated meta-model techniques are employed, the alignment with the 1:1 line becomes significantly better.

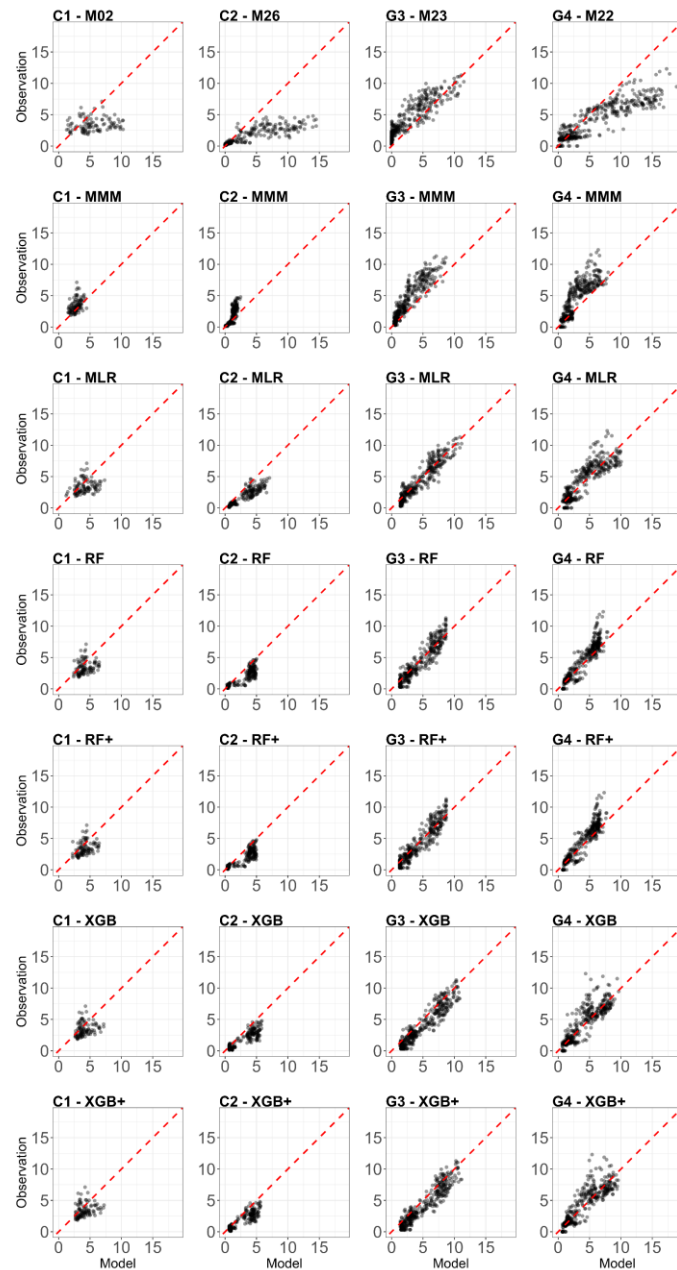


Figure 6: Comparison of the best individual model, the multi-model median and the constructed meta-models with observations for RECO based on the LOYO approach. Each row represents a different model type, and columns correspond to the sites (from left to right: C1, C2, G3, and G4). The top row shows the best individual models with their identifiers (M13 at C1, M01 at C2, M22 at G3 and G4). The remaining rows show the MMM, MLR, RF, RF+, XGB and XGB+. All units are in $\text{g C m}^{-2} \text{ day}^{-1}$. The red dashed line represents the 1:1 relationship.

470 **Table 4:** Statistical evaluation of the best-performing individual model, the multi-model median (MMM) and the applied meta-models (MLR, RF, RF+, XGB and XGB+) for RECO. Three performance metrics are used: root mean square error (RMSE), bias and Pearson's correlation coefficient (r). Only validation data were used for the calculation of the statistics. RMSE and BIAS are provided in gC m⁻² day⁻¹ units.

Site	Metric	Best individual model	MMM	MLR	RF		XGB	XGB+
C1	RMSE	2.61	1.72	0.96	0.84		1.03	0.92
	BIAS	1.56	-1.29	-0.32	-0.23		-0.14	-0.17
	r	0.381	0.469	0.707	0.777		0.607	0.707
C2	RMSE	2.72	2.24	1.30	0.79		0.94	0.93
	BIAS	1.48	-1.09	0.01	0.01		0.03	0.05
	r	0.599	0.556	0.821	0.940		0.912	0.912
G3	RMSE	2.42	2.72	1.56	1.27		1.19	1.19
	BIAS	0.44	-1.69	0.08	0.06		0.05	0.02
	r	0.641	0.700	0.855	0.907		0.918	0.918
G4	RMSE	2.36	2.52	1.97	1.36		1.40	1.35
	BIAS	0.51	-1.08	0.04	0.01		0.06	0.05
	r	0.714	0.720	0.798	0.912		0.905	0.912

Site	Metric	best base model	MMM	MLR	RF	RF+	XGB	XGB+
C1	RMSE 70/30	2.61	1.72	0.96	0.84	0.75	1.03	0.92
	RMSE LOYO	1.65	1.57	3.04	1.69	1.58	1.72	1.60
	BIAS 70/30	1.56	-1.29	-0.32	-0.23	0.17	-0.14	-0.17
	BIAS LOYO	-0.76	-1.10	-1.69	-0.23	-0.17	-0.13	-0.01
	r 70/30	0.381	0.469	0.707	0.777	0.818	0.607	0.707
r LOYO	0.418	0.549	0.370	0.309	0.434	0.295	0.415	
C2	RMSE 70/30	2.72	2.24	1.30	0.79	0.78	0.94	0.93
	RMSE LOYO	2.16	2.09	2.84	1.69	1.71	1.69	1.65
	BIAS 70/30	1.48	-1.09	0.01	0.01	0.00	0.03	0.05
	BIAS LOYO	-1.10	-1.13	-0.24	-0.07	-0.09	0.13	-0.01
	r 70/30	0.599	0.556	0.821	0.940	0.947	0.912	0.912
r LOYO	0.617	0.685	0.727	0.775	0.768	0.781	0.778	
G3	RMSE 70/30	2.42	2.72	1.56	1.27	1.57	1.19	1.19
	RMSE LOYO	2.16	2.49	1.71	1.66	1.66	1.96	1.94
	BIAS 70/30	0.44	-1.69	0.08	0.06	0.00	0.05	0.02
	BIAS LOYO	0.09	-1.75	0.06	0.00	0.00	0.23	0.25
	r 70/30	0.641	0.700	0.855	0.907	0.843	0.918	0.918
r LOYO	0.830	0.820	0.888	0.879	0.879	0.862	0.866	

G4	RMSE 70/30	<u>2.36</u>	<u>2.52</u>	<u>1.97</u>	<u>1.36</u>	1.78	<u>1.40</u>	<u>1.35</u>
	RMSE LOYO	<u>2.26</u>	<u>2.50</u>	<u>2.38</u>	<u>2.20</u>	<u>2.20</u>	<u>2.50</u>	<u>2.44</u>
	BIAS 70/30	<u>0.51</u>	<u>-1.08</u>	<u>0.04</u>	<u>0.01</u>	0.00	<u>0.06</u>	<u>0.05</u>
	BIAS LOYO	<u>0.47</u>	<u>-1.13</u>	<u>0.02</u>	<u>-0.03</u>	<u>-0.03</u>	<u>-0.01</u>	<u>0.00</u>
	r 70/30	<u>0.714</u>	<u>0.720</u>	<u>0.798</u>	<u>0.912</u>	0.851	<u>0.905</u>	<u>0.912</u>
	r LOYO	<u>0.768</u>	<u>0.759</u>	<u>0.787</u>	<u>0.798</u>	<u>0.798</u>	<u>0.742</u>	<u>0.744</u>

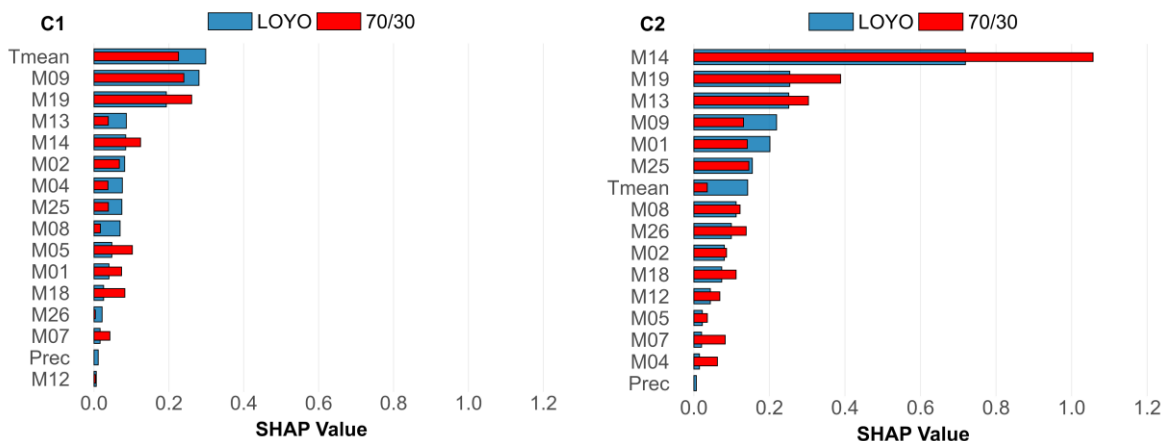
475

480

485

490

Table 4-5 provides statistics calculated based on the validation dataset both for 70/30 and LOYO strategy. A comparison of the MMM and the best individual models reveals some key differences. At C1 the MMM exhibits lower RMSE values, indicating better accuracy. The correlation coefficient is higher than the best individual model at C1 (0.469 vs. 0.381 for 70/30, while 0.549 vs. 0.418 for LOYO) but slightly lower at C2 (0.556 vs. 0.599). At the grassland sites (G3 and G4), the MMM shows slightly higher RMSE values but a better correlation coefficient than for the best individual models. The MMM at the C1 and C2 sites behaves differently compared to the other models. Overall, the meta-models demonstrate a distinct improvement over both the MMM and the best individual models (except for G4 with the LOYO strategy). Among the meta-models, RF, RF+, XGB and XGB+ are the top performers. At the grassland sites, the performance differences between RF, RF+, XGB, and XGB+ were minimal, with all three models demonstrating strong performance across all metrics under the LOYO strategy. Overall, explained variance correlation coefficient typically increases by 19-38.5% for the best performing metamodel compared to MMM in a variable fashion (C2 was associated with the largest increase both under LOYO and 70/30, while the increase was marginal for the grassland sites at C4 this was the lowest, and largest at C2). The meta-models typically show almost unbiased estimates, with the exception of site C1.



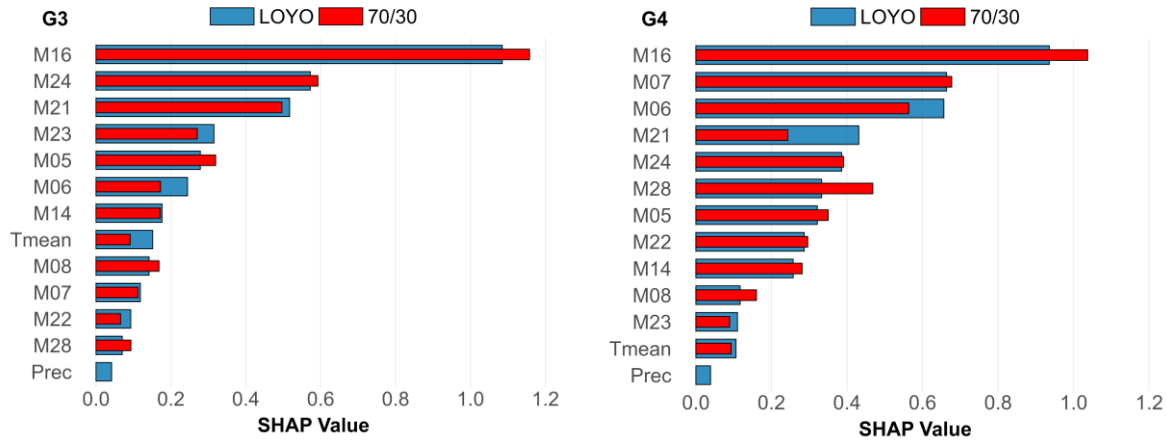


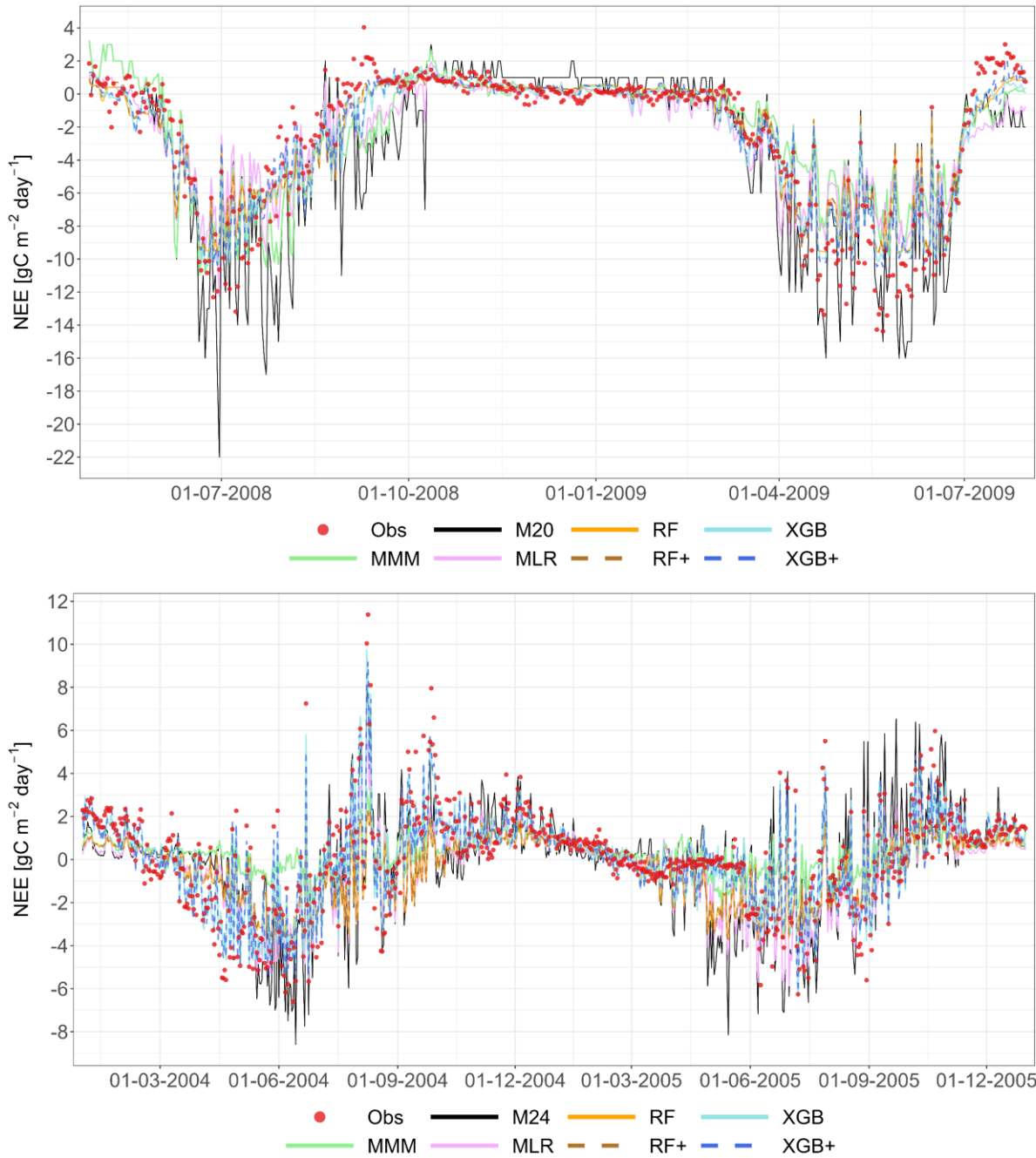
Figure 7: The SHAP values of the XGB+ meta-model for RECO based on the 70/30 strategy (red) and the LOYO strategy (blue). Larger values mean stronger contribution to the resulting RECO. a) C1 site; b) C2 site; c) G3 site; d) G4 site. Tmean stands for daily mean temperature, and Prec is daily precipitation.

SHAP values (Fig. 7) indicate that model outputs are the primary contributors of RECO predictions. Among environmental predictors, mean temperature emerges as an important contributor, especially at site C1, where its influence nearly matches top models M19 and M09 for 70/30, and it is the most important for LOYO. Precipitation influence on RECO is negligible across all sites.

3.3 NEE

Fig. 8 illustrates the simulated and observed NEE for Grignon (C2) and Easter Bush (G4) over two years based on the LOYO strategy. Appendix A contains the complete simulated dataset for all sites, and for all years, for the 70/30 strategy as well.

The MMM shows greater consistency with other meta-models at C2 compared to its performance for RECO in Fig. 5. For both sites, M19-M20 (best model) tends to diverge most from the other models during observation peaks (this is emphasized for grasslands) ~~for C2~~, whereas RF, RF+, XGB and XGB+ are consistently following a similar ~~traeepattern~~, suggesting similar performance for C2.



515 **Figure 8:** Performance of the multi-model median (MMM, green), the constructed meta-models and the best-
 performing individual models for simulating NEE based on the LOYO strategy. The top panel shows results for the
 Grignon cropland site (C2), which includes maize and winter wheat. The bottom panel shows two years of data for
 the Easter Bush grassland site (G4). Observations are marked by red circles. The meta-models include Multiple
 Linear Regression (MLR, purple), Random Forest (RF, orange), XGBoost (XGB, light blue), Random Forest+ (RF+,
 520 hatched brown) and XGBoost+ (XGB+, hatched dark blue). The meta-models include Multiple Linear Regression
 (MLR, hatched light blue), Random Forest (RF, hatched orange), RF+ (brown) and XGBoost (XGB, hatched
 purple), and XGBoost+ (XGB+, blue). The best-performing individual models (M20¹⁹ at C2, M24³ at G4) are
 shown in black. Dates are provided in the format of dd-mm-yyyy.

525

To provide a more objective assessment, Fig. 9 presents scatterplots ~~for the validation year comparing the observations and the models~~ The figures were constructed using one validation year selected based on the performance of the XGB+ method ~~entire dataset~~. The MMM aligns more closely with the meta-models (unlike the case with RECO in Fig. 5). While this holds true for G4 as well, the correlations for the meta-models were 20-40% higher than at G3. At the crop sites (C1 and C2), the meta-models, particularly RF, RF+, XGB and XGB+, show a strong linear relationship with the observed data, explaining a large portion of the variance.

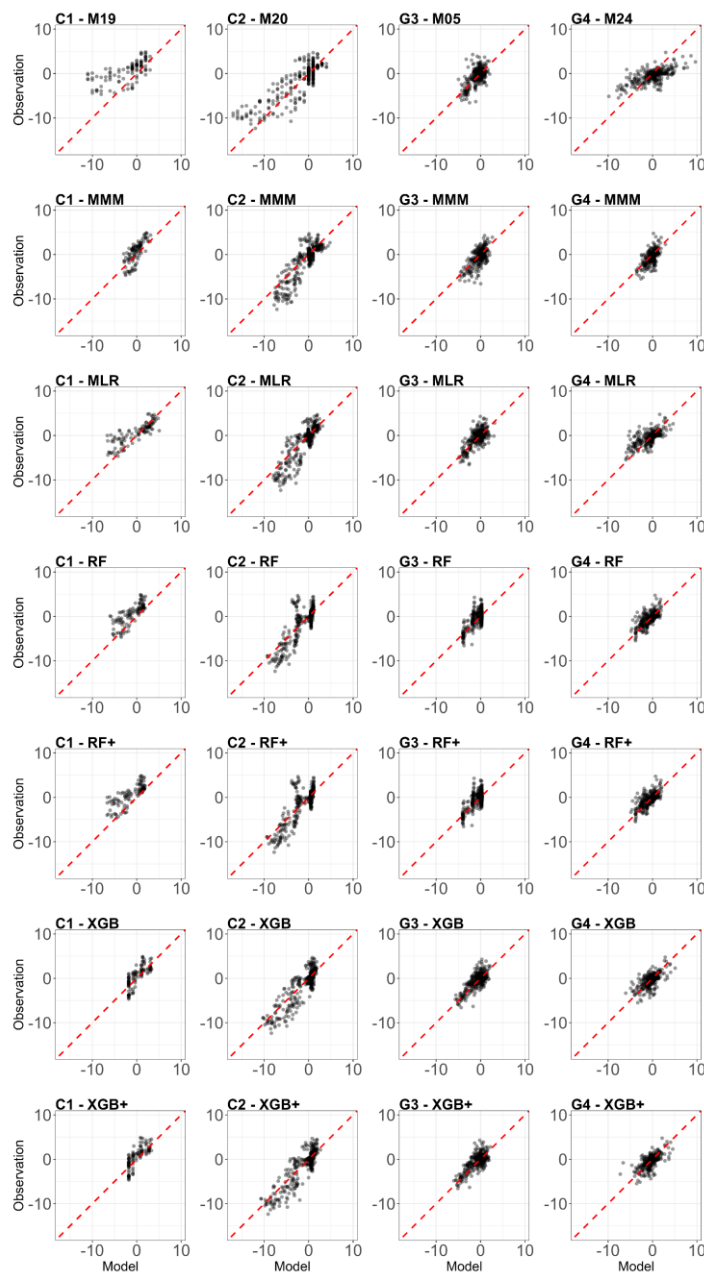


Figure 9: Comparison of the best individual model, the multi-model median and the constructed meta-models with observations for NEE using the LOYO approach. Each row represents a different model type, and columns correspond to the sites (from left to right: C1, C2, G3, and G4). The top row shows the best individual models with their identifiers (M20 at C1, M19 at C2, M22 at G3, M23 at G4). The remaining rows show the MMM, MLR, RF, RF+, XGB and XGB+. All units are in $\text{g C m}^{-2} \text{ day}^{-1}$. The red dashed line represents the 1:1 relationship.

540

Table 5: Statistical evaluation of the best-performing individual model, the multi-model median (MMM) and the applied meta-models (MLR, RF, XGB and XGB+) for NEE, based on the three validation strategies (70/30, LOYO and the RECO-GPP approach that is referred as INDEP). Three performance metrics are used: root mean square error (RMSE), bias and Pearson's correlation coefficient (r). Only validation data were used for the calculation of the statistics. RMSE and BIAS are provided in $\text{g C m}^{-2} \text{d}^{-1}$ units.

Site	Metric	<u>best base model</u>	MMM	MLR	RF	XGB	<u>RF+</u>	XGB+
C1	<u>RMSE 70/30</u>	3.87	3.06	1.77	1.78	1.81	1.71	1.89
	<u>RMSE LOYO</u>	<u>2.98</u>	<u>2.48</u>	<u>2.51</u>	<u>2.83</u>	<u>3.47</u>	<u>2.98</u>	<u>3.44</u>
	<u>RMSE INDEP</u>	<u>3.04</u>	<u>2.57</u>	<u>2.66</u>	<u>2.46</u>	<u>2.52</u>	<u>2.78</u>	<u>2.776</u>
	<u>BIAS 70/30</u>	-0.48	0.1	0.38	0.46	0.66	0.00	0.52
	<u>BIAS LOYO</u>	<u>-1.11</u>	<u>0.00</u>	<u>0.49</u>	<u>0.12</u>	<u>1.78</u>	<u>0.01</u>	<u>1.75</u>
	<u>BIAS INDEP</u>	<u>-1.15</u>	<u>-1.03</u>	<u>-1.18</u>	<u>-1.16</u>	<u>-1.21</u>	<u>-1.82</u>	<u>-1.866</u>
	<u>r 70/30</u>	0.382	0.759	0.909	0.929	0.921	0.915	0.910
	<u>r LOYO</u> ‡	<u>0.772</u>	<u>0.766</u>	<u>0.864</u>	<u>0.816</u>	<u>0.683</u>	<u>0.830</u>	<u>0.770</u>
	<u>r INDEP</u> ‡	<u>0.698</u>	<u>0.755</u>	<u>0.818</u>	<u>0.84</u>	<u>0.839</u>	<u>0.818</u>	<u>0.825</u>
C2	<u>RMSE 70/30</u>	3.98	2.29	2.15	1.42	1.48	1.76	1.44
	<u>RMSE LOYO</u>	<u>2.71</u>	<u>2.23</u>	<u>2.38</u>	<u>2.23</u>	<u>2.26</u>	<u>2.22</u>	<u>2.25</u>
	<u>RMSE INDEP</u>	<u>4.146</u>	<u>3.929</u>	<u>2.768</u>	<u>2.593</u>	<u>2.594</u>	<u>2.063</u>	<u>1.955</u>
	<u>BIAS 70/30</u>	1.03	0.4	-0.1	-0.07	-0.02	0.00	0.02
	<u>BIAS LOYO</u>	<u>0.06</u>	<u>0.48</u>	<u>-0.02</u>	<u>-0.06</u>	<u>0.01</u>	<u>-0.07</u>	<u>0.01</u>
	<u>BIAS INDEP</u>	0.35	<u>-1.2327</u>	<u>0.2658</u>	<u>0.3879</u>	<u>0.361</u>	<u>0.3986</u>	<u>0.284</u>
	<u>r 70/30</u>	0.584	0.761	0.785	0.913	0.904	0.875	0.909
	<u>r LOYO</u>	<u>0.703</u>	<u>0.789</u>	<u>0.775</u>	<u>0.793</u>	<u>0.791</u>	<u>0.791</u>	<u>0.788</u>
	<u>r INDEP</u> ‡	<u>0.601</u>	<u>0.695</u>	<u>0.705</u>	<u>0.747</u>	<u>0.746</u>	<u>0.850</u>	<u>0.865</u>
G3	<u>RMSE 70/30</u>	2.82	1.87	1.78	1.53	1.55	1.78	1.55
	<u>RMSE LOYO</u>	<u>1.89</u>	<u>1.88</u>	<u>1.82</u>	<u>1.77</u>	<u>1.77</u>	<u>1.77</u>	<u>1.76</u>
	<u>RMSE</u>	4.72	<u>2.184</u>	<u>1.884</u>	<u>1.991</u>	<u>2.0106</u>	<u>1.60</u>	<u>1.562</u>
	<u>BIAS 70/30</u>	0.44	0.31	-0.03	0.01	0.02	0.00	-0.01
	<u>BIAS LOYO</u>	<u>0.13</u>	<u>0.32</u>	<u>-0.02</u>	<u>-0.01</u>	<u>-0.03</u>	<u>-0.01</u>	<u>-0.03</u>
	<u>BIAS</u>	-2.31	<u>-0.1545</u>	<u>-0.04</u>	<u>-0.082</u>	<u>-0.0987</u>	<u>0.023</u>	<u>0.025</u>
	<u>r 70/30</u>	0.299	0.584	0.623	0.741	0.734	0.625	0.734
	<u>r LOYO</u>	<u>0.573</u>	<u>0.583</u>	<u>0.620</u>	<u>0.647</u>	<u>0.653</u>	<u>0.645</u>	<u>0.656</u>
	<u>r INDEP</u> ‡	0.270	<u>0.452</u>	<u>0.581</u>	<u>0.52</u>	<u>0.515</u>	<u>0.726</u>	<u>0.741</u>
G4	<u>RMSE 70/30</u>	2.61	2.06	1.64	1.39	1.39	1.53	1.36
	<u>RMSE LOYO</u>	<u>2.04</u>	<u>1.95</u>	<u>1.80</u>	<u>1.67</u>	<u>1.84</u>	<u>1.67</u>	<u>1.81</u>
	<u>RMSE</u>	2.13	<u>2.1329</u>	<u>1.8327</u>	<u>1.923</u>	<u>1.92</u>	<u>1.9106</u>	<u>1.868</u>
	<u>BIAS 70/30</u>	0.48	0.67	-0.03	-0.01	0.03	0.00	0.02
	<u>BIAS LOYO</u>	<u>0.20</u>	<u>0.67</u>	<u>0.05</u>	<u>0.03</u>	<u>0.13</u>	<u>0.03</u>	<u>0.12</u>
	<u>BIAS INDEP</u>	<u>0.33</u>	<u>0.2435</u>	<u>0.10097</u>	<u>-0.08</u>	<u>-0.0879</u>	<u>0.0106</u>	<u>0.005</u>
	<u>r 70/30</u>	0.435	0.653	0.751	0.829	0.829	0.758	0.836
	<u>r LOYO</u>	<u>0.718</u>	<u>0.680</u>	<u>0.737</u>	<u>0.763</u>	<u>0.702</u>	<u>0.764</u>	<u>0.705</u>
	<u>r INDEP</u> ‡	<u>0.680</u>	<u>0.511</u>	<u>0.683</u>	<u>0.621</u>	<u>0.623</u>	<u>0.663</u>	<u>0.677</u>

545

Table 57 shows statistics for all the models using three metrics based on the validation subset, for all three validation approaches (70/30, LOYO, and the NEE estimation using meta-model based RECO-GPP, abbreviated here as INDEP). Across all the four sites, the RF, RF+, XGB and XGB+ values differ little from each other in all three metrics, resulting in a similar performance, which is also visible in Fig. 8 for 70/30 strategy. The MLR meta-model is on par with these three-four meta-models, except at C2, where its performance is worse across all three metrics, making it more comparable to the MMM for 70/30 (but not for LOYO and INDEP). The best-performing individual

550

models typically have poor statistics compared to all other models. At the crop sites, they produce the worst values, with RMSE values that are, on average, 50% higher and a r value that is 36% lower than that of the MMM. At the grassland sites, the performance gap is slightly smaller, with the MMM's RMSE values being, on average, 38% better and its correlation coefficient being 41% higher than that of the best individual models. Overall, the explained variance generally correlation coefficient increased by ~15-18% in the range of 0.004-0.289 for the best-performing meta-model compared to MMM, with the most pronounced improvement observed at G43 using the INDEP strategy. Bias shows similarity to those presented for GPP and RECO, meaning that with the exception of C1 the meta-models provide results that are almost bias-free.

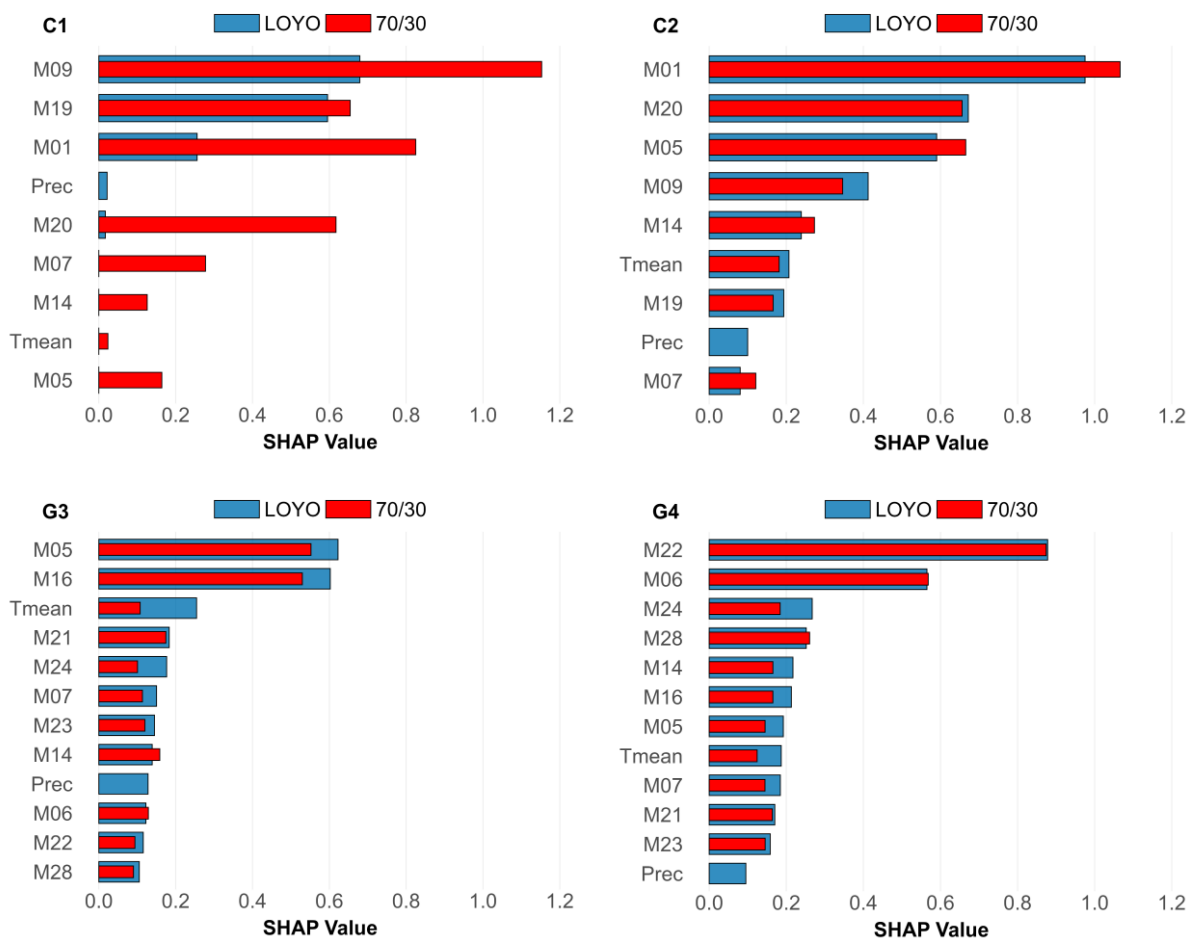


Figure 10: The SHAP values of the XGB+ meta-model for NEE based on the 70/30 strategy (red) and the LOYO strategy (blue). Larger values mean stronger contribution to the resulting NEE. Tmean stands for daily mean temperature, and Prec is daily precipitation.

SHAP analysis presented in Fig. 10 reveals that a few key model outputs primarily determine NEE predictions for the XGB+ method, just like in the case of GPP and RECO. Meteorological variables, particularly temperature and precipitation, contribute modestly but importantly, with a stronger effect noted at grassland sites G3 and G4, with larger contribution in case of LOYO.

4 Discussion

4.1 Synthesis of the meta-model approaches

~~Across all sites and flux components,~~ The stacking-based meta-models (MLR, RF, RF+, XGB, XGB+) consistently outperformed both the best individual process-based models and the traditional MMM [for sites with sufficient data coverage](#). By combining ensemble learning with key environmental covariates, [RF+ and XGB+](#) emerged as a good candidate as well, in some cases achieving lower errors and higher correlations than all other approaches. Thus, while the MMM retained its role as a robust benchmark, its predictive power was consistently surpassed by the stacking-based methods.

This aligns with findings from Shahhosseini et al. (2020, 2021), who demonstrated that ensemble learning approaches can surpass the performance of individual models for crop yield prediction, and with Zhang et al. (2022), who reported similar benefits of ensemble learning in winter wheat yield modelling. The added value of explicitly incorporating drivers such as temperature into the meta-modelling framework also supports the conclusions of Mathieu and Aires (2018), who emphasised that agro-climatic indices like temperature and precipitation can significantly enhance model accuracy. Our results go beyond these earlier studies by demonstrating that such improvements are really possible (even without incorporating meteorology) across multiple flux components (GPP, RECO, NEE) and agroecosystem types, including both croplands and grasslands.

Novelty of the study is the XGBoost and RF with environmental covariates (which means stacking with meteorological data) that represents a hybrid, regime-dependent integration framework rather than a purely statistical aggregation. This method seems to have potential that needs to be exploited in the future at sites with better temporal data coverage.

4.2 Cross-comparison of model contributions and environmental drivers for XGB+

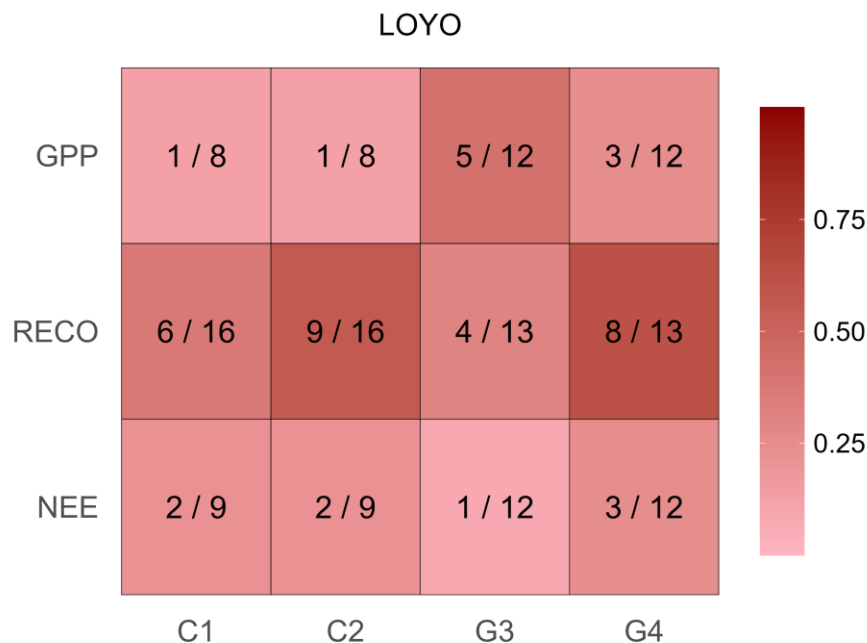
Across all three fluxes (GPP, RECO, NEE), XGB+ also heavily relies on individual model outputs, confirming that the meta-model is successfully leveraging model consensus to improve predictive performance. However, the consistent appearance of temperature - particularly at the C1 site for RECO and at grassland sites for NEE - highlights that certain temperature-driven processes are not fully captured by the base models and need to be explicitly considered. Precipitation, while generally having less impact, may still play a role in certain site-specific cases (e.g. GPP at C1), suggesting localised interactions between water availability and C fluxes. Importantly, the climate characteristics of the study sites provide important context for interpreting these results. These locations lie within mid-latitude temperate zones with well-defined seasonality, and some (e.g. Ottawa) experience high continentality, marked by large annual temperature ranges and pronounced growing season transitions. In such climates, temperature becomes the primary constraint on biological activity during both dormancy and active periods, while precipitation is often more evenly distributed or limiting only during episodic droughts (Baldocchi, 2008; Koster et al., 2004; Sun et al., 2025). This climatic backdrop helps explain why temperature consistently

605 emerges as a key predictor across sites and flux types, while precipitation plays a more site-specific and secondary role. These patterns align with broader findings from temperate ecosystems, where thermal constraints dominate respiration and photosynthesis processes, particularly outside of water-limited systems.

The dominant role of specific models in GPP predictions, supplemented by temperature's influence (Fig. 4), suggests that while ensemble model outputs capture much of the variability, temperature-dependent processes remain only
610 partially resolved by the base models. This aligns with global studies such as Zhu et al. (2016) and Bellocchi et al. (2023), who identified temperature as a key driver of GPP dynamics, especially in temperate and high-latitude ecosystems. The minimal role of precipitation in GPP prediction indicates that water availability was not a limiting factor at the examined sites, consistent with ecosystem-specific findings reported by Reichstein et al. (2013), which showed temperature or radiation often dominate in temperate regions.

615 For RECO, the strong temperature effect (Fig. 7) corroborates well-established biological principles, such as the temperature sensitivity of respiration processes described by Lloyd and Taylor (1994). The negligible role of precipitation further suggests these sites are not subject to drought stress, echoing findings from Xu et al. (2025) who highlighted thermal thresholds as primary controls over ecosystem carbon fluxes.

NEE's XGB+ related sensitivity to meteorological variables at grassland sites (Fig. 10) confirms the known climate sensitivity of these systems (Baldocchi et al., 2018). The significant influence of temperature and soil water content on GPP and RECO in grasslands, as noted by Xia et al. (2024), explains the prominence of these variables in NEE predictions. These findings underscore the importance of climate drivers in modulating carbon fluxes beyond what model ensembles alone capture.



625

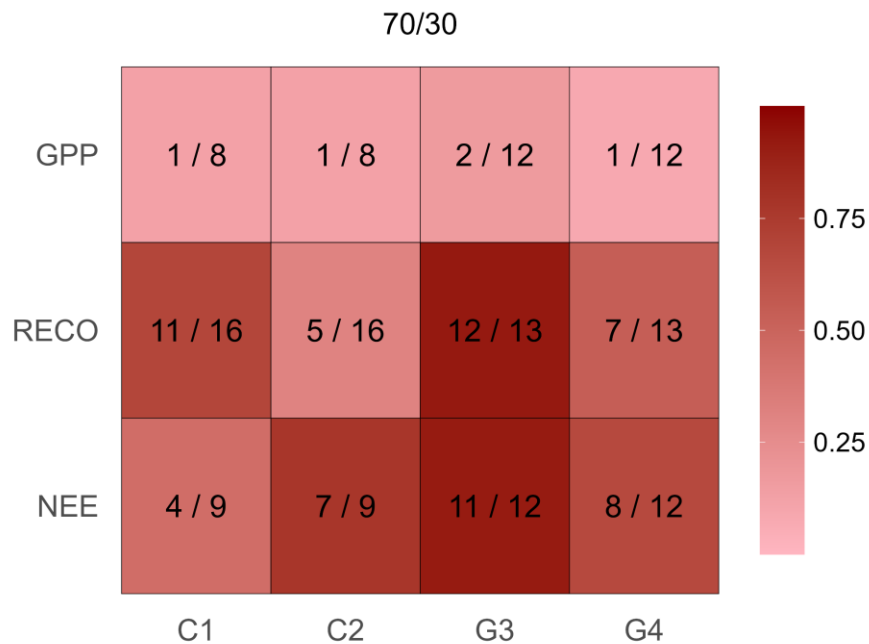


Figure 11: Ranking of the top-performing individual models (selected based on RMSE) across each site and model output based on their contribution to the XGB+ model. The first number in each cell indicates the ranking for the best model among the other models according to the SHAP value, while the second number is the total number of models. Red shades are just visual representations of the first number relative to the second indicating how important or negligible the best model's influence was.

Fig. 11 provides deeper insight into the functioning of XGB+ by ranking the influence of the top-performing process-based models (using SHAP values) for each flux and site. Several distinct patterns emerge. For RECO predictions, the influence of the highest-performing models was less prominent than for GPP~~minimal~~, particularly at site G3 for both approaches~~strategies~~, where the best model ranked only 12th out of 13. This indicates that, for RECO, the ensemble relied less on the best individual models. In contrast, for GPP, the top-performing models had a substantial impact for the crop sites across all sites, ranking first at both C1 and C2 for both the LOYO and 70/30 approach~~strategy~~. This suggests that XGB+ leveraged structurally diverse yet individually strong models to enhance predictive accuracy. For grassland sites the influence of the best models remains strong, especially for the 70/30 strategy. In case of NEE, the 70/30 approach~~strategy~~ exhibited moderate to low contributions from top-performing models - especially at grassland sites, pointing to a more balanced integration of individual models and ensemble diversity. This differs for the LOYO strategy where the top-performing individual models provide notable influence across all sites in the meta-model results.

-These findings reinforce a key principle of ensemble learning: the models with the highest standalone accuracy are not always the most influential within the ensemble. By contributing unique and non-redundant information, even structurally weaker models can significantly improve an ensemble's predictive ability. This finding, based on SHAP analysis, is consistent with the principle of ensemble diversity highlighted by Chergui and Kechadi (2022), which posits that combining a variety of models with different strengths and weaknesses leads to more robust and accurate predictions. However, our SHAP analysis adds a novel layer of interpretability by quantifying the relative influence

of top-performing versus structurally diverse models within the ensemble, providing diagnostic insights that go beyond earlier ensemble studies (Shahhosseini et al., 2020).

655 Gains in performance were more pronounced for croplands than for grasslands, especially for GPP and NEE. This aligns with previous research (Bansal et al., 2024; Nand et al., 2025) which found that management-intensive crop systems, like maize and winter wheat, benefit more from dynamic environmental and management data due to their seasonal and management-driven variability. For instance, Nand et al. (2025) demonstrated that weighted multi-model averaging, specifically the Granger-Ramanathan B method for actual evapotranspiration (ET_a), reduced RRMSE by 4–8.5% in croplands. The Granger-Ramanathan B method is a multi-model averaging approach that
660 requires non-negative weights that sum to one, and it provides the closest match to measured values for daily ET_a in maize simulations. Conversely, grasslands, characterised by more stable phenological cycles, show smaller improvements. Their flux variability is often more strongly influenced by biotic controls rather than environmental drivers alone (Reichstein et al., 2007; Stoy et al., 2013). This is because grasslands exhibit more stable, biologically mediated carbon fluxes, while the sharp seasonal transitions and management-driven dynamics of crop systems
665 make them particularly responsive to external data.

Overall, the XGB+ meta-model achieved good predictive performance across diverse agro-environmental contexts, while also providing enhanced interpretability by quantifying the contributions of individual models and environmental drivers. These dual benefits - improved performance and diagnostic insight - position XGB+ as a powerful framework for advancing predictive modelling and guiding process-model refinement.

670 **4.3 Implications and applications**

The demonstrated improvements in predictive performance of stacking-based meta-models have direct implications for crop and grassland biogeochemical modelling. By consistently outperforming both the best-performing individual models and the MMM, these approaches provide a pathway for enhancing C-flux predictions across diverse agro-environmental contexts. This is particularly relevant for applications such as greenhouse gas
675 inventorying, site-specific management planning, and scenario analysis under climate change, where reliability is critical.

Beyond performance gains, the interpretability of the meta-models offers valuable diagnostic insights for process modellers. The analysis of regression coefficients and feature contributions highlights the value of retaining structurally diverse models in ensembles, rather than limiting selection to the top-performing candidates. Moreover,
680 identifying temperature as a dominant external contributor points to opportunities for refining process-based models, such as improving their representation of phenological and temperature response mechanisms. These insights can also inform calibration practices: by quantifying the relative influence of models and drivers, the meta-modelling framework can guide targeted recalibration and prioritisation of model improvement efforts. In this way, meta-model outputs can serve as both a predictive tool and a diagnostic instrument for iterative process model development.

685 Together, these findings have broader implications for how model ensembles should be constructed and applied. Our results highlight that the traditional practice of equal-weight multi-model averaging (like with the MMM) may not be sufficient for delivering credible predictions. As noted in Section 4.4, the approach depends on long, high-quality time series for training, which may limit application in some contexts. Consistent with the arguments of Mathieu and Aires (2018), Eyring et al. (2019), Shahhosseini et al. (2020) and Chergui and Kechadi (2022), who

690 emphasised that structurally dependent and unevenly performing models require differentiated treatment, our findings demonstrate that stacking-based meta-models - combining adaptive weighting with key environmental drivers - consistently outperform both the best individual models and the MMM. This evidence calls for a paradigm shift in ensemble design: future model intercomparison and synthesis efforts should move toward performance-informed, diagnostic-driven weighting strategies that explicitly incorporate relevant covariates. Such approaches not only improve predictive accuracy but also generate actionable insights for refining underlying process-based models, ultimately accelerating progress toward more reliable and process-rich representations of agroecosystem C dynamics. This calls for coordinated action by the modelling community to adopt adaptive, performance-informed ensemble frameworks in future intercomparison efforts. Furthermore, our framework could be applied as a post-processing step to archived ensemble outputs from major multi-model initiatives (discussed in Section 5), maximising the value of existing model intercomparison investments without requiring new simulations.

4.4 Limitations and future research

While the proposed meta-modelling framework offers notable advantages, several limitations warrant acknowledgment. ~~First,~~

705 The approach depends on sufficiently long and consistent time series for training and evaluation, which were not uniformly available across all sites and flux components, limiting generalisability in data-scarce regions (e.g. C1 site). This data dependence is highlighted in Section 4.3 as a key consideration for ensemble design.

While the results indicated that the models show high temporal fidelity, spatial extrapolation to unobserved sites was not the objective of this work. This needs further investigation in forthcoming studies.

710 ~~Second,~~ Incorporating external covariates improves performance but increases complexity and introduces dependencies on auxiliary datasets that may not always be accessible or reliable. Our analysis also focused on a limited set of covariates (temperature and precipitation), leaving unexplored the potential benefits of integrating hydrological or soil-related variables. Residual analysis can potentially be used to identify site-specific environmental variables that could be included as additional covariates, of course considering the potential collinearity issues.

715 The interpretability of regression coefficients also comes with caveats: while they provide insight into model influence within the ensemble, they do not directly reveal mechanistic underpinnings, and the relationships captured remain largely empirical. Consequently, care must be taken when using these findings to inform process-level changes.

720 Future research should expand the set of environmental covariates to include soil moisture, global radiation, management practices, and hydrological variables, which are likely to improve representation of key drivers in both crops and grasslands. There is a great potential in including the same environmental variables in a more sophisticated way that can include average (or cumulative) conditions (like heat-sum) for longer time periods and also considering lagged effects using asynchronous climate data. Testing the framework across a broader range of management systems, crop types, and climatic zones would also help assess scalability and robustness. Moreover, integrating advanced interpretability tools (e.g., causal inference methods) could move beyond purely statistical associations toward more mechanistically grounded insights. Finally, co-developing meta-model frameworks with process-based

modellers could establish a feedback loop in which ensemble diagnostics directly inform iterative improvements to individual models, accelerating convergence toward more reliable, process-rich representations.

5 Conclusions

730 International initiatives that foster collaborations between researchers working on agricultural and grassland models are creating new opportunities in the field of process-oriented modelling. By gathering outputs from several models with different representations of plant and soil processes and using standardised protocols, exploitation of the potential of the ensembles becomes possible. However, those multi-model ensemble techniques are still at their infancy, as typically simple multi-model means or medians are constructed as robust estimations that typically
735 overperform the individual models. Some studies attempted to use more sophisticated methods like skill-based model selection and even machine learning, but the potential of the multi-model frameworks is still being explored. In this study, building on a previous multi-model exercise performed under the umbrella of international initiatives, new combinations of models are tested that we call here as meta-models.

The introduced meta-models significantly improved the accuracy of C-flux estimates in crop and grassland
740 ecosystems compared to individual process-based models and traditional multi-model medians. By integrating structurally diverse models and incorporating key environmental variables - particularly temperature -, these meta-models deliver not only more reliable predictions but also diagnostic insights into the relative contributions of models and environmental drivers. This underscores the importance of maintaining model diversity in ensembles and highlights opportunities to refine process-based models, especially regarding temperature responses and
745 phenological processes.

Perhaps the most important element of our modelling framework is the presentation of a method to goes beyond the static nature of meta-models. As the changing environmental conditions can alter the relevance of the base-models, the optimal meta-model may vary over time. Without the environmental variables continuous retraining is needed to maintain accuracy. Our solution is a step forward for more reliable and scientifically sound projections under
750 changing climate.

Performance gains were more pronounced in crop systems than in grasslands, likely reflecting the stronger influence of management and pronounced seasonal dynamics. Nevertheless, the approach relies on long, high-quality datasets and auxiliary covariates, and its empirical nature limits direct mechanistic interpretation. These limitations were
755 detailed in Section 4.4.

Importantly, this framework opens the door to re-analyzing outputs from major multi-model initiatives like AgMIP (Agricultural Model Intercomparison and Improvement Project; <https://agmip.org>) and MACSUR (Modelling European Agriculture with Climate Change for Food Security; <https://www.facejpi.net/en/facejpi/actions/core-theme-1/knowledge-hub-macsur.htm>). Rather than requiring new simulations, archived ensemble datasets from
760 these projects could be post-processed using stacking meta-models to enhance predictive skill and extract new diagnostic insights - maximising the value of past investments in large-scale model intercomparison. We strongly encourage international modelling communities to pilot such stacking-based re-analyses, which offer a low-cost, high-impact opportunity to unlock new insights and improve ensemble predictions.

765 While promising, this approach requires long, high-quality datasets and auxiliary inputs and remains empirical in
nature, calling for caution when inferring mechanistic causation. Future research should expand the set of
environmental drivers (e.g., soil and hydrological variables), test scalability across broader agroecosystems, and
apply advanced interpretability tools. Collaborative development with process-based modellers could translate these
statistical gains into mechanistic improvements, ultimately leading to a new generation of hybrid ensemble
770 frameworks for agricultural and grassland biogeochemistry. We encourage the international modelling communities
to pilot such stacking-based re-analyses, leveraging their rich archives to unlock new insights and improve ensemble
predictions without additional simulation costs.

Code and Data availability

775 The exact versions of the R scripts used to produce the results presented in this paper are available from the GitHub
repository: https://github.com/hollorol/metamodeling_of_c under the GPL-3 licence. The input data used to produce
the results presented in this paper is archived on the Harvard Dataverse repository under
doi:10.7910/DVN/5TO4HE.

Author contribution

780 Roland Hollós: Methodology, Conceptualization, Visualization, Writing (original draft preparation, [revised draft
preparation](#))
Nándor Zrinyi: Software, Visualization, Writing (original draft preparation, [revised draft preparation](#))
Zoltán Barcza: Methodology, Writing (original draft preparation, [revised draft preparation](#))
Gianni Bellocchi: Methodology, Writing (original draft preparation, [revised draft preparation](#)), Supervision
Renáta Sándor: Data curation, Validation
785 János Ruff: Conceptualization, Formal analysis
Nándor Fodor: Funding acquisition, Resources, Project administration, [Writing \(original draft preparation, revised
draft preparation\)](#)

Acknowledgements

790 The present article was published under the auspices of the MACSUR (Modelling European Agriculture with
Climate Change for Food Security) Science-Policy Knowledge Forum (MACSUR SciPol Pilot, June 2021-
December 2022, and MACSUR SciPolNet, May 2024–April 2026), with the support of the INRAE metaprogramme
“Climate change in agriculture and forests: Adaptation and mitigation” (CLIMAE) and INRAE’s Public Policy-
Support Directorate (DAPP). It falls within the thematic area of the French government IDEX-ISITE initiative
(reference: 16-IDEX-0001; project CAP 20-25). This work has been partly implemented by the National
795 Multidisciplinary Laboratory for Climate Change (RRF-2.3.1-21-2022-00014) project within the framework of
Hungary's National Recovery and Resilience Plan supported by the Recovery and Resilience Facility of the

European Union. This work was also supported by the National Research, Development and Innovation Office, Hungary [project ID: ADVANCED_24 150795]. Also supported by the FK 131813 project, implemented with support provided by the National Research, Development and Innovation Fund of Hungary, financed under the FK_19 funding scheme. Also supported by the TKP2021-NVA-29 project of the Hungarian National Research, Development and Innovation Fund, with the support provided by the Ministry of Culture and Innovation of Hungary. RH and ZB was Also supported by the “Advanced methods of greenhouse gases emission reduction and sequestration in agriculture and forest landscape for climate change mitigation” (CZ.02.01.01/00/22_008/0004635) project. RS, RH and GB received mobility funding from the French-Hungarian bilateral partnership through the BALATON (N° 44703TF)/TÉT (2019-2.1.11-TÉT-2019-00031) programme. Support was also provided by the TKP2021-NKTA-06 project that has been implemented with the support provided by the Ministry of Innovation and Technology of Hungary from the National Research, Development and Innovation Fund, financed under the [TKP2021-NKTA] funding scheme. Also supported by the AI4Impact programme of the Hungarian Research Network (HUN-REN). The authors are grateful to Gergő Szabó for his support.

810

References

- Anuga, S.W., Chirinda, N., Nukpezah, D., Ahenkan, A., Andrieu, N., Gordon, C.: Towards low carbon agriculture: Systematic-narratives of climate-smart agriculture mitigation potential in Africa. *Current Research in Environmental Sustainability* 2, 100015. <https://doi.org/10.1016/j.crsust.2020.100015> , 2020.
- 815 Asseng, S., Ewert, F., Rosenzweig, C., Jones, J.W., Hatfield, J.L., Ruane, A.C., Boote, K.J., Thorburn, P.J., Rötter, R.P., Cammarano, D., Brisson, N., Basso, B., Martre, P., Aggarwal, P.K., Angulo, C., Bertuzzi, P., Biernath, C., Challinor, A.J., Doltra, J., Gayler, S., Goldberg, R., Grant, R., Heng, L., Hooker, J., Hunt, L.A., Ingwersen, J., Izaurralde, R.C., Kersebaum, K.C., Müller, C., Naresh Kumar, S., Nendel, C., O’Leary, G., Olesen, J.E., Osborne, T.M., Palosuo, T., Priesack, E., Ripoche, D., Semenov, M.A., Shcherbak, I., Steduto, P., Stöckle, C., Stratonovitch, P., Streck, T., Supit, I., Tao, F., Travasso, M., Waha, K., Wallach, D., White, J.W., Williams, J.R., Wolf, J.: Uncertainty in simulating wheat yields under climate change. *Nature Climate Change* 3, 827-832. <https://doi.org/10.1038/nclimate1916>, 2013.
- 825 Bai, Y., Zhang, S., Bhattarai, N., Mallick, K., Liu, Q., Tang, L., Im, J., Guo, L., Zhang, J. : On the use of machine learning based ensemble approaches to improve evapotranspiration estimates from croplands across a wide environmental gradient. *Agricultural and Forest Meteorology* 298–299, 108308. <https://doi.org/10.1016/j.agrformet.2020.108308>, 2021.
- 830 Baldocchi, D.: ‘Breathing’ of the terrestrial biosphere: Lessons learned from a global network of carbon dioxide flux measurement systems. *Australian Journal of Botany* 56, 1–26. <https://doi.org/10.1071/BT07151>, 2008.

- Baldocchi, D., Chu, H., Reichstein, M.: Intercomparison of ten eddy covariance flux partitioning methods with a global dataset of CO₂ fluxes. *Agricultural and Forest Meteorology* 256-257, 223-233. 835 <https://doi.org/10.1016/j.agrformet.2017.05.015>, 2018.
- Bansal, Y., Lillis, D., Kechadi, M.T.: A neural meta model for predicting winter wheat crop yield. *Machine Learning* 113: 3771–3788. <https://doi.org/10.1007/s10994-023-06455-1>, 2024.
- 840 Bassu, S., Brisson, N., Durand, J.L., Boote, K.J., Lizaso, J., Jones, J.W., Rosenzweig, C., Adam, M., Basso, B., Baron, C., Basso, B., Biernath, C., Boogaard, H., Conijn, S., Corbeels, M., Deryng, D., De Sanctis, G., Gayler, S., Grassini, P., Hatfield, J., Hoek, S., Izaurralde, C., Jongschaap, R., Kemanian, A.R., Kersebaum, K.C., Kim, S.-H., Kumar, N.S., Makowski, D., Müller, C., Nendel, C., Priesack, E., Pravia, M.V., Sau, F., Shcherbak, I., Tao, F., Teixeira, E., Timlin, D., Waha, K.: How do various maize crop models vary in their responses to climate change 845 factors? *Global Change Biology* 20, 2301-2320. <https://doi.org/10.1111/gcb.12520>, 2014.
- Beer, C., Reichstein, M., Tomelleri, E., Ciais, P., Jung, M., Carvalhais, N., Rödenbeck, C., Arain, M. A., Baldocchi, D., Bonan, G. B., Bondeau, A., Cescatti, A., Lasslop, G., Lindroth, A., Lomas, M., Luysaert, S., Margolis, H., Oleson, K.W., Rouspard, O., Veenendaal, E., Viovy, N., Williams, C., Woodward, F.I., Papale, D.: Terrestrial gross 850 carbon dioxide uptake: Global distribution and covariation with climate. *Science* 329, 834–838. <https://doi.org/10.1126/science.1184984>, 2010.
- Bellocchi, G.: MACSUR SciPol Policy brief 5: Assessing Emissions and Mitigation Practices in Agriculture, towards an effective use of models for policy. Zenodo. <https://doi.org/10.5281/zenodo.8038881>, 2023. 855
- Bellocchi, G., Barcza, Z., Hollós, R., Acutis, M., Bottyán, E., Doro, L., Hidy, D., Lellei-Kovács, E., Ma, S., Minet, J., Pacskó, V., Perego, A., Ruget, F., Seddaiu, G., Wu, L., Sándor, R.: Sensitivity of simulated soil water content, evapotranspiration, gross primary production and biomass to climate change factors in Euro-Mediterranean grasslands. *Agricultural and Forest Meteorology* 343, 109778. <https://doi.org/10.1016/j.agrformet.2023.109778>, 860 2023.
- Bellocchi, G., Rivington, M., Donatelli, M., Matthews, K.: Validation of biophysical models: issues and methodologies. A review. *Agronomy for Sustainable Development* 30, 109-113. <https://doi.org/10.1051/agro/2009001>, 2010. 865
- Bilotto, F., Harrison, M.T., Migliorati, M.D.A., Christie, K.M., Rowlings, D.W., Grace, P.R., Smith, A.P., Rawnsley, R.P., Thorburn, P.J., Eckard, R.J.: Can seasonal soil N mineralisation trends be leveraged to enhance pasture growth? *Science of the Total Environment* 772:145031. <https://doi.org/10.1016/j.scitotenv.2021.145031>, 870 2021.
- Breiman, L.: Stacked regressions. *Machine Learning* 24, 123–140. <https://doi.org/10.1007/BF00058655>, 1996.

- Breiman, L.: Stacked regressions. *Machine Learning* 24, 49–64. <https://doi.org/10.1007/BF00117832>, 2001a.
- 875 Breiman, L.: Random forests. *Machine Learning* 45, 5–32. <https://doi.org/10.1023/A:1010933404324>, 2001b.
- Brilli, L., Bechini, L., Bindi, M., Carozzi, M., Cavalli, D., Conant, R., Dorich, C.D., Doro, L., Ehrhardt, F., Farina, R., Ferrise, R., Fitton, N., Francaviglia, R., Grace, P., Iocola, I., Klumpp, K., Léonard, J., Martin, R., Massad, R.S., Recous, S., Seddaiu, G., Sharp, J., Smith, P., Smith, W.N., Soussana, J-F., Bellocchi, G.: Review and analysis of strengths and weaknesses of agro-ecosystem models for simulating C and N fluxes. *Science of the Total Environ.* 598, 445-470. <https://doi.org/10.1016/j.scitotenv.2017.03.208>, 2017.
- 880
- Calanca, P., Deléglise, C., Martin, R., Carrère, P., Mosimann, E.: Testing the ability of a simple grassland model to simulate the seasonal effects of drought on herbage growth. *Field Crops Research* 187, 12-23. <https://doi.org/10.1016/j.fcr.2015.12.008>, 2016.
- 885
- Challinor, A.J., Smith, M.S., Thornton, P.: Use of agro-climate ensembles for quantifying uncertainty and informing adaptation. *Agricultural and Forest Meteorology* 170, 2-7. <https://doi.org/10.1016/j.agrformet.2012.09.007>, 2013.
- 890
- Chandel, S., Kleber, M., Jahn, R., Vogel, C.: Soil science-informed machine learning. *Geoderma* 452, 117094. <https://doi.org/10.1016/j.geoderma.2024.117094>, 2024.
- Chen, T., Guestrin, C.: XGBoost: A scalable tree boosting system. In: *KDD '16: Proceedings of the 22nd ACM SIGKDD International Conference on Knowledge Discovery and Data Mining*, pp. 785-794. <https://doi.org/10.1145/2939672.2939785>, 2016.
- 895
- Chergui, N., Kechadi, M.T.: Data analytics for crop management: a big data view. *Journal of Big Data* 9, 1-37. <https://doi.org/10.1186/s40537-022-00668-2>, 2022.
- 900
- Dietterich, T.G.: Ensemble methods in machine learning. In: *Multiple classifier systems. MCS 2000. Lecture Notes in Computer Science*, vol 1857. Springer, Berlin, Heidelberg. https://doi.org/10.1007/3-540-45014-9_1, 2000.
- Dormann, C.F., Elith, J., Bacher, S., Buchmann, C., Carl, G., Carré, G., Marquéz, J.R.G., Gruber, B., Lafourcade, B., Leitão, P.J., Münkemüller, T., McClean, C., Osborne, P.E., Reineking, B., Schröder, B., Skidmore, A.K., Zurell, D., Lautenbach, S.: Collinearity: A review of methods to deal with it and a simulation study evaluating their performance. *Ecography* 36, 27–46. <https://doi.org/10.1111/j.1600-0587.2012.07348.x>, 2013.
- 905
- Ehrhardt, F., Soussana, J-F., Bellocchi, G., Grace, P., McAuliffe, R., Recous, S., Sándor, R., Smith, P., Snow, V., Migliorati, M.D.A., Basso, B., Bhatia, A., Brilli, L., Doltra, J., Dorich, C.D., Doro, L., Fitton, N., Giacomini, S.J., Grant, B., Harrison, M.T., Jones, S.K., Kirschbaum, M.U.F., Klumpp, K., Laville, P., Léonard, J., Liebig, M., Lieffering, M., Martin, R., Massad, R.S., Meier, E., Merbold, L., Moore, A.D., Myrriotis, V., Newton, P., Pattey, E., Rolinski, S., Sharp, J., Smith, W.N., Wu, L., Zhang, Q.: Assessing uncertainties in crop and pasture ensemble
- 910

model simulations of productivity and N₂O emissions. *Global Change Biology* 24, e603-e616. <https://doi.org/10.1111/gcb.13965>, 2018.

915

Eyring, V., Cox, P.M., Flato, G.M., Friedlingstein, P., Hall, A., Hawkins, E., Hewitt, H.T., Joshi, M., Klein, S.A., Knutti, R., Meehl, G.A., O'Neill, B.C., Piani, C., Raper, S.C.B., Riahi, K., Roeckner, E., Sanderson, B.M., Wenzel, S.: Taking climate model evaluation to the next level. *Nature Climate Change* 9, 102–110. <https://doi.org/10.1038/s41558-018-0355-y>, 2019.

920

Farina, R., Sándor, R., Abdalla, M., Álvaro-Fuentes, J., Bechini, L., Bolinder, M.A., Brilli, L., Chenu, C., Clivot, H., De Antoni Migliorati, M., Di Bene, C., Dorich, C.D., Ehrhardt, F., Ferchaud, F., Fitton, N., Francaviglia, R., Franko, U., Giltrap, D.L., Grant, B.B., Guenet, B., Harrison, M.T., Kirschbaum, M.U.F., Kuka, K., Kulmala, L., Liski, J., McGrath, M.J., Meier, E., Menichetti, L., Moyano, F., Nendel, C., Recous, S., Reibold, N., Shepherd, A.,
925 Smith, W.N., Smith, P., Soussana, J.-F., Stella, T., Taghizadeh-Toosi, A., Tsutsikh, E., Bellocchi, G.: Ensemble modelling, uncertainty and robust predictions of organic carbon in long-term bare-fallow soils. *Global Change Biology* 27, 904-928. <https://doi.org/10.1111/gcb.15441>, 2021.

930

Faticchi, S., Pappas, C., Zscheischler, J., Leuzinger, S.: Modelling carbon sources and sinks in terrestrial vegetation. *New Phytologist* 221, 652-668. <https://doi.org/10.1111/nph.15451>, 2019.

935

Gascuel-Oudou, C., Lescourret, F., Dedieu, B., Detang-Dessendre, C., Favardin, P., Hazard, L., Litrico-Chiarelli, I., Petit, S., Roques, L., Reboud, X., Tixier-Boichard, M., de Vries, H., Caquet, T.: A research agenda for scaling up agroecology in European countries. *Agronomy for Sustainable Development* 42, 53. <https://doi.org/10.1007/s13593-022-00786-4>, 2022.

Granger, C.W.J., Ramanathan R.: Improved methods of combining forecasts. *Journal of Forecasting* 3:197–204. <https://doi.org/10.1002/for.3980030207>, 1984.

940

Hagedorn, R., Doblas-Reyes, F.J., Palmer, T.N.: The rationale behind the success of multi-model ensembles in seasonal forecasting – I. Basic concept. *Tellus A: Dynamic Meteorology and Oceanography* 57, 219–233. <https://doi.org/10.1111/j.1600-0870.2005.00103.x>, 2005.

945

Hansen, L.K., Salamon, P.: Neural network ensembles. *IEEE Transactions on Pattern Analysis and Machine Intelligence* 12, 993–1001. <https://doi.org/10.1109/34.58871>, 1990.

Harrison, M.T., Evans, J.R., Moore, A.D.: Using a mathematical framework to examine physiological changes in winter wheat after livestock grazing: 1. Model derivation and coefficient calibration. *Field Crops Research* 136, 116-126. <https://doi.org/10.1016/j.fcr.2012.06.015>, 2012.

950

Hengl, T., de Jesus, J.M., Heuvelink, G.B., Gonzalez, M.R., Kilibarda, M., Blagotić, A., Shangquan, W., Wright, M.N., Geng, X., Bauer-Marschallinger, B., Guevara, M.A., Vargas, R., MacMillan, R.A., Batjes, N.H., Leenaars,

- J.G.B., Ribeiro, E., Wheeler, I., Mantel, S., Kempen, B.: SoilGrids250m: Global gridded soil information based on machine learning. *PLoS ONE* 12, e0169748. <https://doi.org/10.1371/journal.pone.0169748>, 2018.
- 955 Hijmans, R.J., Cameron, S.E., Parra, J.L., Jones, P.G., Jarvis, A.: Very high-resolution interpolated climate surfaces for global land areas. *International Journal of Climatology* 25, 1965-1978. <https://doi.org/10.1002/joc.1276>, 2005.
- Hou, J., Hou, B.: Farmers' adoption of low-carbon agriculture in China: An extended theory of the planned behavior model. *Sustainability* 11, 1399. <https://doi.org/10.3390/su11051399>, 2019.
- 960 Jackson, R. B., Lajtha, K., Crow, S. E., Hugelius, G., Kramer, M. G., Rhodes, C.: The ecology of soil carbon: pools, vulnerabilities, and biotic and abiotic controls. *Annual Review of Ecology, Evolution, and Systematics* 48, 419-445. <https://doi.org/10.1146/annurev-ecolsys-112414-054234>
- 965 Janes-Bassett, V., Davies, J., Rowe, Ed C., Tipping, E., 2020. Simulating long-term carbon nitrogen and phosphorus biogeochemical cycling in agricultural environments. *Science of the Total Environment* 714, 136599. <https://doi.org/10.1016/j.scitotenv.2020.136599>, 2017.
- 970 Jones, J.W., Antle, J.M., Basso, B.O., Boote, K.J., Conant, R.T., Foster, I., Godfray, H.C.J., Herrero, M., Howitt, R.E., Janssen, S., Keating, B.A., Muñoz-Carpena, R., Porter, C.H., Rosenzweig, C., Wheeler, T.R.: Brief history of agricultural systems modelling. *Agricultural Systems* 155, 240-254. <https://doi.org/10.1016/j.agsy.2016.05.014>, 2017.
- 975 Jung, M., Vetter, M., Herold, M., Churkina, G., Reichstein, M., Zaehle, S., Ciais, P., Viovy, N., Bondeau, A., Chen, Y., Trusilova, K., Feser, F., Heimann, M.: Uncertainties of modelling gross primary productivity over Europe: A systematic study on the effects of using different drivers and terrestrial biosphere models. *Global Biogeochemical Cycles* 21, GB4021. <https://doi.org/10.1029/2006GB002915>, 2007.
- 980 Keskin, H., Grunwald, S., Basso, B.: Machine learning advances to predict crop yield for agricultural systems. *Soil Science Society of America Journal* 83, 1521-1531. <https://doi.org/10.2136/sssaj2019.06.0203>, 2019.
- Knutti, R., Baumberger, C., Hirsch Hadorn, G.: Uncertainty quantification using multiple models - prospects and challenges. In: Beisbart C., Saam N.J. (eds.) *Computer simulation validation: fundamental concepts, methodological frameworks, and philosophical perspectives*. Springer: Cham, pp. 835–855, 2019.
- 985 Kobayashi, K., Salam, M.U.: Comparing simulated and measured values using mean squared deviation and its components. *Agronomy Journal* 92, 345-352. <https://doi.org/10.2134/agronj2000.922345x>, 2000.
- 990 Kollas, C., Kersebaum, K.C., Nendel, C., Manevski, K., Müller, C., Palosuo, T., Armas-Herrera, C.M., Beaudoin, N., Bindi, M., Charfeddine, M., Conradt, T., Constantin, J., Eitzinger, J., Ewert, F., Ferrise, R., Gaiser, T., Garcia de Cortazar-Atauri, I., Giglio, L., Hlavinka, P., Hoffmann, H., Hoffmann, M.P., Launay, M., Manderscheid, R.,

- Mary, B., Mirschel, W., Moriondo, M., Olesen, J.E. Öztürk, I., Pacholski, A., Ripoche-Wachter, D., Roggero, P.P., Roncossek, S., Rötter, R.P., Ruget, F., Sharif, B., Trnkam, M., Ventrella, D., Waha, K., Wegehenkel, M., Weigel, H.-J., Wu, L.: Crop rotation modelling - A European model intercomparison. *European Journal of Agronomy* 70, 98–111. <https://doi.org/10.1016/j.eja.2015.06.007>, 2015.
- 995
- Koster, R.D., Dirmeyer, P.A., Guo, Z., Bonan, G., Chan, E., Cox, P., Gordon, C.T., Kanae, S., Kowalczyk, E., Lawrence, D., Liu, P., Lu, C.-H., Malyshev, S., McAvaney, B., Mitchell, K., Mocko, D., Oki, T., Oleson, K., Pitman, A., Sud, Y. C., Taylor, C. M., Versegny, D., Vasic, R., Xue, Y., Yamada, T.: Regions of strong coupling between soil moisture and precipitation. *Science* 305, 1138–1140. <https://doi.org/10.1126/science.1100217>, 2004.
- 1000
- Kutner, M.H., Nachtsheim, C.J., Neter, J. and Li, W.: *Applied linear statistical models*. 5th Edition, McGraw-Hill, Irwin, New York, 2005.
- 1005
- Lambin, E.F., Meyfroidt, P.: Global land use change, economic globalization, and the looming land scarcity. *Proceedings of the National Academy of Sciences* 108, 3465-3472. <https://doi.org/10.1073/pnas.1100480108>, 2011.
- Lembaid, I., Moussadek, R., Mrabet, R., Bouhaouss, A.: Modeling soil organic carbon changes under alternative climatic scenarios and soil properties using DNDC model at a semi-arid Mediterranean environment. *Climate* 10, 23. <https://doi.org/10.3390/cli10020023>, 2022.
- 1010
- Lembaid, I., Moussadek, R., Mrabet, R., Doauik, A., Bouhaouss, A.: Modeling the effects of farming management practices on soil organic carbon stock under two tillage practices in a semi-arid region, Morocco. *Heliyon*. 7, e05889. <https://doi.org/10.1016/j.heliyon.2020.e05889>, 2021.
- 1015
- Li, T., Cui, L., Kuhnert, M., McLaren, T.I., Pandey, R., Liu, H., Wang, W., Xu, Z., Xia, A., Dalal, R.C., Dang, Y.P.: A comprehensive review of soil organic carbon estimates: Integrating remote sensing and machine learning technologies. *Journal of Soils and Sediments* 24, 3556-3571. <https://doi.org/10.1007/s11368-024-03913-8>, 2015.
- 1020
- Li, C., Farahbakhshazad, N., Jaynes, D.B., Dinnes, D.L., Salas, W., McLaughlin, D.: Modeling nitrate leaching with a biogeochemical model modified based on observations in a row-crop field in Iowa. *Ecological Modelling* 196, 116-130. <https://doi.org/10.1016/j.ecolmodel.2006.02.007>, 2006.
- 1025
- Li, T., Hasegawa, T., Yin, X., Zhu, Y., Boote, K., Adam, M., Bregalio, S., Buis, S., Confalonieri, R., Fumoto T., Gaydon, D., Marcaida III, M., Nakagawa, H., Oriol, P., Ruane, A.C., Ruget, F., Balwinder-Singh, B., Singh, U., Tang, L., Tao, F., Wilkens, P., Yoshida, H., Zhang, Z., Bouman, B.: Uncertainties in predicting rice yield by current crop models under a wide range of climatic conditions. *Global Change Biology* 21, 1328–1341. <https://doi.org/10.1111/gcb.12758>, 2015.
- 1030
- Liaw, A., Wiener, M.: Classification and regression by randomForest. *R News* 2, 18-22. <http://CRAN.R-project.org/doc/Rnews>, 2002.

- 1035 Lobell, D.B., Schlenker, W., Costa-Roberts, J.: Climate trends and global crop production since 1980. *Science* 333, 616-620. <https://doi.org/10.1126/science.1204531>, 2011.
- Lloyd, J., Taylor, J.A.: On the temperature dependence of soil respiration. *Functional Ecology* 8, 315–323. <https://doi.org/10.2307/2389824>, 1994.
- 1040 Lundberg, S.M., Erion, G., Lee, S.-I.: Consistent individualized feature attribution for tree ensembles. arXiv:1802.03888. <https://doi.org/10.48550/arXiv.1802.03888>, 2020.
- Lundberg, S.M., Lee, S.-I., 2017. A unified approach to interpreting model predictions. Proceedings of the 31st International Conference on Neural Information Processing Systems, Long Beach, 4-9 December, pp. 4766-4777.
- 1045 Luo, Y., Weng, E., Wu, X., Gao, C., Zhou, X., Zhang, L.: Parameter identifiability, constraint, and equifinality in data assimilation with ecosystem models. *Ecological Applications* 19, 571-574. <https://doi.org/10.1890/08-0561.1>, 2009.
- Mangani, R., Tesfamariam, E., Engelbrecht, C.J., Bellocchi, G., Hassen, A., Mangani, T.: Potential impacts of extreme weather events in main maize (*Zea mays* L.) producing areas of South Africa under rainfed conditions. *Regional Environmental Change* 19, 1441-1452. <https://doi.org/10.1007/s10113-019-01486-8>, 2019.
- Martre, P., Wallach, D., Asseng, S., Ewert, F., Jones, J.W., Rotter, R.P., Boote, K.J., Ruane, A.C., Thorburn, P.J., Cammarano, D., Hatfield, J.L., Rosenzweig, C., Aggarwal, P.K., Angulo, C., Basso, B., Bertuzzi, P., Biernath, C., 1055 Brisson, N., Challinor, A.J., Doltra, J., Gayler, S., Goldberg, R., Grant, R.F., Heng, L., Hooker, J., Hunt, L.A., Ingwersen, J., Izaurralde, R.C., Kersebaum, K.C., Müller, C., Kumar, S.N., Nendel, C., O’leary, G., Olesen, J.E., Osborne, T.M., Palosuo, T., Priesack, E., Ripoche, D., Semenov, M.A., Shcherback, I., Steduto, P., Stöckle, C.O., Stratonovitch, P., Streck, T., Supit, I., Tao, F., Travasso, M., Waha, K., White, J.W., Wolf, J., 2015. Multimodel ensembles of wheat growth: many models are better than one. *Global Change Biology* 21, 911-925.
- 1060 Mathieu, J.A., Aires, F.: Assessment of the agro-climatic indices to improve crop yield forecasting. *Agricultural and Forest Meteorology* 253-254:15-30. <https://doi.org/10.1016/j.agrformet.2018.01.031>, 2018.
- Nand, V., Qi, Z., Ma, L., Helmers, M.J., Madramootoo, C.A., Smith, W.N., Zhang, T., Weber, T.K.D., Pattey, E., Li, Z., Wang, J., Jin, V.L., Jiang, Q., Tenuta, M., Trout, T.J., Cheng, H., Harmel, R.D., Kimball, B.A., Thorp, K.R., 1065 Boote, K.J., Stockle, C., Suyker, A.E., Evett, S.R., Brauer, D.K., Coyle, G.G., Copeland, K.S., Marek, G.W., Colaizzi, P.D., Acutis, M., Alimagham, S.M., Archontoulis, S., Babacar, F., Barcza, Z., Basso, B., Bertuzzi, P., Constantin, J., De Antoni Migliorati, M., Dumont, B., Durand, J.L., Fodor, N., Gaiser, T., Garofalo, P., Gayler, S., Giglio, L., Grant, R., Guan, K., Hoogenboom, G., Kim, S.H., Kisekka, I., Lizaso, J., Masia, S., Meng, H., Mereu, V., Mukhtar, A., Perego, A., Peng, B., Priesack, E., Shelia, V., Snyder, R., Soltani, A., Spano, D., Srivastava, A., 1070 Thomson, A., Timlin, D., Trabucco, A., Webber, H., Willaume, M., Williams, K., van der Laan, M., Ventrella, D., Viswanathan, M., Xu, X., Zhou, W.: Evaluation of multimodel averaging approaches for ensembling

- evapotranspiration and yield simulations from maize models. *Journal of Hydrology* 661: 133631. <https://doi.org/10.1016/j.jhydrol.2025.133631>, 2025.
- 1075 Olesen, J.E., Bindi, M.: Consequences of climate change for European agricultural productivity, land use and policy. *European Journal of Agronomy* 16, 239-262. [https://doi.org/10.1016/S1161-0301\(02\)00004-7](https://doi.org/10.1016/S1161-0301(02)00004-7), 2002.
- Opitz, D., Maclin, R.: Popular ensemble methods: An empirical study. *Journal of Artificial Intelligence Research* 11, 169–198. <https://doi.org/10.1613/jair.614>, 1999.
- 1080 Ostle, N.J., Smith, P., Fisher, R., Woodward, F.I., Fisher, J.B., Smith, J.U., Galbraith, D., Levy, P., Meir, P., McNamara, N.P., Bardgett, R.D.: Integrating plant–soil interactions into global carbon cycle models. *Journal of Ecology* 97, 851–863. <https://doi.org/10.1111/j.1365-2745.2009.01547.x>, 2009.
- 1085 Pappas, C., Papalexiou, S.M., Koutsoyiannis D.: A quick gap filling of missing hydrometeorological data. *Journal of Geophysical Research Atmosphere* 119, 9290–9300. <https://doi.org/10.1002/2014JD021633>, 2014.
- Raj, R., Hamm, N.A.S., van de Tol, C., Stein, A.: Uncertainty analysis of gross primary production partitioned from net ecosystem exchange measurements. *Biogeosciences* 13, 1409-1422. <https://doi.org/10.5194/bg-13-1409-2016>, 2006.
- 1090 Reichstein, M., Bahn, M., Ciais, P., Frank, D., Mahecha, M. D., Seneviratne, S. I., Zscheischler, J., Beer, C., Buchmann, N., Frank, D. C., Papale, D., Rammig, A., Smith, P., Thonicke, K., van der Velde, M., Vicca, S., Walz, A., Wattenbach, M.: Climate extremes and the carbon cycle. *Nature* 500, 287–295. <https://doi.org/10.1038/nature12350>, 2013.
- 1095 Reichstein, M., Camps-Valls, G., Stevens, B., Jung, M., Denzler, J., Carvalhais, N., Prabhat: Deep learning and process understanding for data-driven Earth system science. *Nature* 566, 195–204. <https://doi.org/10.1038/s41586-019-0912-1>, 2019.
- 1100 Riccio, G., Giunta, G., Galmarini, S.: Seeking for the rational basis of the Median Model: the optimal combination of multi-model ensemble results. *Atmospheric Chemistry and Physics* 7, 6085-6098. <https://doi.org/10.5194/acp-7-6085-2007>, 2007.
- 1105 Richter, K., Atzberger, C., Hank, T.B., Mauser, W.: Derivation of biophysical variables from Earth observation data: validation and statistical measures. *Journal of Applied Remote Sensing* 6, 063557. <https://doi.org/10.1117/1.JRS.6.063557>, 2012.
- 1110 Reichstein, M., Ciais, P., Papale, D., Valentini, R., Running, S., Viovy, N., Cramer, W., Granier, A., Ogée, J., Allard, V., Aubinet, M., Bernhofer, C., Buchmann, N., Carrara, A., Grünwald, T., Heimann, M., Heinesch, B., Knohl, A., Kutsch, W., Loustau, D., Manca, G., Matteucci, G., Miglietta, F., Ourcival, J.M., Pilegaard, K., Pumpanen, J.,

- Rambal, S., Schaphoff, S., Seufert, G., Soussana, J.-F., Sanz, M.-J., Vesala, T., Zhao, M.: Reduction of ecosystem productivity and respiration during the European summer 2003 climate anomaly: A joint flux tower, remote sensing and modelling analysis. *Global Change Biology* 13, 634-651. <https://doi.org/10.1111/j.1365-2486.2006.01224.x>, 2007.
- 1115
- Reichstein, M., Falge, E., Baldocchi, D., Papale, D., Aubinet, M., Berbigier, P., Bernhofer, C., Buchmann, N., Gilmanov, T., Granier, A., Grünwald, T., Havránková, K., Ilvesniemi, H., Janous, D., Knohl, A., Laurila, T., Lohila, A., Loustau, D., Matteucci, G., Meyers, T., Miglietta, F., Ourcival, J.-M., Pumpanen, J., Rambal, S., Rotenberg, E., 1120 Sanz, M., Tenhunen, J., Seufert, G., Vaccari, F., Vesala, T., Yakir, D., Valentini, R.: On the separation of net ecosystem exchange into assimilation and ecosystem respiration: Review and improved algorithm. *Global Change Biology* 11, 1424-1439. <https://doi.org/10.1111/j.1365-2486.2005.001002.x>, 2005.
- Robeson, S.M., Willmott, C.J.: Decomposition of the mean absolute error (MAE) into systematic and unsystematic 1125 components. *PLoS ONE* 18, e0279774. <https://doi.org/10.1371/journal.pone.0279774>, 2023.
- Rosenzweig, C., Elliott, J., Deryng, D., Ruane, A.C., Müller, C., Arneth, A., Boote, K.J., Folberth, C., Glotter, M., Khabarov, N., Neumann, K., Piontek, F., Pugh, T.A.M., Schmid, E., Stehfest, E., Yang, H., Jones, J.W.: Assessing agricultural risks of climate change in the 21st century in a global gridded crop model intercomparison. *Proceedings of the National Academy of Sciences of the United States of America* 111, 3268-3273. <https://doi.org/10.1073/pnas.1222463110>, 2014.
- 1130
- Ruane, A.C., Hudson, N.I., Asseng, S., Camarrano, D., Ewert, F., Martre, P., Boote, K.J., Thorburn, P.J., Aggarwal, P.K., Angulo, C., Basso, B., Bertuzzi, P., Biernath, C., Brisson, N., Challinor, A.J., Doltra, J., Gayler, S., Goldberg, 1135 R., Grant, R.F., Heng, L., Hooker, J., Hunt, L.A., Ingwersen, J., Izaurralde, R.C., Kersebaum, K.C., Kumar, S.N., Müller, C., Nendel, C., O'Leary, G., Olesen, J.E., Osborne, T.M., Palosuo, T., Priesack, E., Ripoche, D., Rötter, R.P., Semenov, M.A., Shcherbak, I., Steduto, P., Stöckle, C.O., Stratonovitch, P., Streck, T., Supit, I., Tao, F., Travasso, M., Waha, K., Wallach, D., White, J.W., Wolf, J.: Multi-wheat-model ensemble responses to interannual climate variability. *Environmental Modelling & Software* 81, 86-101. <https://doi.org/10.1016/j.envsoft.2016.03.008>, 2016.
- 1140
- Ruane, A.C., Rosenzweig, C., Asseng, S., Boote, K.J., Elliott, J., Ewert, F., Jones, J.W., Martre, P., McDermid, S.P., Müller, C., Snyder, A., Thorburn, P.J.: An AgMIP framework for improved agricultural representation in integrated assessment models. *Environmental Research Letters* 12, 125003. <https://doi.org/10.1088/1748-9326/aa8da6>, 2017.
- 1145
- Sagi, O., Rokach, L.: Ensemble learning: A survey. *Wiley Interdisciplinary Reviews: Data Mining and Knowledge Discovery* 8, e1249. <https://doi.org/10.1002/widm.1249>, 2018.
- Sándor, R., Barcza, Z., Acutis, M., Doro, L., Hidy, D., Köchy, M., Minet, J., Lellei-Kovács, E., Ma, S., Perego, A., 1150 Rolinski, S., Ruget, F., Sanna, M., Seddaiu, G., Wu, L., Bellocchi, G.: Multi-model simulation of soil temperature,

soil water content and biomass in Euro-Mediterranean grasslands: Uncertainties and ensemble performance. *European Journal of Agronomy* 88, 22-40. <https://doi.org/10.1016/j.eja.2016.06.006>, 2017.

1155 Sándor, R., Ehrhardt, F., Basso, B., Bellocchi, G., Bhatia, A., Brilli, L., Migliorati, M.D., Doltra, J., Dorich, C.,
Doro, L., Fitton, N., Giacomini, S.J., Grace, P., Grant, B., Harrison, M.T., Jones, S., Kirschbaum, M.U.F., Klumpp,
K., Laville, P., Léonard, J., Liebig, M., Lieffering, M., Martin, R., McAuliffe, R., Meier, E., Merbold, L., Moore,
A., Myrگیotis, V., Newton, P., Pattey, E., Recous, S., Rolinski, S., Sharp, J., Massad, R.S., Smith, P., Smith, W.,
Snow, V., Wu, L., Zhang, Q., Soussana, J.-F.: C and N models Intercomparison – benchmark and ensemble model
estimates for grassland production. *Advances in Animal Biosciences* 7, 245-247.
1160 <https://doi.org/10.1017/S2040470016000297>, 2016.

Sándor, R., Ehrhardt, F., Brilli, L., Carozzi, M., Recous, S., Smith, P., Snow, V., Soussana, J.F., Dorich, C.D., Fuchs,
K., Fitton, N., Gongadze, K., Klumpp, K., Liebig, M., Martin, R., Merbold, L., Newton, P.C.D., Rees, R.M.,
Rolinski, S., Bellocchi, G.: The use of biogeochemical models to evaluate mitigation of greenhouse gas emissions
1165 from managed grasslands. *Science of the Total Environment* 15, 292-306.
<https://doi.org/10.1016/j.scitotenv.2018.06.020>, 2018.

Sándor, R., Ehrhardt, F., Grace, P., Recous, S., Smith, P., Snow, V., Soussana, J.-F., Basso, B., Bhatia, A., Brilli,
L., Doltra, J., Dorich, C.D., Doro, L., Fitton, N., Grant, B., Harrison, M.T., Kirschbaum, M.U.F., Klumpp, K.,
1170 Laville, P., Léonard, J., Martin, R., Massad, R.S., Moore, A., Myrگیotis, V., Pattey, E., Rolinski, R., Sharp, J., Skiba,
U., Smith, W., Wu, L., Zhang, Q., Bellocchi, G.: Ensemble modelling of carbon fluxes in grasslands and croplands.
Field Crops Research 252, 107791. <https://doi.org/10.1016/j.fcr.2020.107791>, 2020.

Sándor, R., Ehrhardt, F., Grace, P., Recous, S., Smith, P., Snow, V., Soussana, J.-F., Basso, B., Bhatia, A., Brilli,
1175 L., Doltra, J., Dorich, C.D., Doro, L., Fitton, N., Grant, B., Harrison, M.T., Kirschbaum, M.U.F., Klumpp, K.,
Laville, P., Léonard, J., Martin, R., Massad, R.S., Moore, A., Myrگیotis, V., Pattey, E., Rolinski, R., Sharp, J., Skiba,
U., Smith, W., Wu, L., Zhang, Q., Bellocchi, G.: Experimental and simulated data for crop and grassland production
and carbon-nitrogen fluxes. *Open Data Journal for Agricultural Research* 24, 22-27. Available at:
<https://odjar.org/article/view/18594>, 2024.

1180 Sándor, R., Ehrhardt, F., Grace, P., Recous, S., Smith, P., Snow, V., Soussana, J.-F., Basso, B., Bhatia, A., Brilli,
L., Doltra, J., Dorich, C.D., Doro, L., Fitton, N., Grant, B., Harrison, M.T., Skiba, U., Kirschbaum, M.U.F., Klumpp,
K., Laville, P., Léonard, J., Martin, R., Massad, R.S., Moore, A., Myrگیotis, V., Pattey, E., Rolinski, R., Sharp, J.,
Smith, W., Wu, L., Zhang, Q., Bellocchi, G.: Residual correlation and ensemble modelling to improve crop and
1185 grassland models. *Environmental Modelling & Software* 161, 105625.
<https://doi.org/10.1016/j.envsoft.2023.105625>, 2023.

Schwalm, C.R., Williams, C.A., Schaefer, K., Arneth, A., Bonal, D., Buchmann, N., Chen, J., Law, B.E., Lindroth,
A., Luysaert, S., Reichstein, M., Richardson, A.D.: Assimilation exceeds respiration sensitivity to drought: A

- 1190 FLUXNET synthesis. *Global Change Biology* 16, 657–670. <https://doi.org/10.1111/j.1365-2486.2009.01991.x>, 2010.
- Scowen, M., Athanasiadis, I. N., Bullock, J. M., Eigenbrod, F., Willcock, S.: The current and future uses of machine learning in ecosystem service research. *Science of the Total Environment* 799, 149263. 1195 <https://doi.org/10.1016/j.scitotenv.2021.14926>, 2021.
- Shahhosseini, M., Hu, G., Archontoulis, S.V.: Forecasting corn yield with machine learning ensembles. *Frontiers in Plant Science* 11, 1120. <https://doi.org/10.3389/fpls.2020.01120>, 2020.
- 1200 Shahhosseini, M., Hu, G., Huber, I., Archontoulis, S.V.: Coupling machine learning and crop modeling improves crop yield prediction in the US Corn Belt. *Scientific Reports* 11, 1606. <https://doi.org/10.1038/s41598-020-80820-1>, 2021.
- Shapley, L.S.: A value for n-person games. In: Kuhn H.W., Tucker A.W. (eds.), *Contributions to the theory of games II* (Vol. 28, pp. 307–317). Princeton University Press. 1953. 1205
- Smith, P., House, J.I., Bustamante, M., Sobocká, J., Harper, R., Pan, G., West, P.C., Clark, J.M., Adhya, T., Rumpel, C., Paustian, K., Kuikman, P., Cotrufo, M.F., Elliott, J.A., McDowell, R., Griffiths, R.I., Asakawa, S., Bondeau, A., Jain, A.K., Meersmans, J., Pugh, T.A.M.: Global change pressures on soils from land use and management. *Global Change Biology* 22, 1008-1028. <https://doi.org/10.1111/gcb.13068>, 2016. 1210
- Snow, V., Rotz, C.A., Moore, A.D., Martin-Clouaire, R., Johnson, I.R., Hutchings, N.J., Eckard, R.J.: The challenges - and some solutions - to process-based modelling of grazed agricultural systems. *Environmental Modelling & Software* 62, 420-436. <https://doi.org/10.1016/j.envsoft.2014.03.009>, 2014. 1215
- Sroufe, R., Watts, A., 2022. Pathways to agricultural decarbonization: Climate change obstacles and opportunities in the US. *Resources, Conservation and Recycling* 182, 106276. <https://doi.org/10.1016/j.resconrec.2022.106276>
- 1220 Stoy, P.C., Mauder, M., Foken, T., Marcolla, B., Boegh, E., Ibrom, A., Arain, M.A., Arneth, A., Aurela, M., Bernhofer, C., Cescatti, A., Dellwik, E., Duce, P., Gianelle, D., van Gorsel, E., Kiely, G., Knohl, A., Margolis, H., McCaughey, H., Merbold, L., Montagnani, L., Papale, D., Reichstein, M., Saunders, M., Serrano-Ortiz, P., Sottocornola, M., Spano, D., Vaccari, F., Varlagin, A.: A data-driven analysis of energy balance closure across FLUXNET research sites: The role of landscape scale heterogeneity. *Agricultural and Forest Meteorology* 171-172, 137-152. <https://doi.org/10.1016/j.agrformet.2012.11.004>, 2013. 1225
- Strobl, C., Boulesteix, A. L., Zeileis, A., Hothorn, T.: Bias in random forest variable importance measures: Illustrations, sources and a solution. *BMC Bioinformatics* 8, 25. <https://doi.org/10.1186/1471-2105-8-25>, 2007.

- 1230 Sun, W., Zhou, S., Yu, B., Zhang, Y., Keenan, T.F., Fu, B.: Soil moisture-atmosphere interactions drive terrestrial carbon-water trade-offs. *Communications Earth & Environment* 6, 169. <https://doi.org/10.1038/s43247-025-02145-z>, 2025.
- 1235 Therond, O., Hengsdijk, H., Casellas, E., Wallach, D., Adam, M., Belhouchette, H., Oomen, R., Russell, G., Ewert, F., Bergez, J.-E., Janssen, S., Wery, J., van Ittersum, M.K.: Using a cropping system model at regional scale: low-data approaches for crop management information and model calibration. *Agriculture, Ecosystems & Environment* 142, 85-94. <https://doi.org/10.1016/j.agee.2010.05.007>, 2011.
- 1240 Thornton, P.K., Whitbread, A., Baedeker, T., Cairns, J., Claessens, L., Beethgen, W., Bunn, C., Friedmann, M., Giller, K.E., Herrero, M., Howden, M., Kilcline, K., Nangia, V., Ramirez-Villegas, J., Kumar, S., West, P.C., Keating, B.: A framework for priority-setting in climate smart agriculture research. *Agricultural Systems* 167, 161-175. <https://doi.org/10.1016/j.agsy.2018.09.009>, 2018.
- 1245 Valin, H., Havlik, P., Mosnier, A., Herrero, M., Schmid, E., Obersteiner, M.: Agricultural productivity and greenhouse gas emissions: trade-offs or synergies between mitigation and food security? *Environmental Research Letters* 8, 035019. <https://doi.org/10.1088/1748-9326/8/3/035019>, 2013
- Van der Laan, M.J., Polley, E.C., Hubbard, A.E.: Super learner. *Statistical Applications in Genetics and Molecular Biology* 6, 25. <https://doi.org/10.2202/1544-6115.1309>, 2007.
- 1250 Van der Velde, M., Tubiello, F.N., Vrieling, A., Bouraoui, F.: Impacts of extreme weather on wheat and maize in France: Evaluating regional crop simulations against observed data. *Climatic Change* 123, 699–711. <https://doi.org/10.1007/s10584-011-0368-2>, 2014.
- 1255 Wallach, D., Martre, P., Liu, B., Asseng, S., Ewert, F., Thonburn, P.J., van Ittersum, M., Aggarwal, P.K., Ahmed, M., Basso, B., Biernath, C., Cammarano, D., Challinor, A.J., De Sanctis, G., Dumont, B., Rezaei, E.E., Fereres, E., Fitzgerald, G.J., Gao, Y., Garcia-Vila, M., Gayler, S., Girousse, C., Hoogenboom, G., Horan, H., Izaurralde, R.C., Jones, C.D., Kassie, B.T., Kersebaum, K.C., Klein, C., Koehler, A.-K., Maiorano, A., Minoli, S., Müller, C., Kumar, S.N., Nendel, C., O’Leary, G.J., Palosuo, T., Priesack, E., Ripoche, D., Rötten, R.P., Semenov, M.A., Stöckle, C., Stratonovitch, P., Streck, T., Supit, I., Fao, F., Wolf, J., Zhang, Z.: Multi-model ensembles improve predictions of crop-environment-management interactions. *Global Change Biology* 24, 5072-5083. <https://doi.org/10.1111/gcb.14411>, 2018.
- 1265 Wang, Z., Liu, Z., Huang, M.: NDVI joint process-based models drive a learning ensemble model for accurately estimating cropland net primary productivity (NPP). *Frontiers in Environmental Science* 11, 1304400. <https://doi.org/10.3389/fenvs.2023.1304400>, 2024.
- Wolpert, D.H., Macready, W.G.: Coevolutionary free lunches. *IEEE Transactions on Evolutionary Computation* 9, 721–35. <https://doi.org/10.1109/TEVC.2005.856205>, 2005.

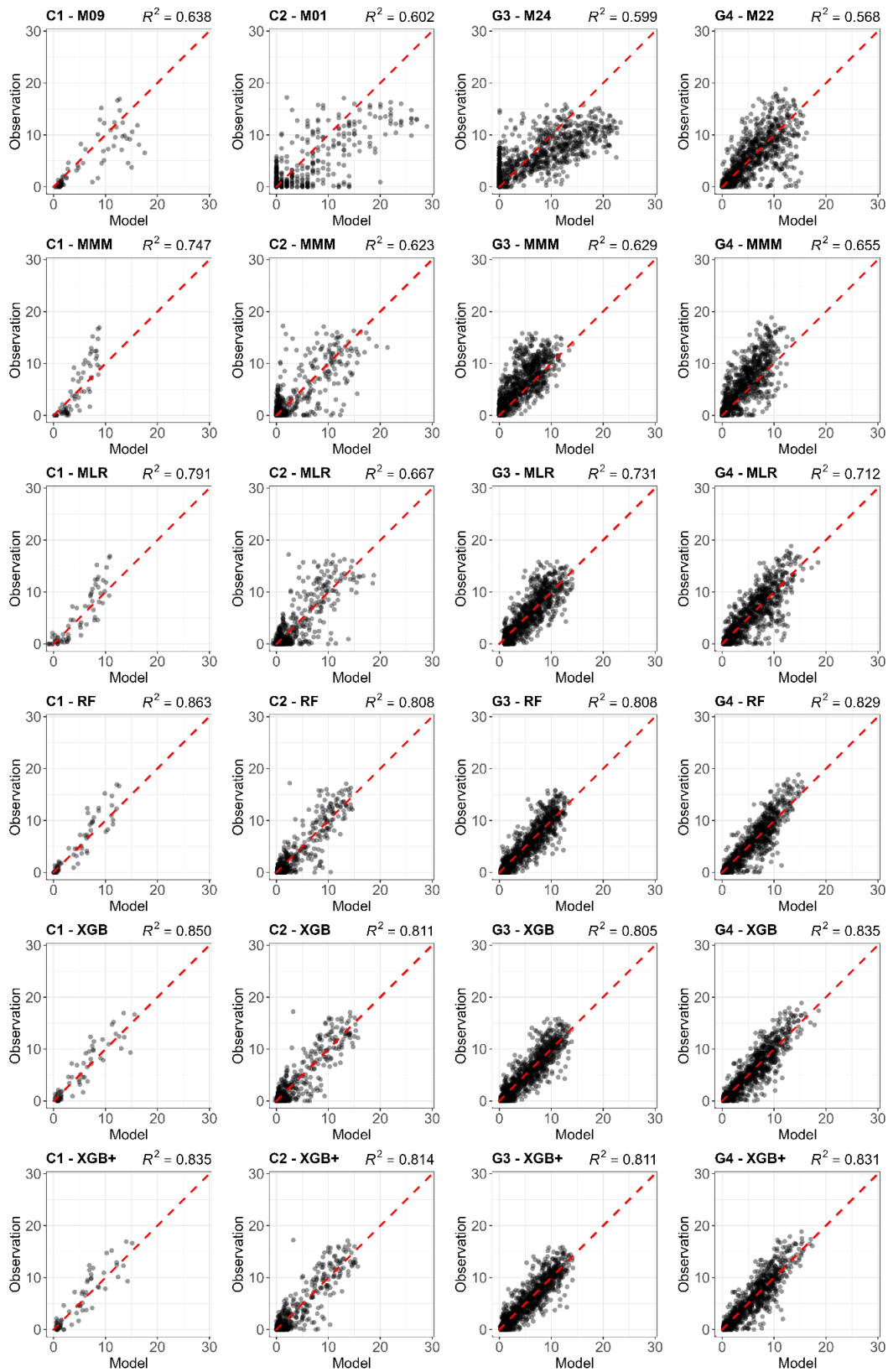
- 1270 Xia, J., Chen, T., Zhang, K., Wang, Y., Chen, G.: Impacts of climate extremes on carbon fluxes and their underlying mechanisms in a typical temperate grassland ecosystem. *Science of the Total Environment* 907, 167755. <https://doi.org/10.1016/j.scitotenv.2023.167755>, 2024.
- Xu, L., Baldocchi, D.D.: Seasonal variation in carbon dioxide exchange over a Mediterranean annual grassland in
1275 California. *Agricultural and Forest Meteorology* 123, 79–96. <https://doi.org/10.1016/j.agrformet.2003.10.004>, 2004.
- Xu, X., Xu, J., Li, B., Li, J., Nie, M.: Ecosystem carbon fluxes exhibit thermal response thresholds at which carbon–climate feedback changes. *Global Ecology and Biogeography* 34, e70030. <https://doi.org/10.1111/geb.70030>, 2025.
- 1280 Zhang, J., Tian, H., Wang, P., Tansey, K., Zhang, S., Li, H.: Improving wheat yield estimates using data augmentation models and remotely sensed biophysical indices within deep neural networks in the Guanzhong Plain, PR China. *Computers and Electronics in Agriculture* 192, 106616. <https://doi.org/10.1016/j.compag.2021.106616>,
| 2022.
- 1285 [Zhu, Z., Piao, S., Myneni, R.B., Huang, M., Zeng, Z., Canadell, J. G., Ciais, P., Sitch, S., Friedlingstein, P., Arneeth, A., Cao, C., Cheng, L., Kato, E., Koven, C., Li, Y., Lian, X., Liu, Y., Liu, R., Mao, J., Pan, Y., Peng, S., Peñuelas, J., Poulter, B., Pugh, T.A.M., Stocker, B. D., Viogy, N., Wang, X., Wang, Y., Xiao, Z., Yang, H., Zaehle, S., Zeng, N.: Greening of the Earth and its drivers. *Nature Climate Change* 6, 791–795. <https://doi.org/10.1038/nclimate3004>,
\[2016\]\(https://doi.org/10.1038/nclimate3004\).](https://doi.org/10.1038/nclimate3004)
- 1290

1295

Appendix A

1300

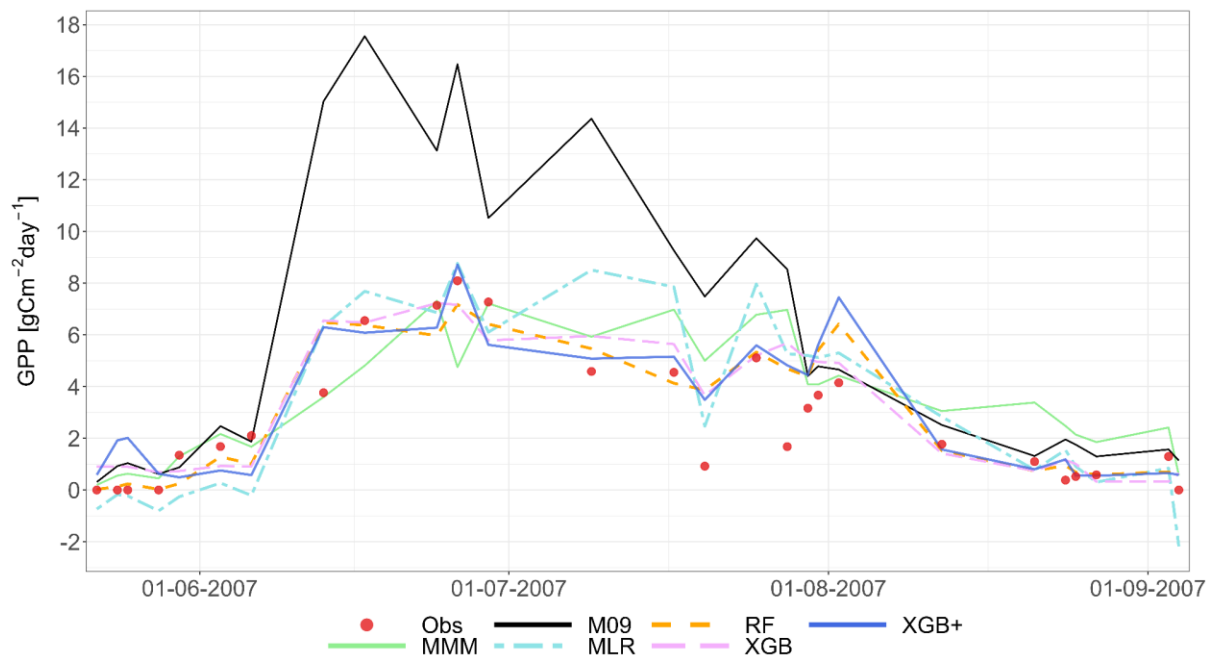
The following figures demonstrate the simulated fluxes of GPP, RECO and NEE for all sites and years included in the study, except those that are presented in the main text. Graphs are presented with a very short caption only containing: flux type, site name and type, covered years. See the main text for explanations.



1305

Figure A1: Comparison of the best individual model, the constructed meta-models and the traditional Multi-Model Median with the observations for all sites (from left to right C1, C2, G3 and G4) and for the entire time series for GPP based on the 70/30 approach. From top to bottom: best individual model with ID, MMM, MLR, RF, RF+, XGB and XGB+. All units are in $\text{g C m}^{-2} \text{ day}^{-1}$. Red dashed line represents the 1:1 relationship.

1310



1315

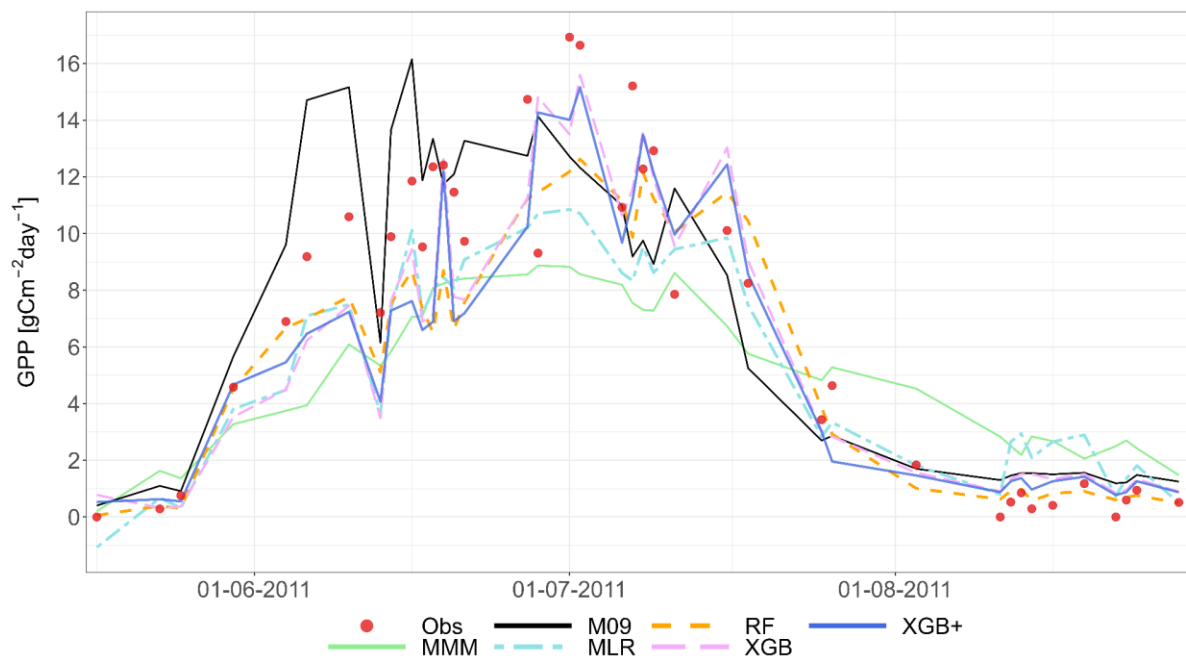


Figure A2: GPP, C1 - Ottawa (CA), cropland, 2007 and 2011, 70/30 strategy.

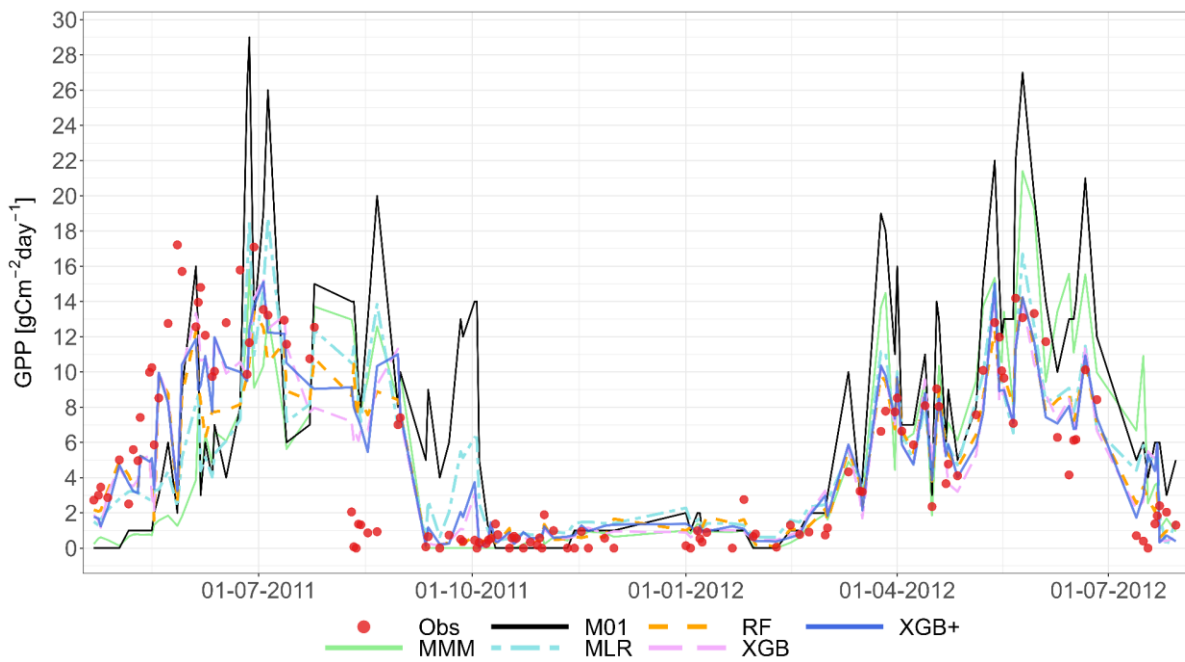
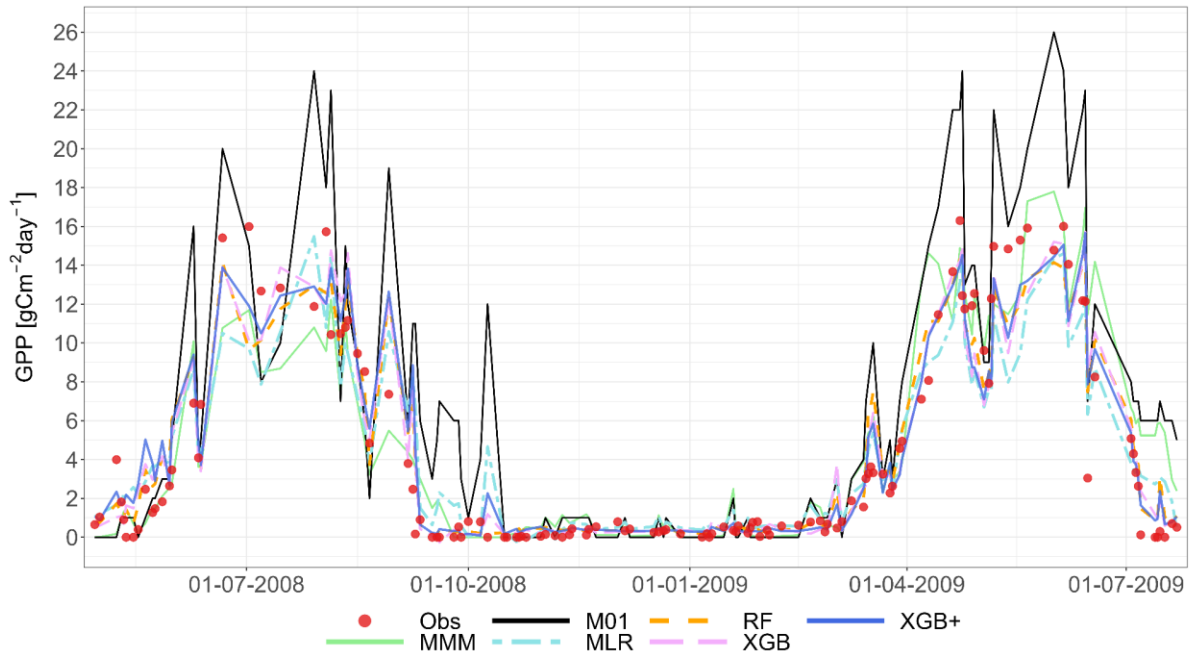
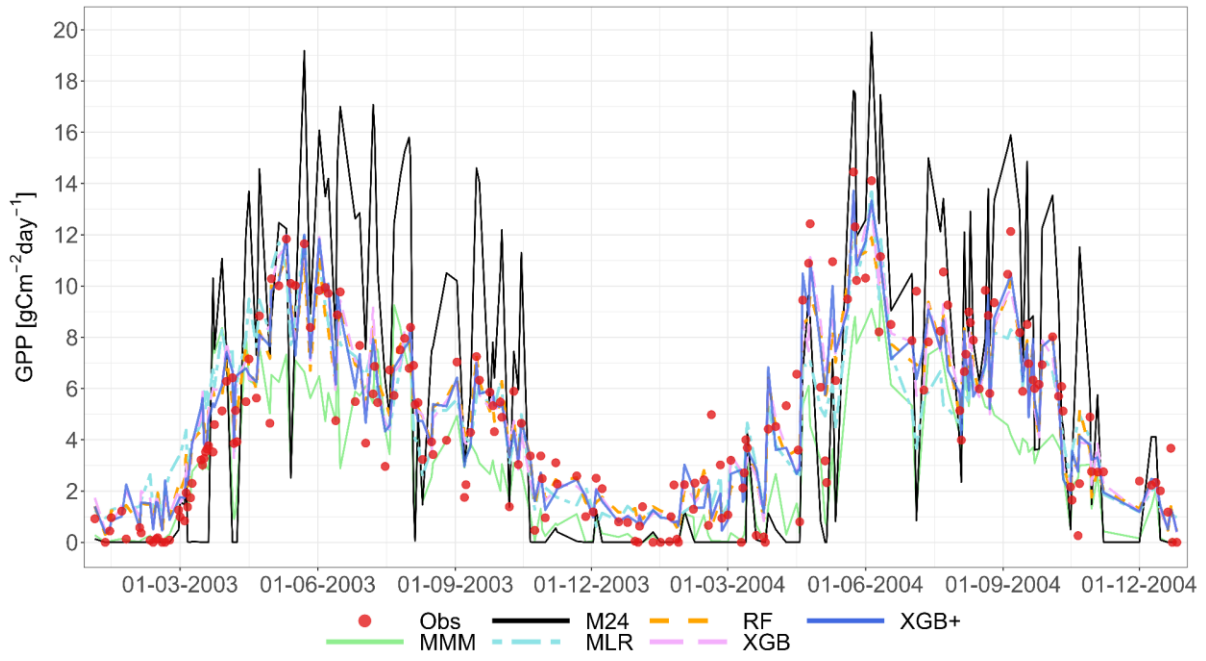
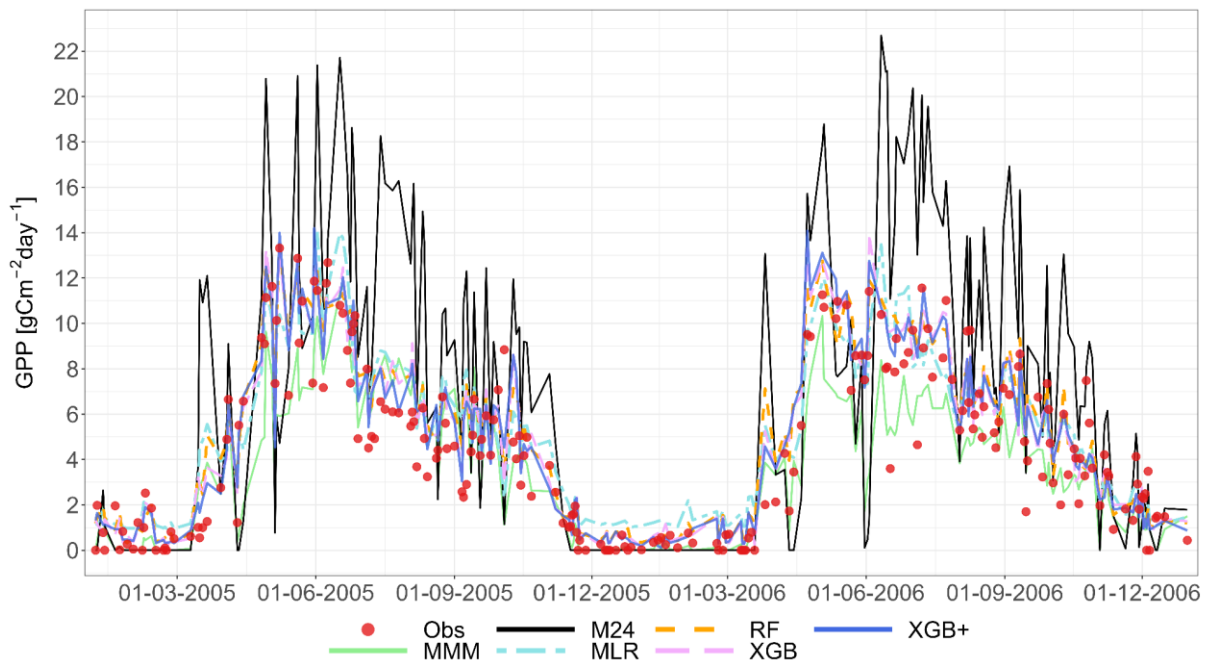
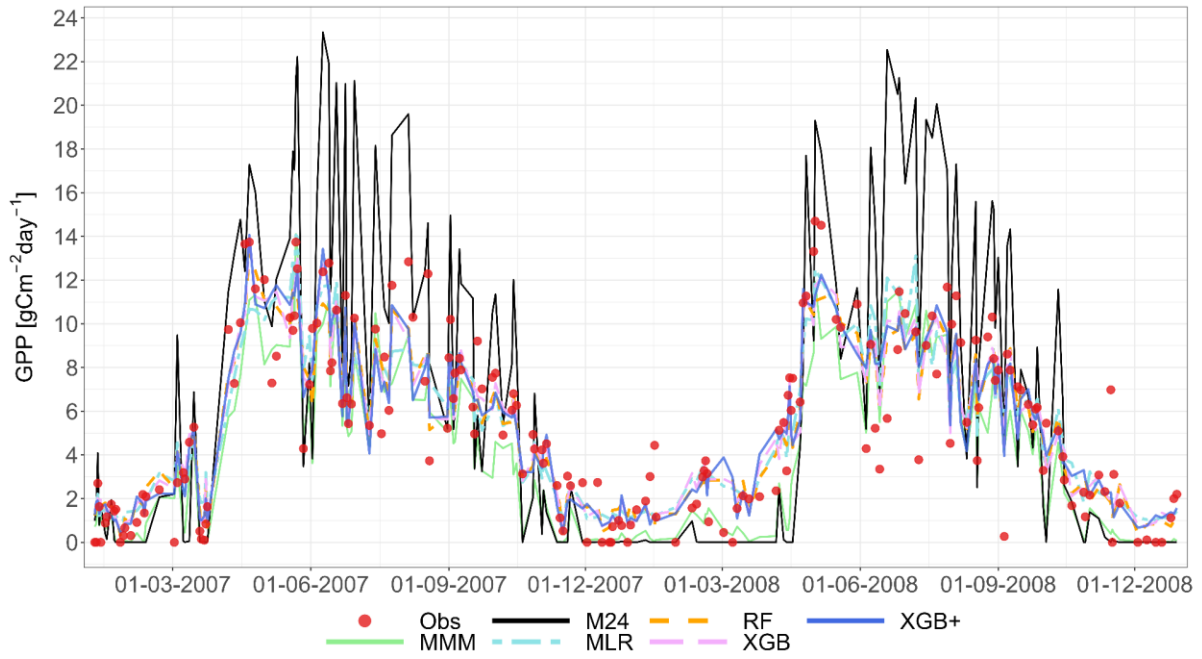


Figure A3: GPP, C2 - Grignon, (FR), cropland, 2008, 2009, 2011 and 2012, 70/30 strategy.



1330





1335

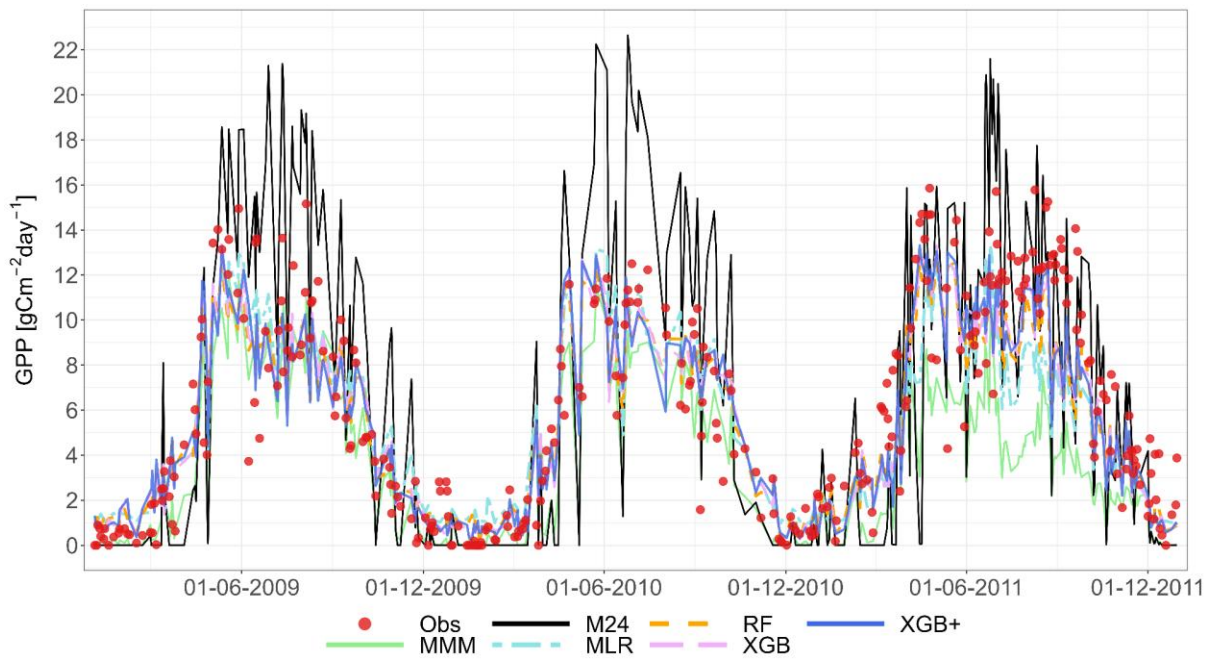
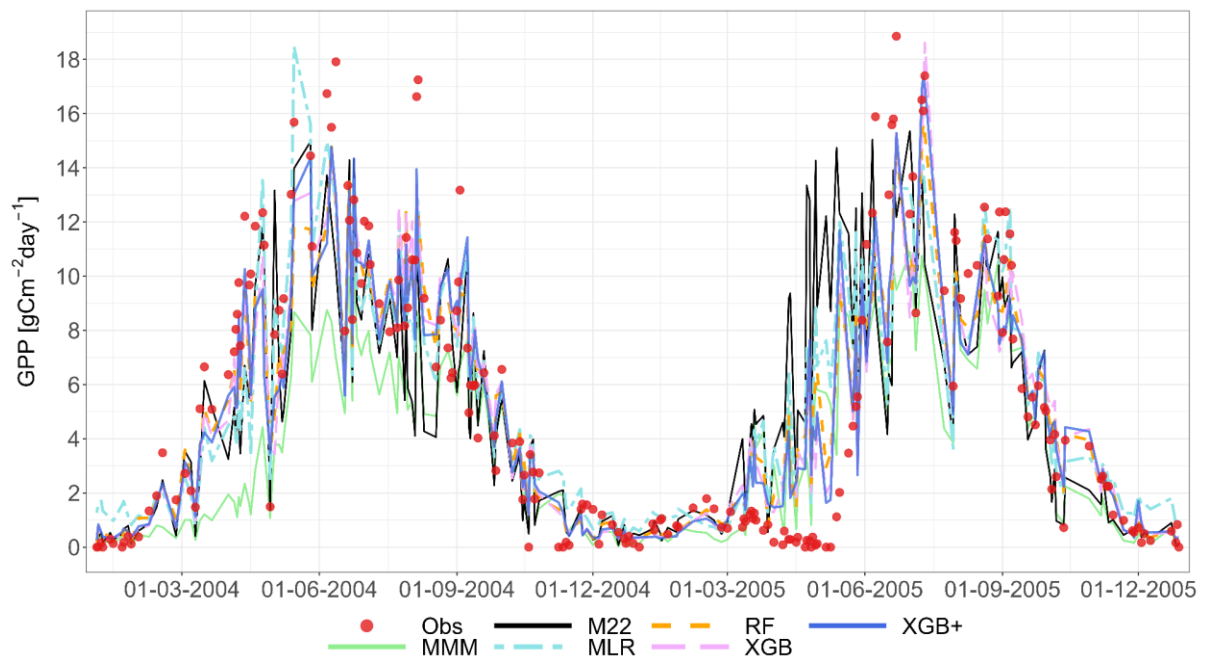
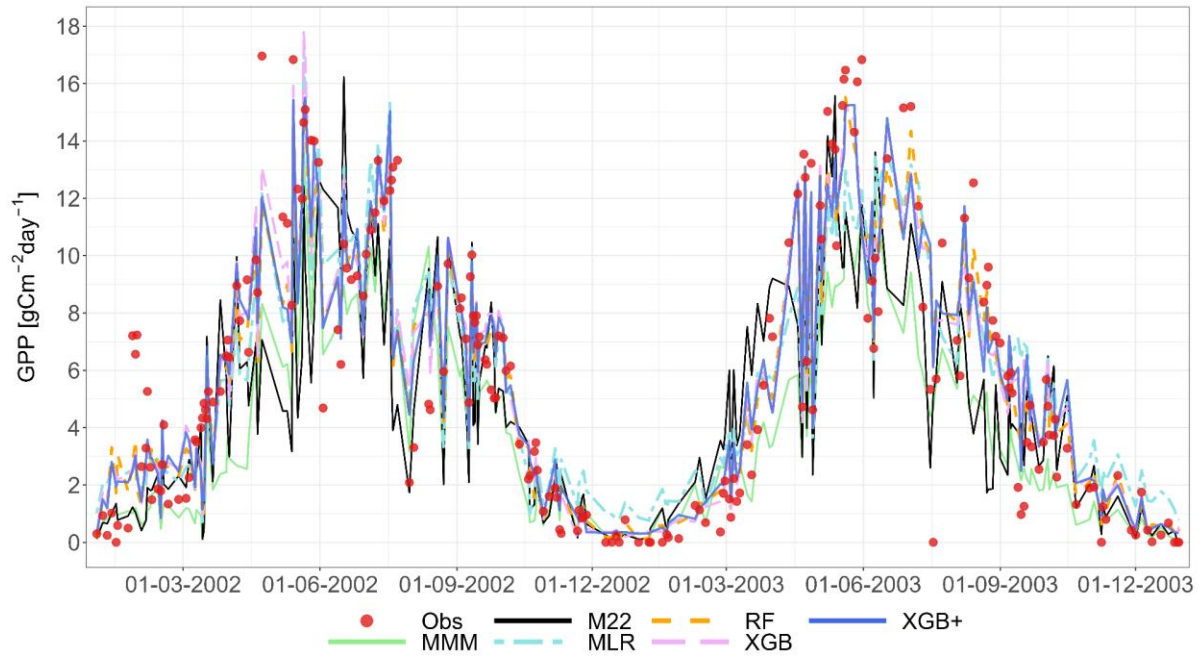
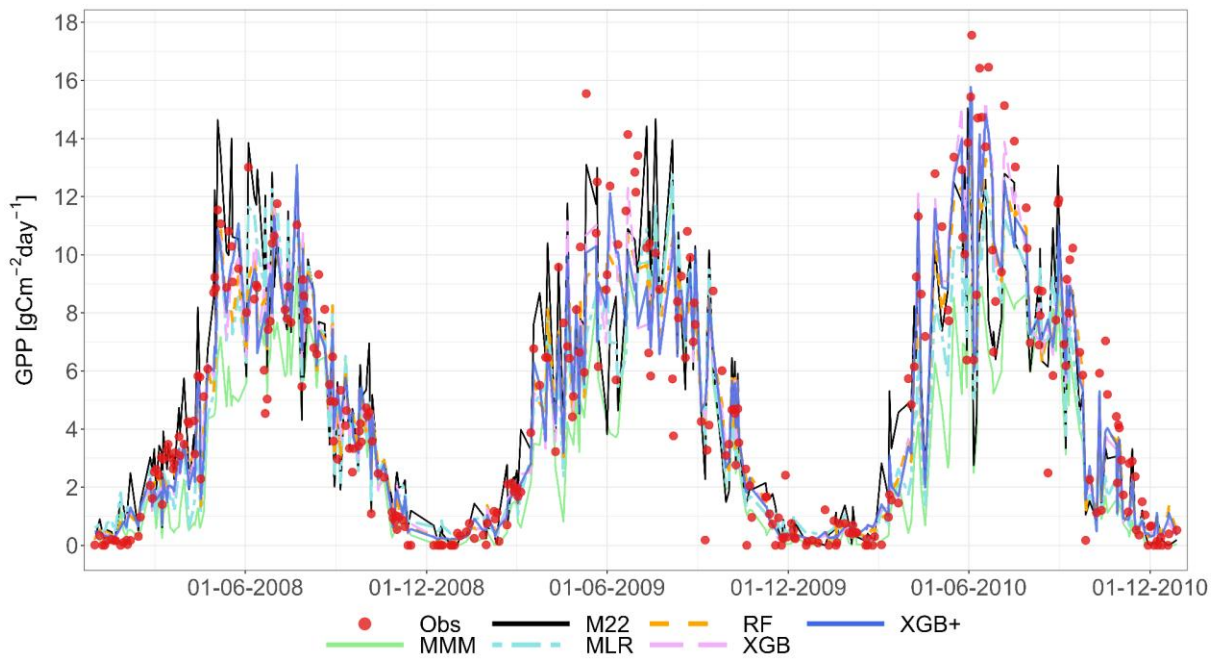
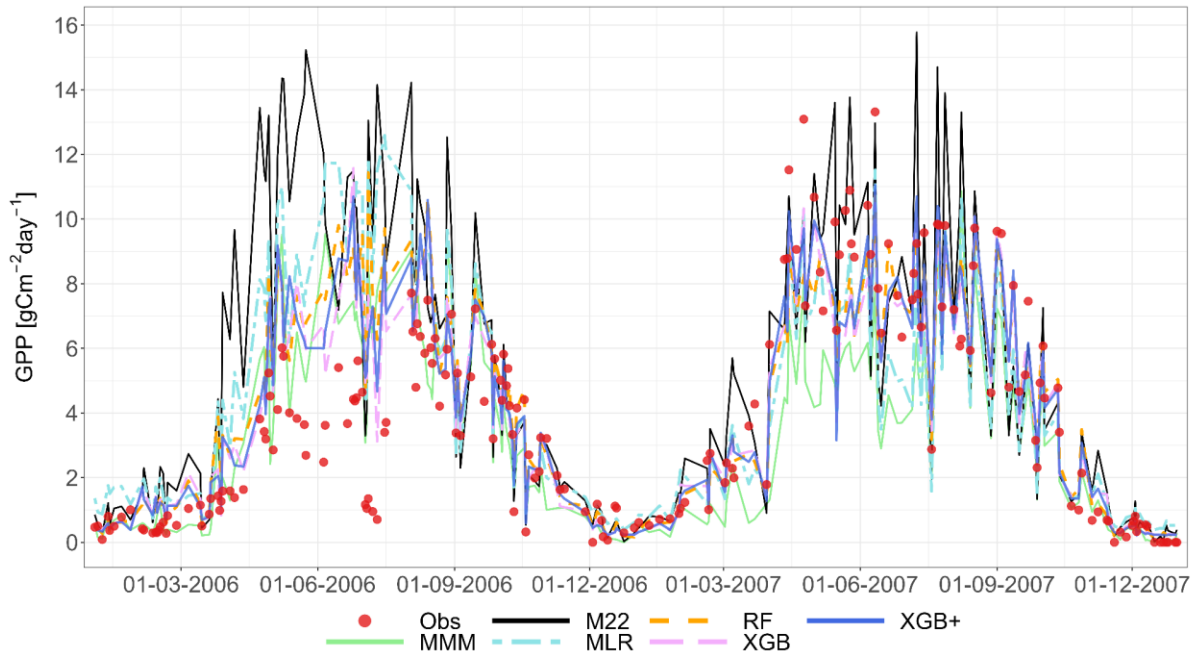


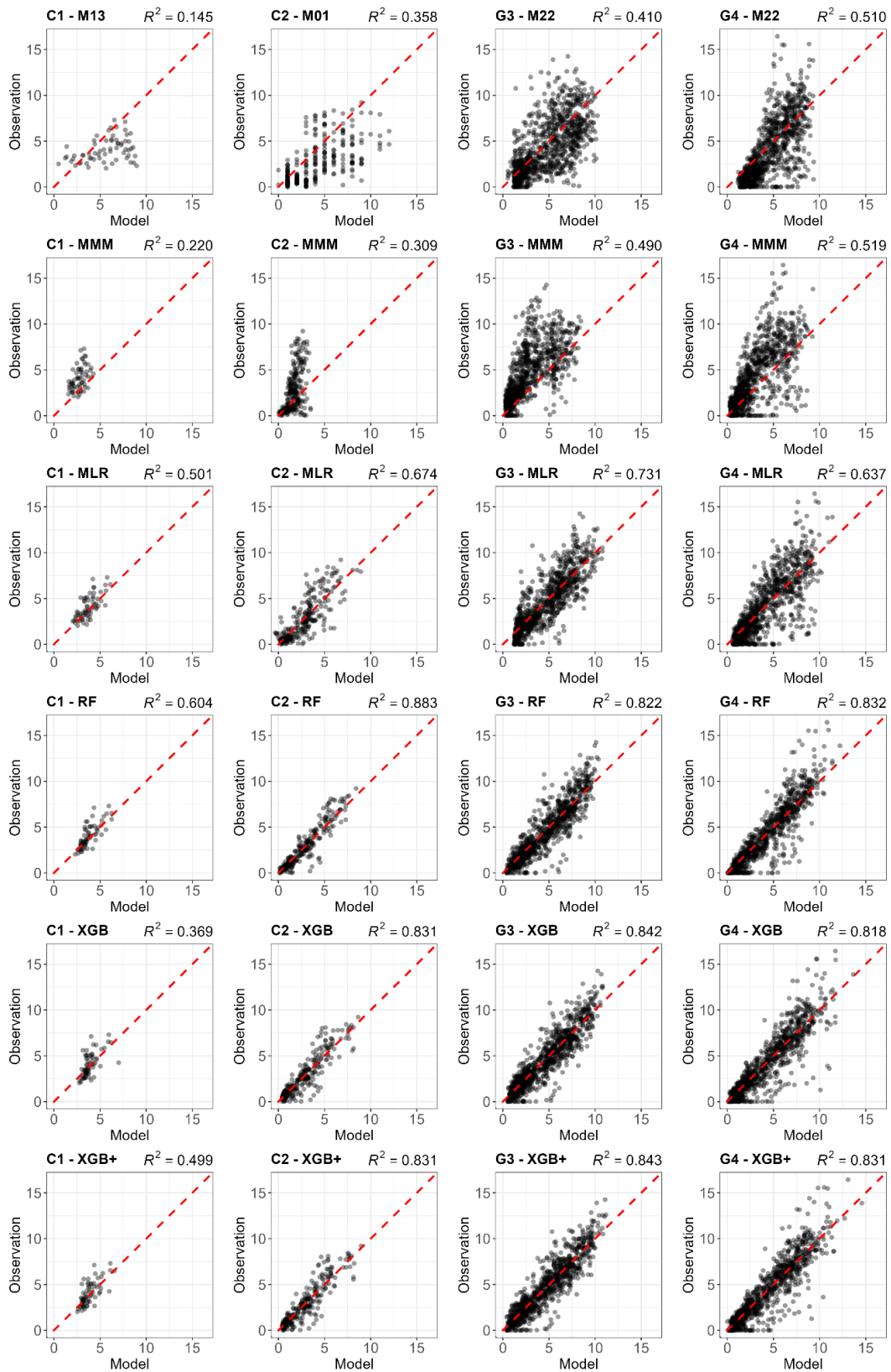
Figure A4: GPP, G3 - Laqueuille (FR), grassland, 2003-2011, 70/30 strategy.





1350

Figure A5: GPP, G4 - Easter Bush (UK), grassland, 70/30 strategy.



1355 **Figure A6:** Comparison of the best individual model, the multi-model median and the constructed meta-models with observations for RECO based on the 70/30 approach. Each row represents a different model type, and columns correspond to the sites (from left to right: C1, C2, G3, and G4). The top row shows the best individual models with their identifiers (M13 at C1, M01 at C2, M22 at G3 and G4). The remaining rows show the MMM, MLR, RF, XGB and XGB+. All units are in $\text{g C m}^{-2} \text{day}^{-1}$. The red dashed line represents the 1:1 relationship.

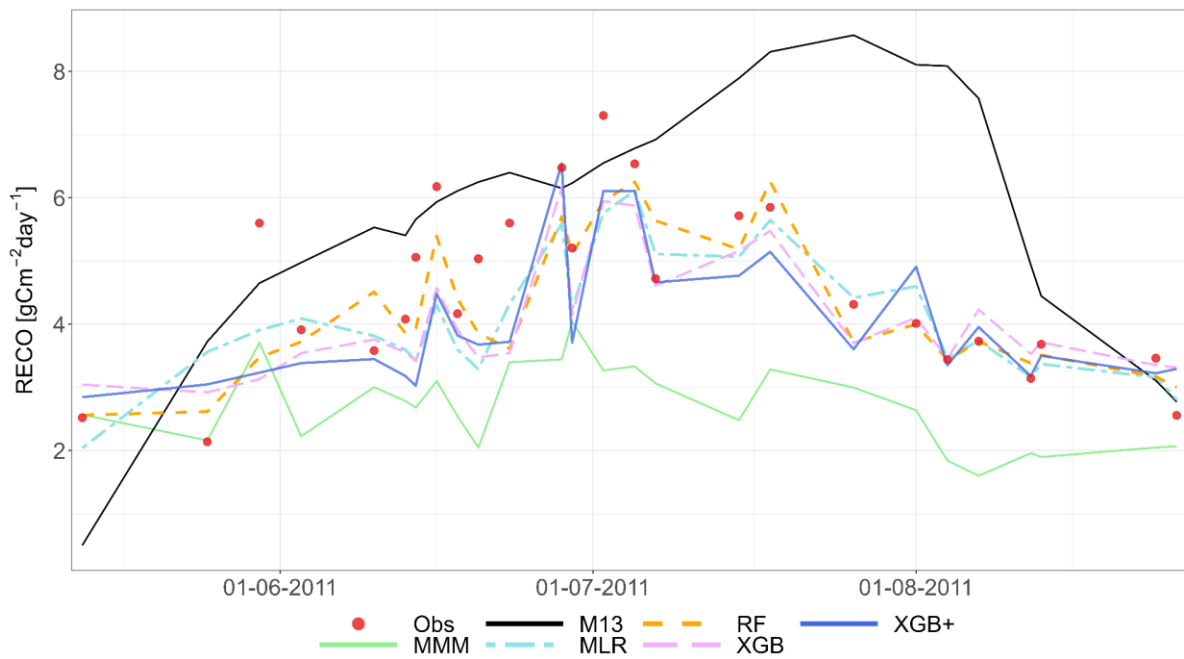
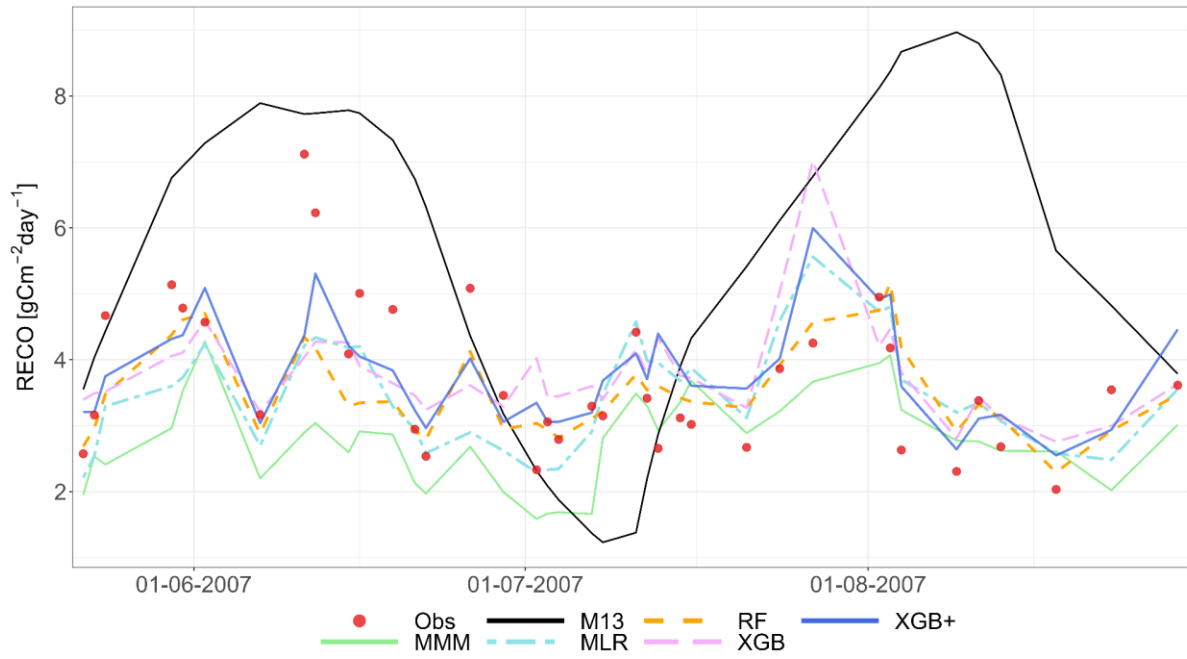
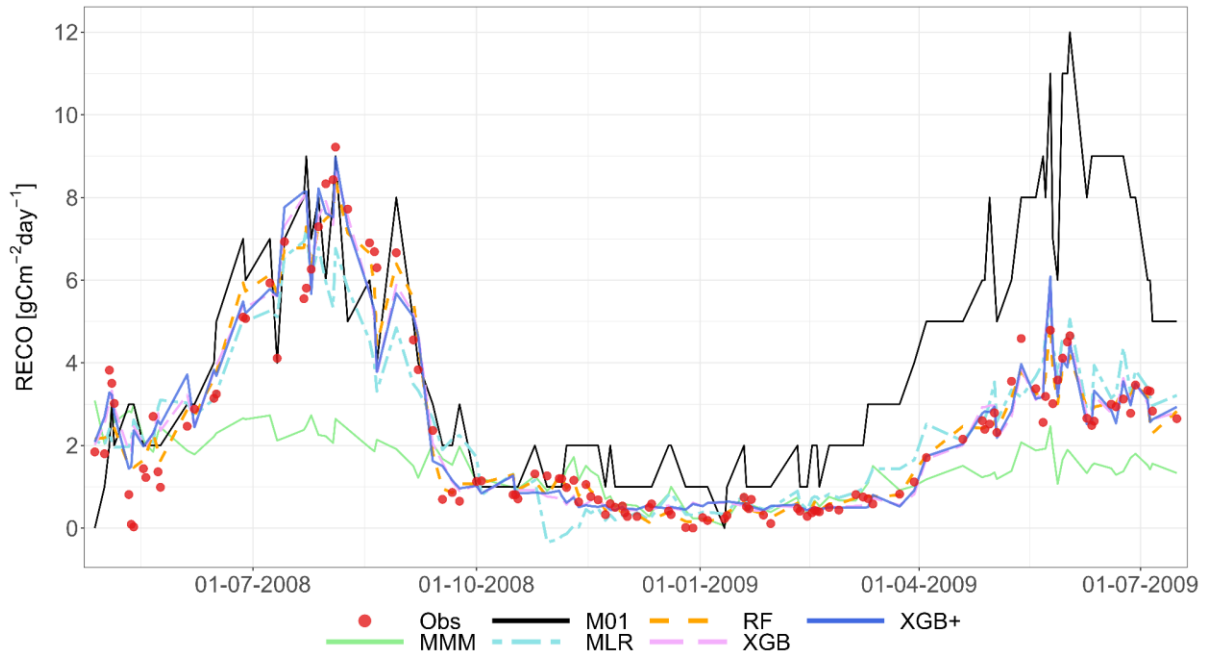


Figure A7: RECO, C1 - Ottawa (CA), cropland, 2007 and 2011, 70/30 strategy.



1370

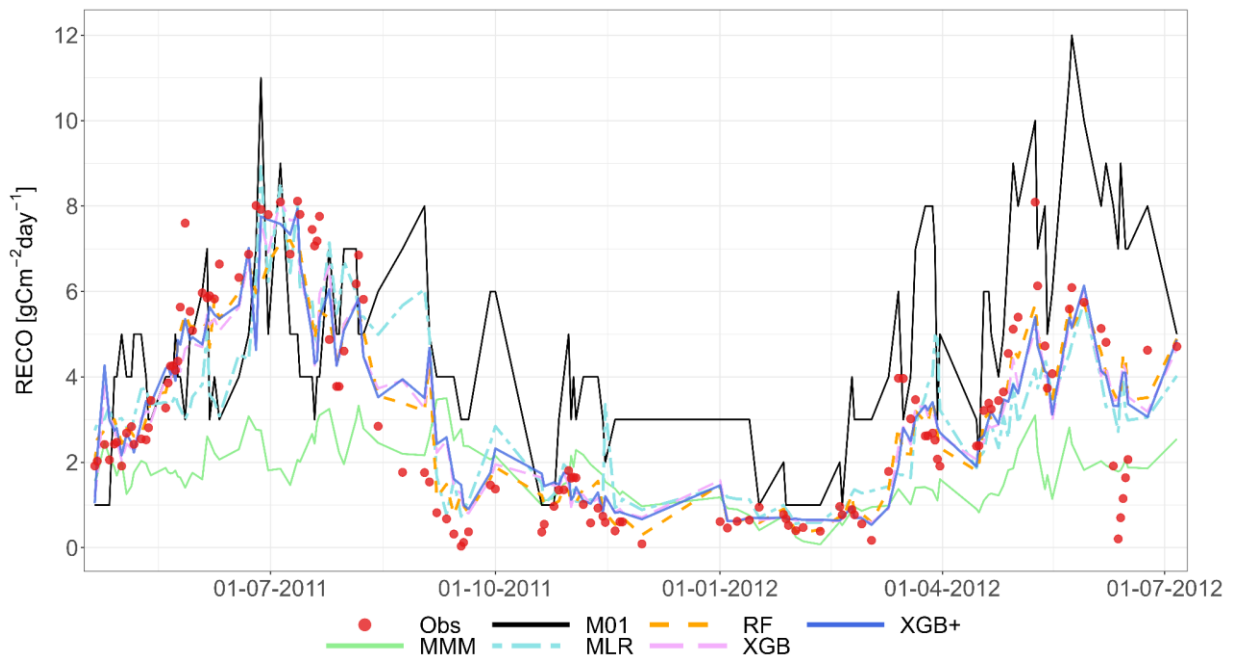
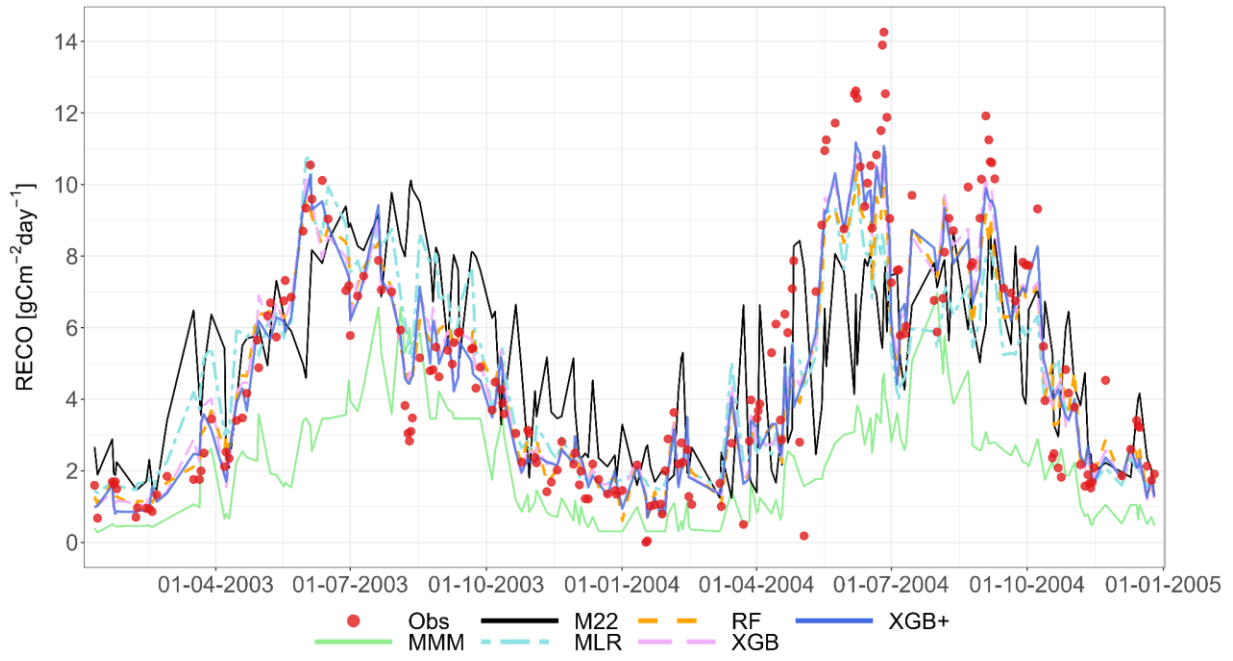
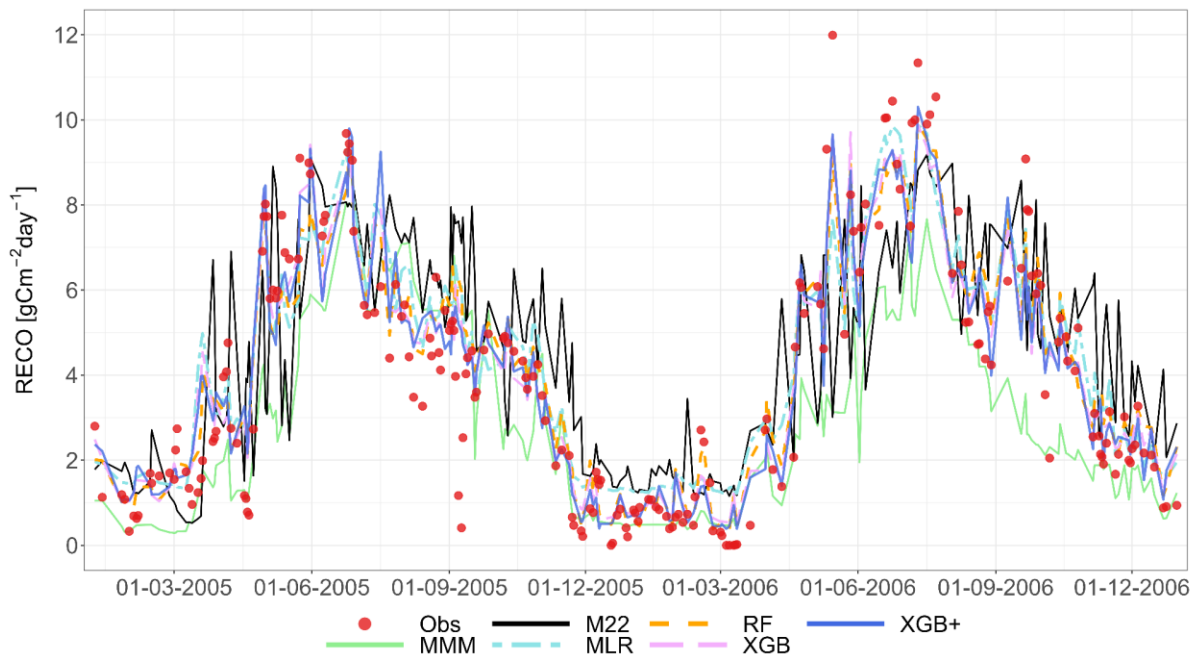


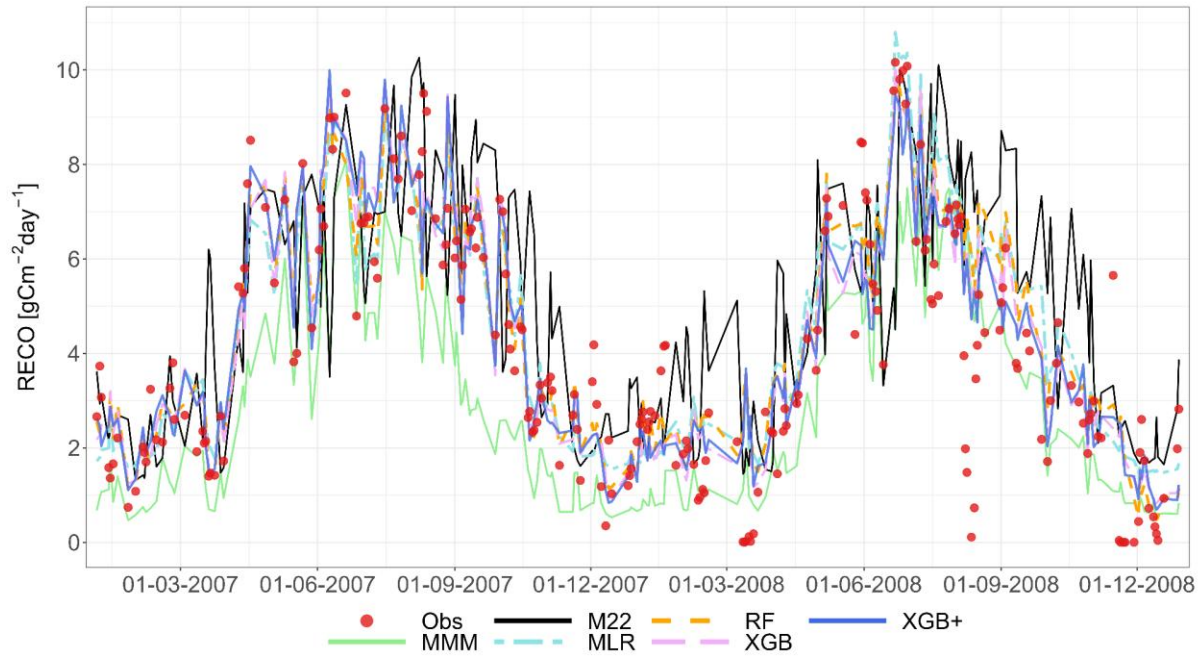
Figure A8: RECO, C2 - Grignon, (FR), cropland, 2007, 2008, 2011 and 2012, 70/30 strategy.

1375



1380





1385

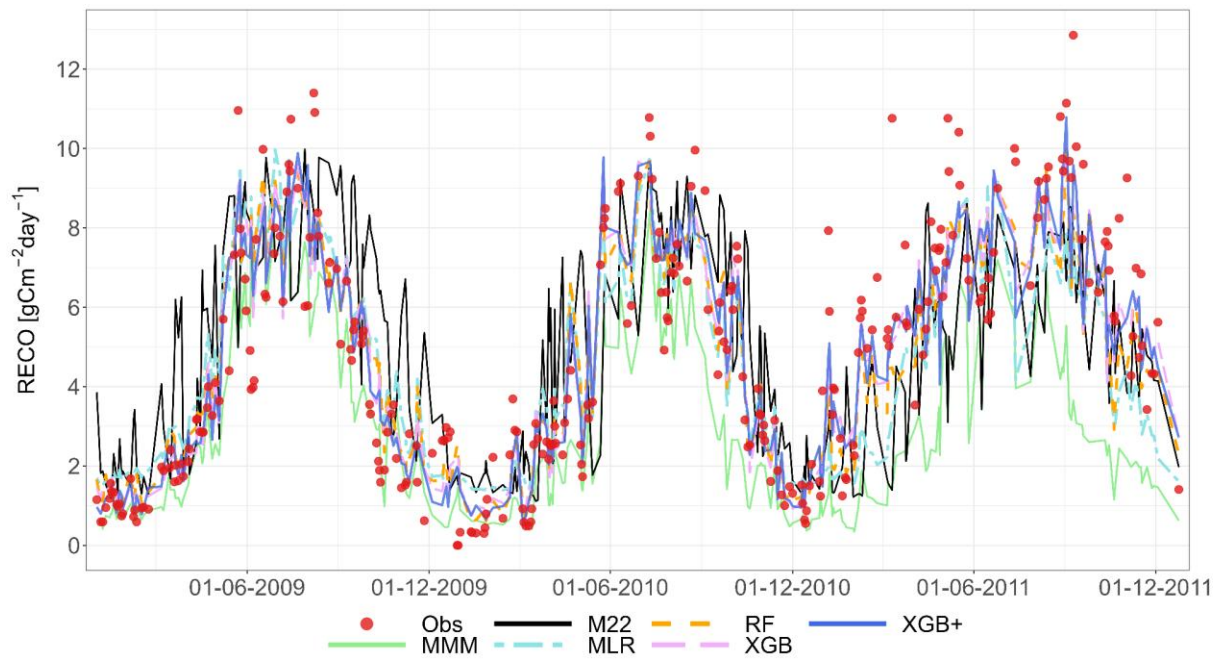
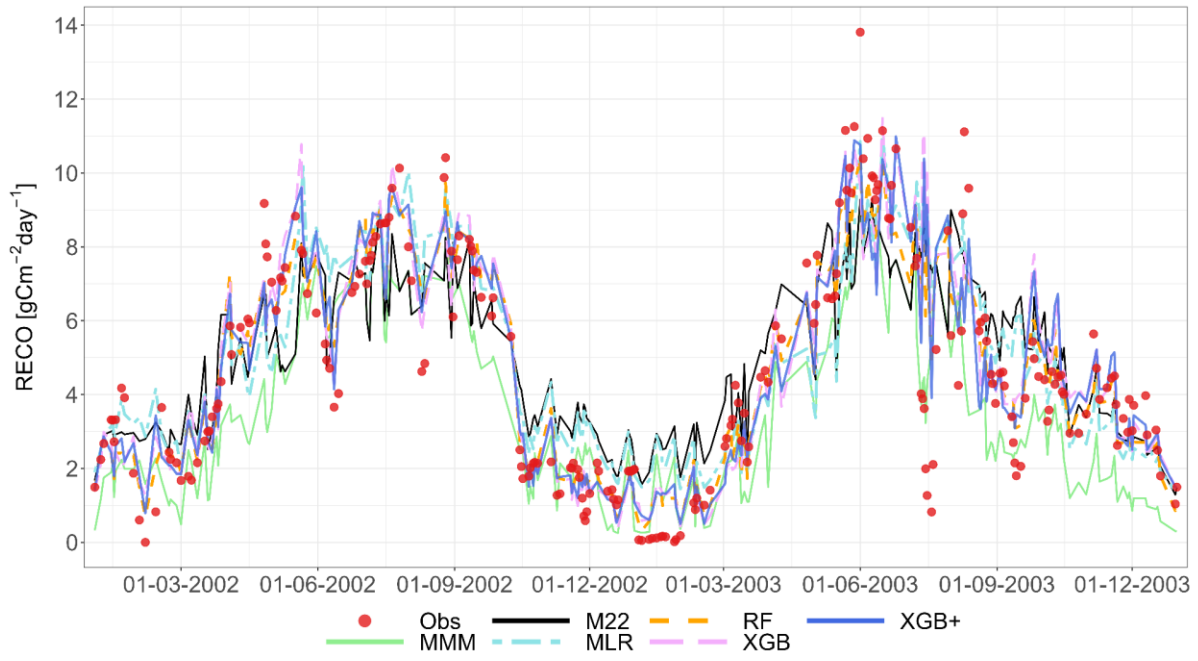
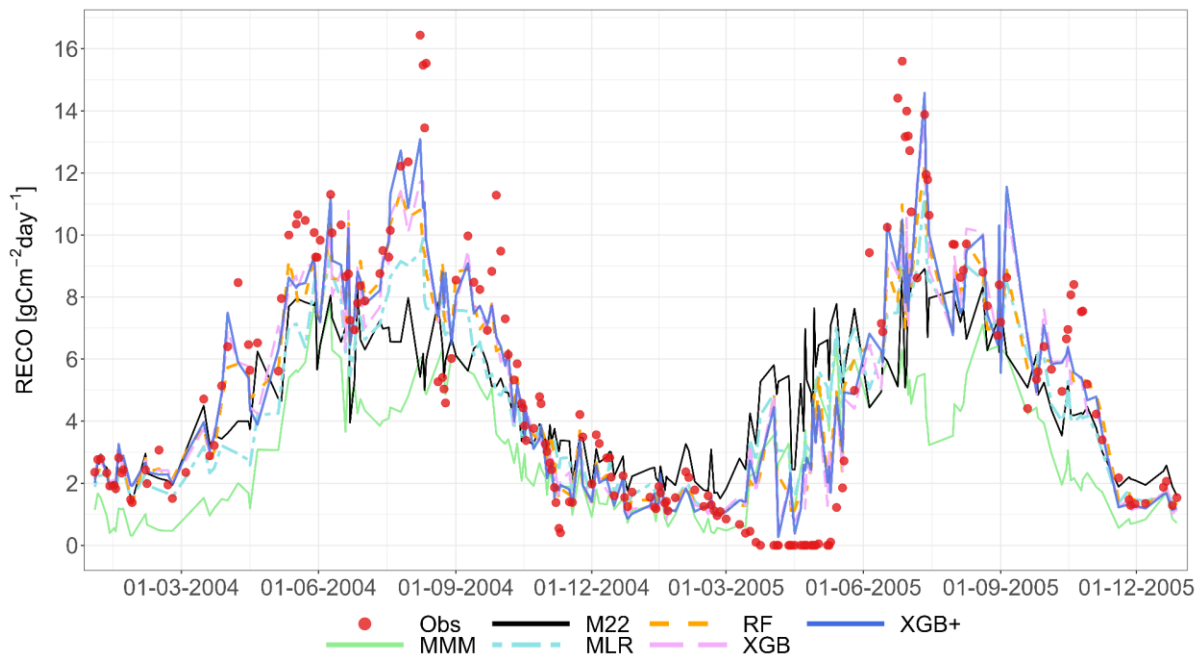


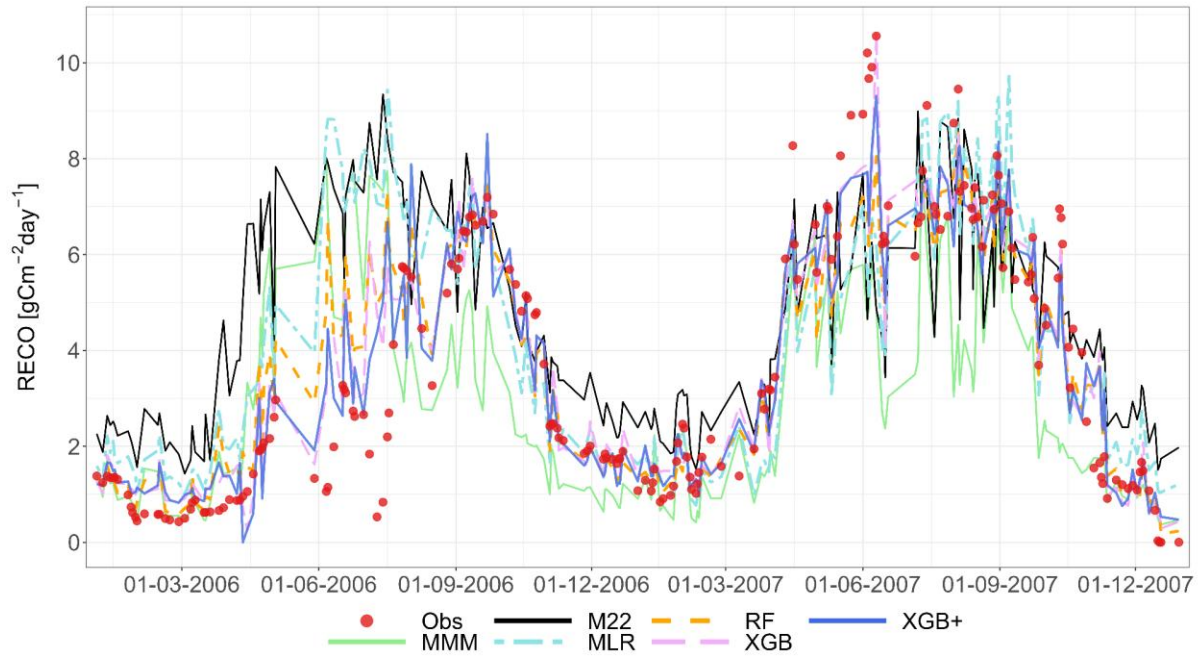
Figure A9: RECO, G3 - Laqueuille (FR), grassland, 2003-2011, 70/30 strategy.



1390



1395



1400

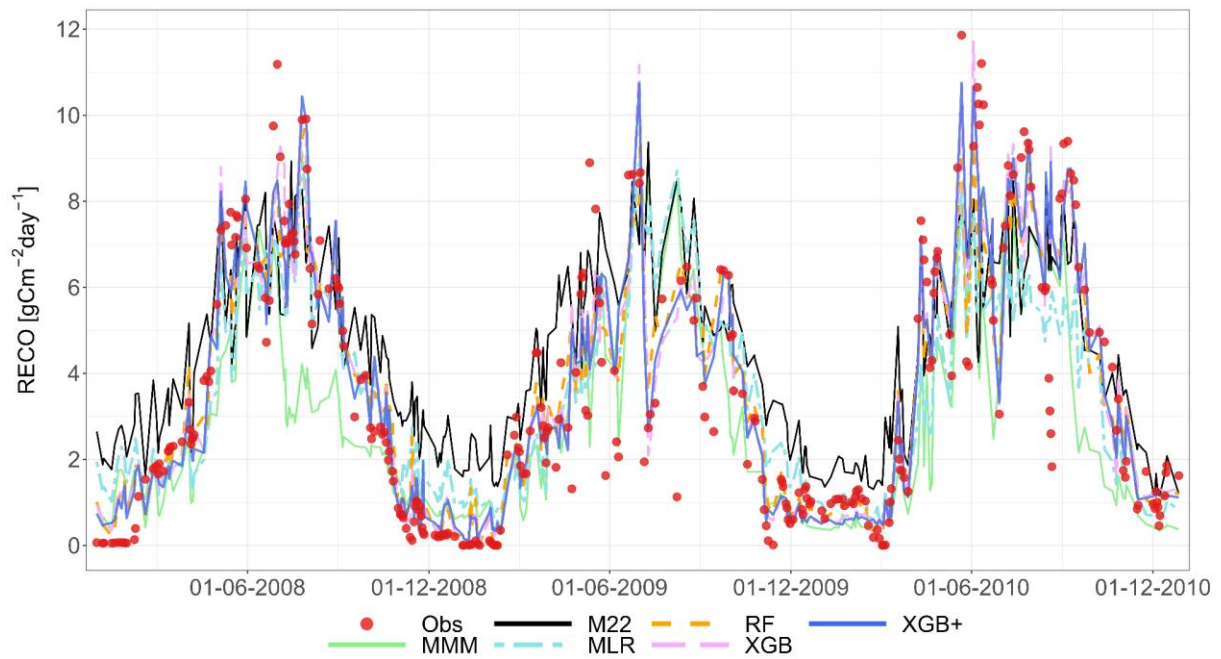
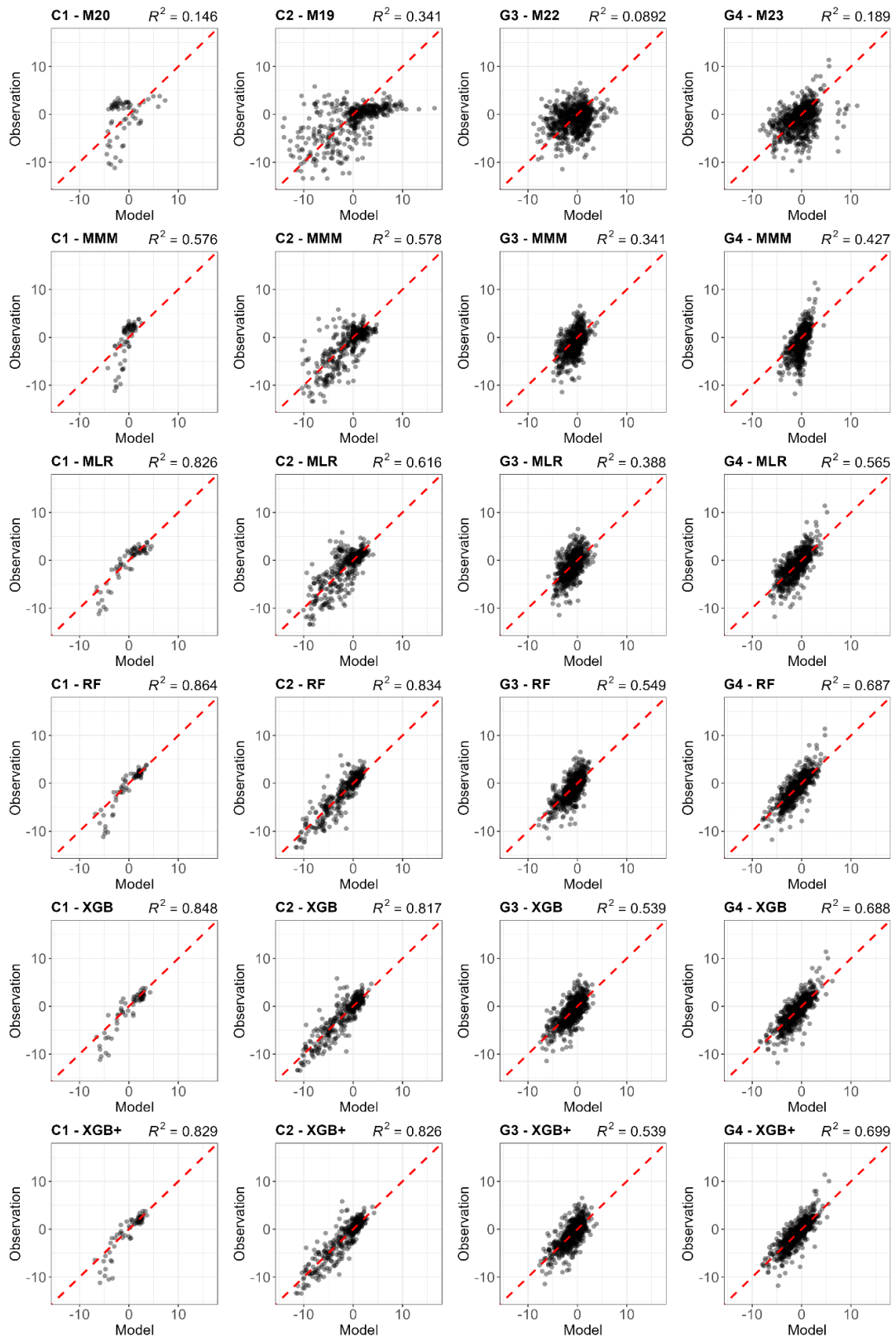


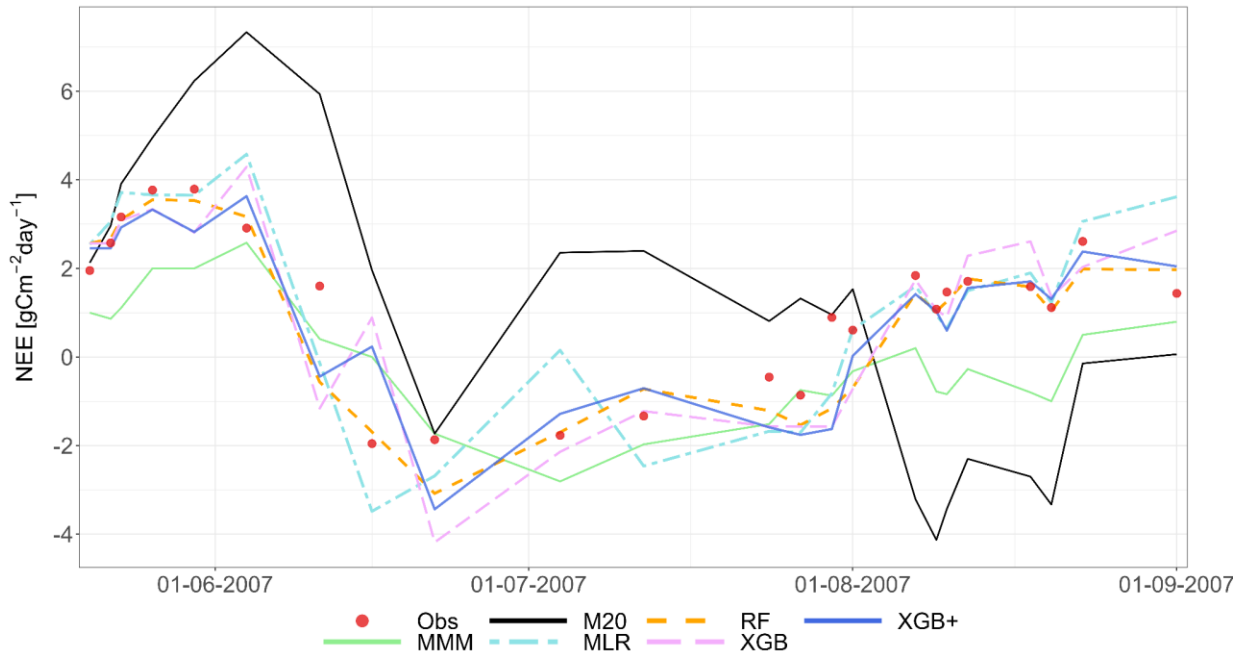
Figure A10: RECO, G4 - Easter Bush (UK), grassland, 70/30 strategy.



1405

Figure A11: Comparison of the best individual model, the multi-model median and the constructed meta-models with observations for NEE using the 70/30 approach. Each row represents a different model type, and columns correspond to the sites (from left to right: C1, C2, G3, and G4). The top row shows the best individual models with their identifiers (M20 at C1, M19 at C2, M22 at G3, M23 at G4). The remaining rows show the MMM, MLR, RF, XGB and XGB+. All units are in $\text{g C m}^{-2} \text{ day}^{-1}$. The red dashed line represents the 1:1 relationship.

1410



1415

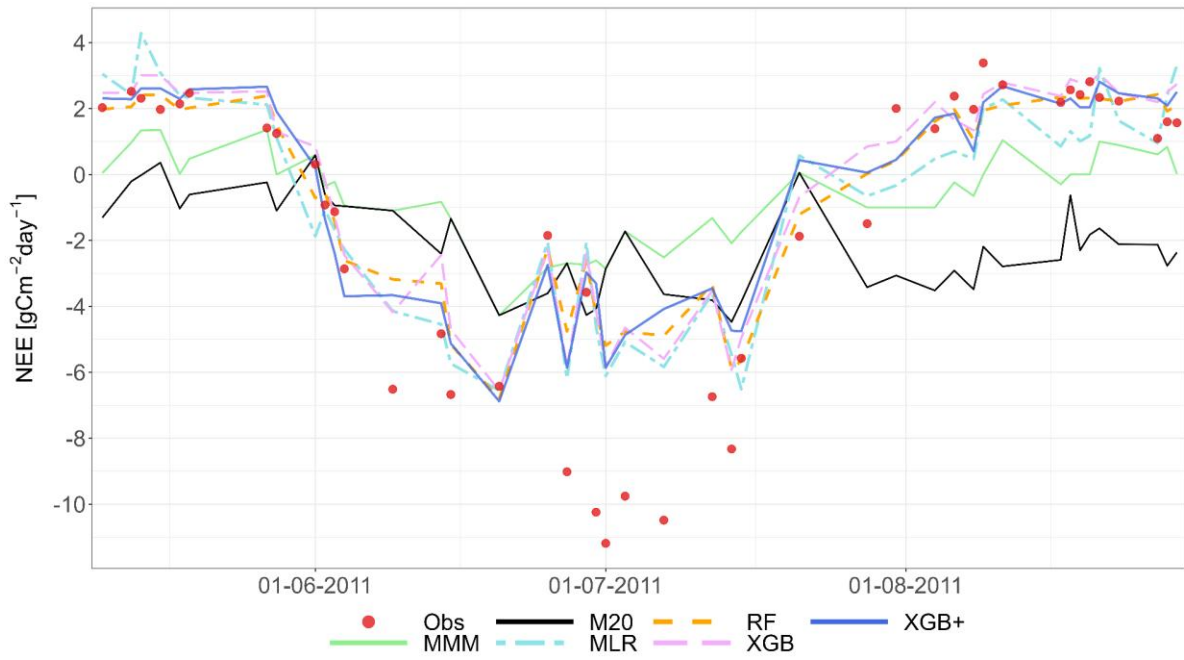
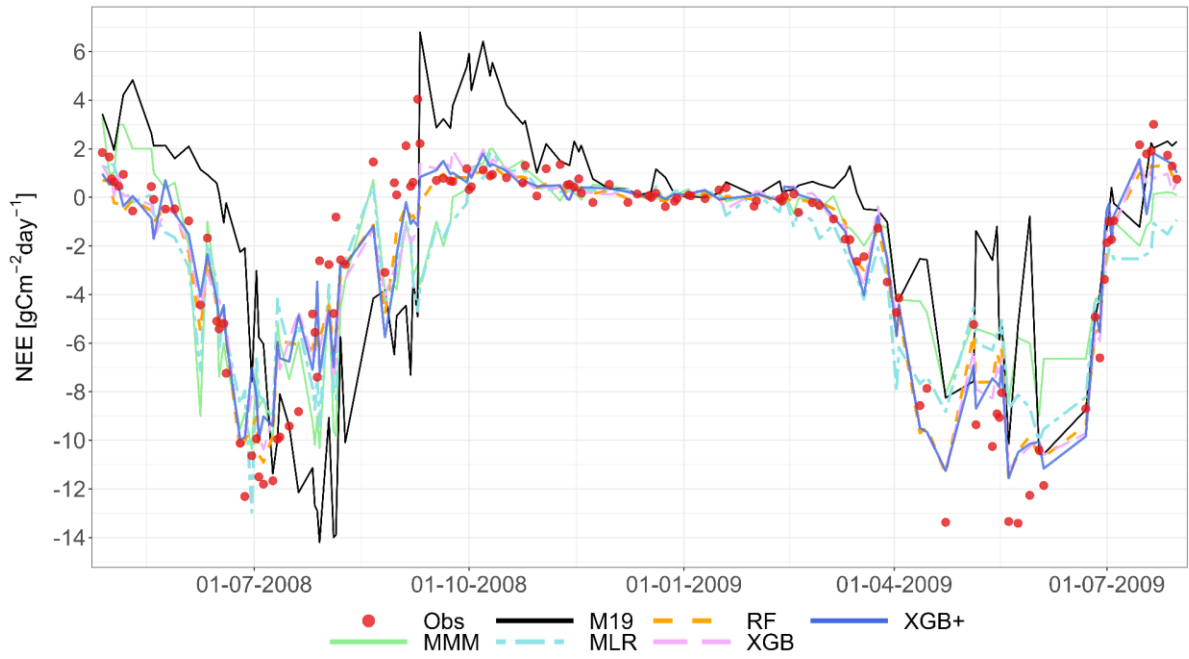


Figure A12: NEE, C1 - Ottawa (CA), cropland, 2007 and 2011, 70/30 strategy.



1420

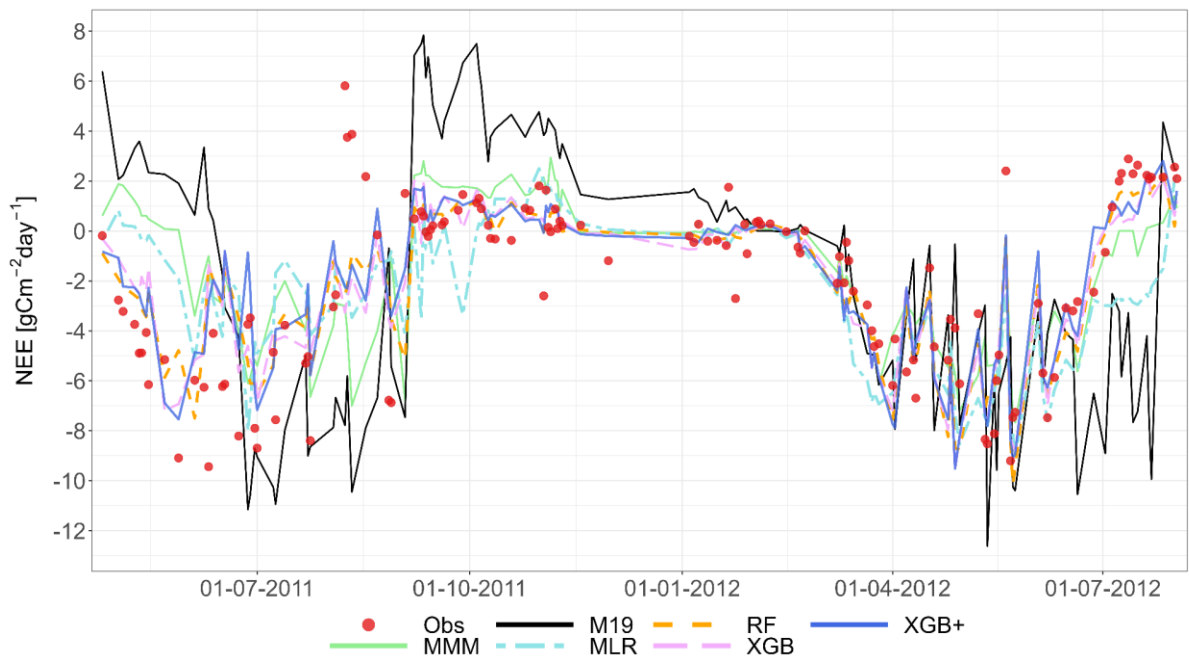
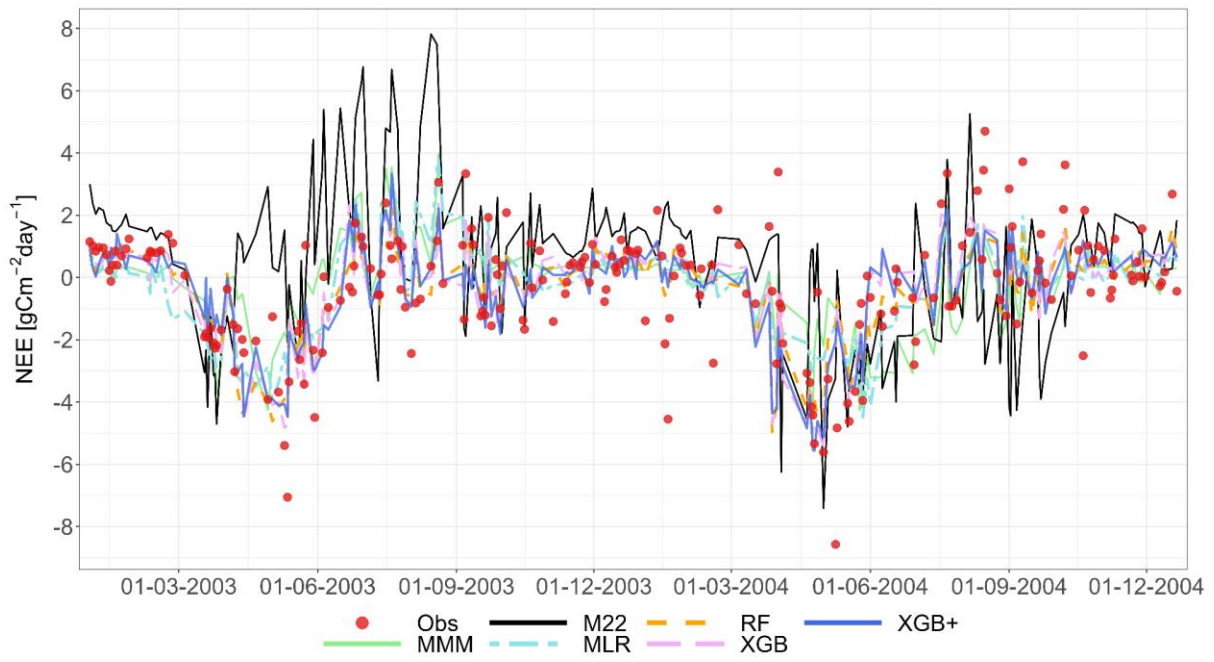
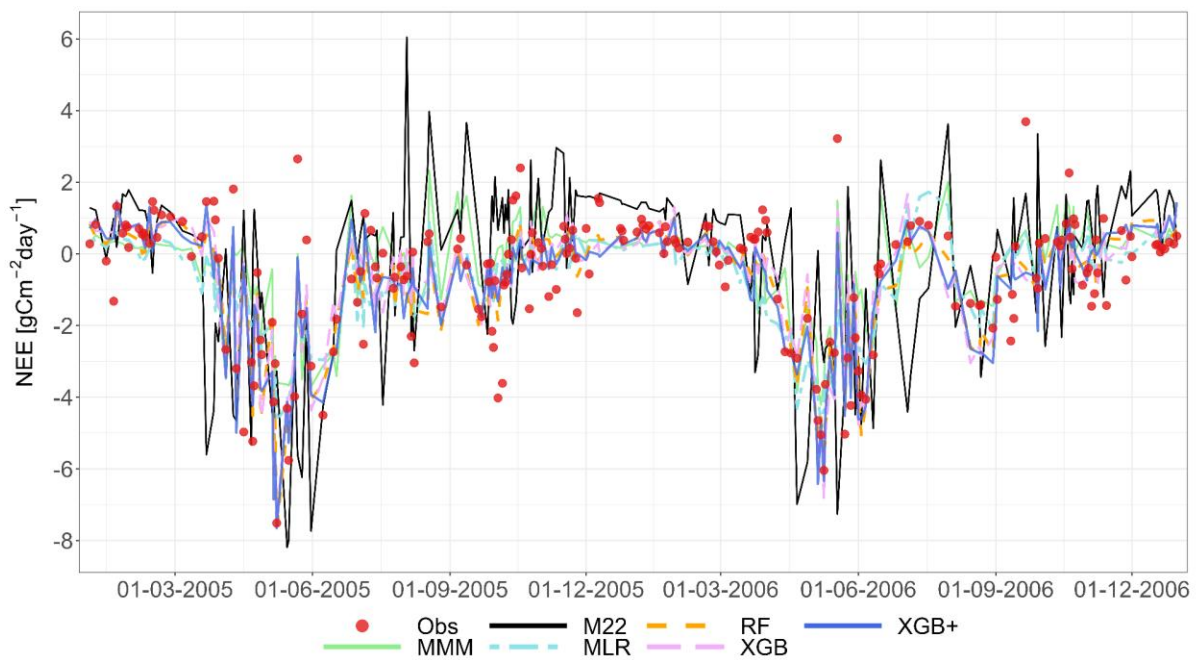


Figure A13: NEE, C2 - Grignon, (FR), cropland, 2008, 2009, 2011 and 2012, 70/30 strategy.

1425



1430



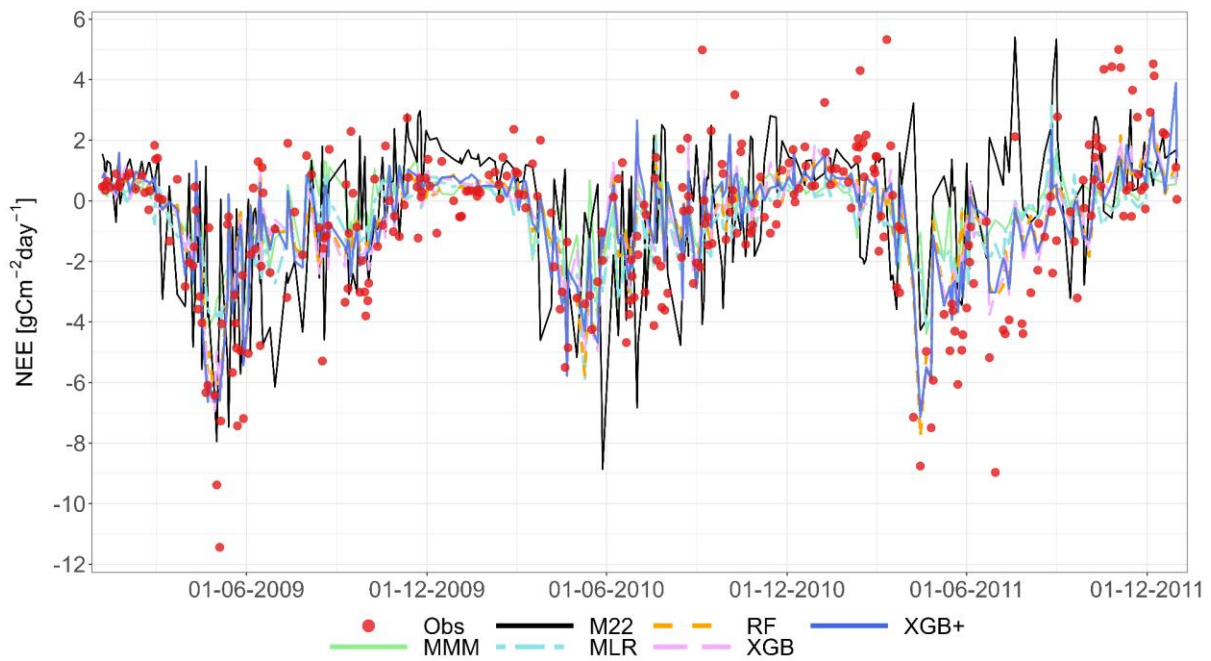
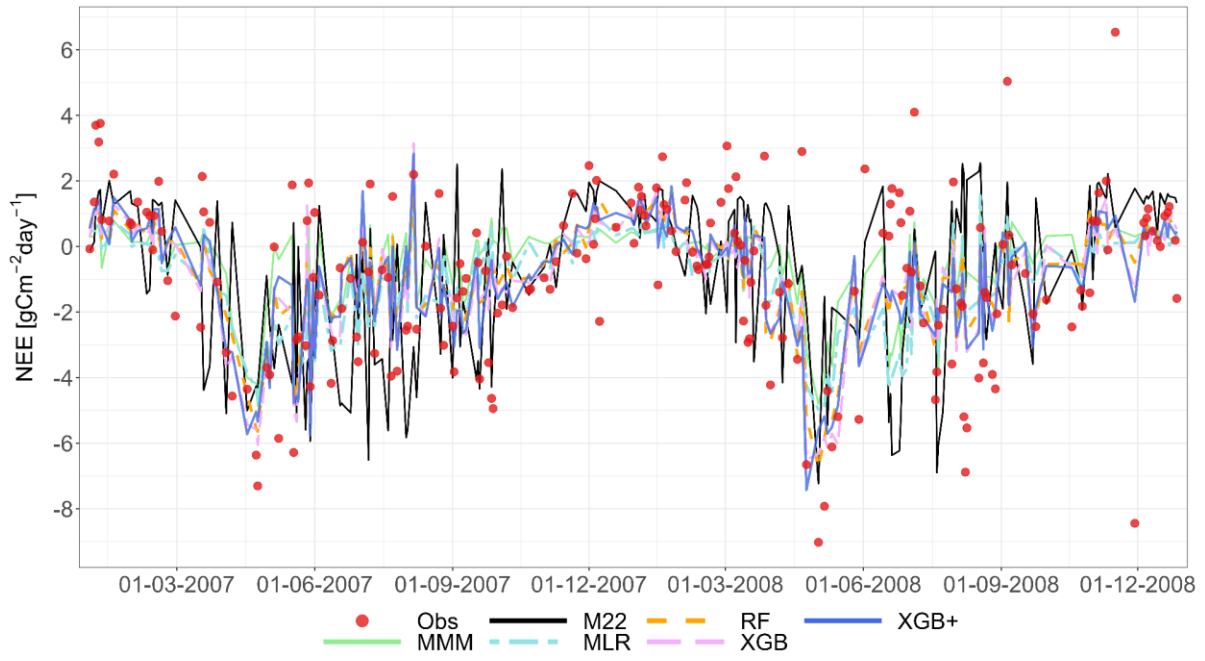
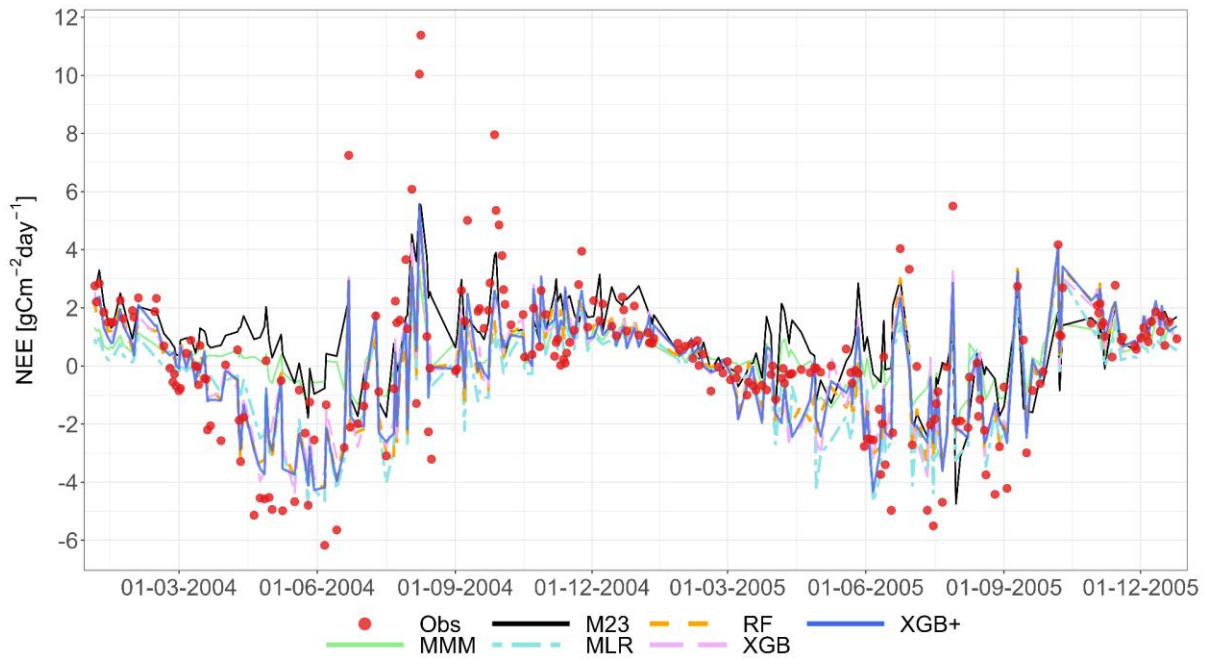
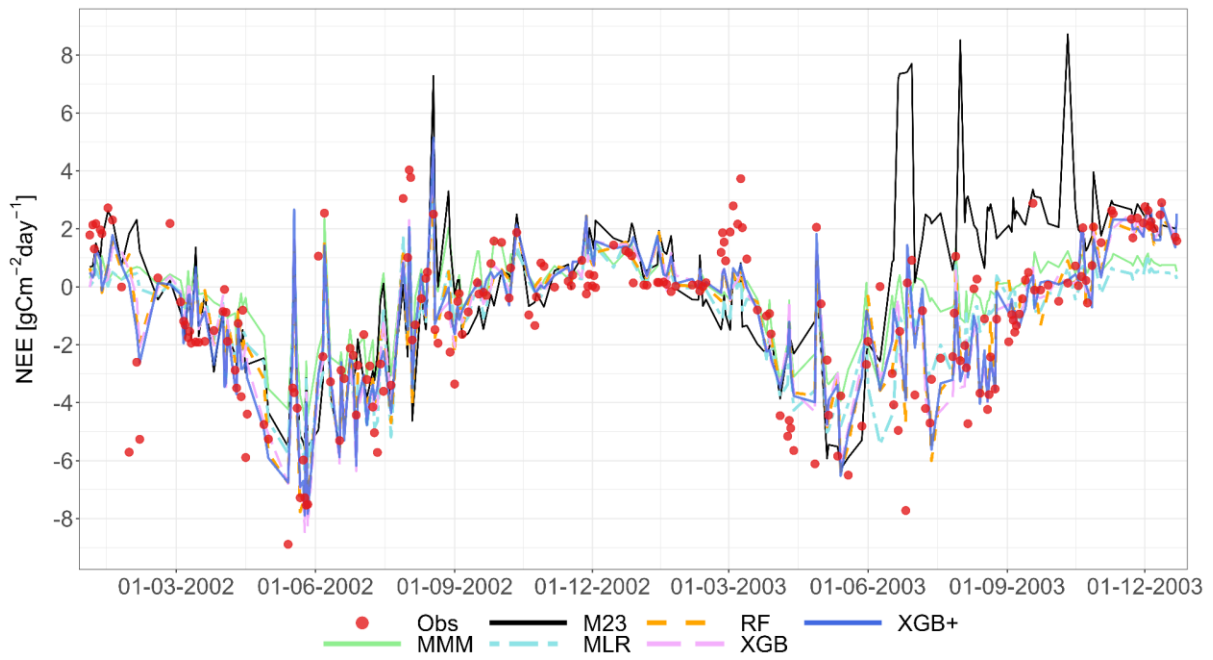
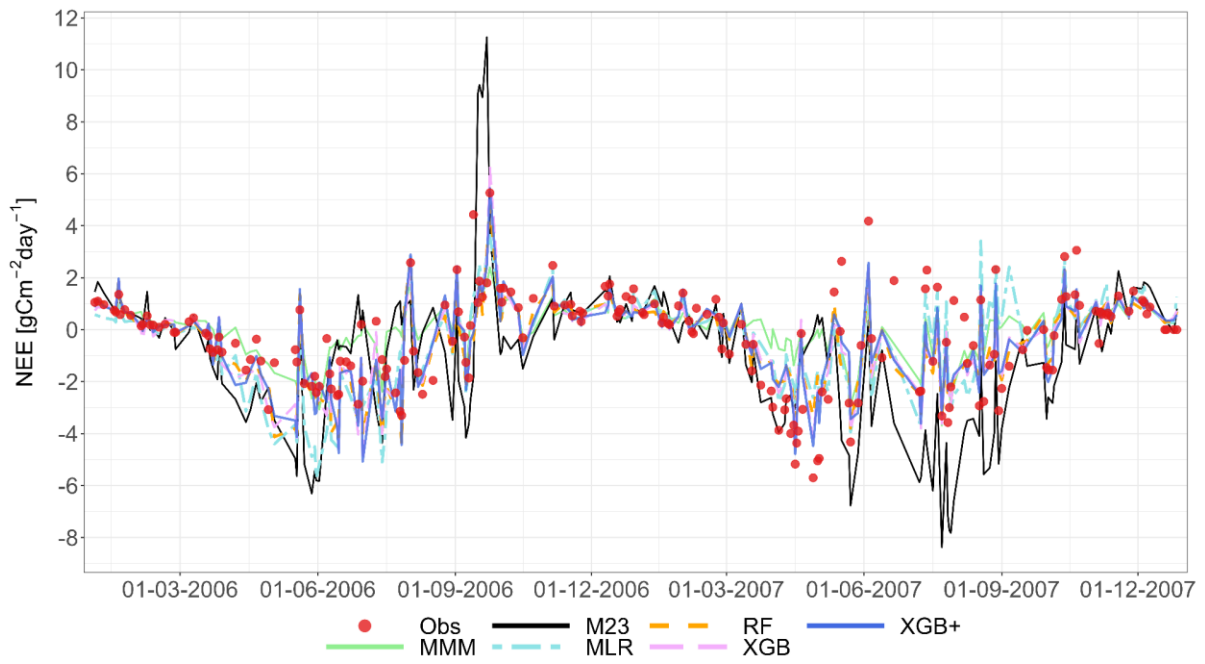


Figure A14: NEE, G3 - Laqueuille (FR), grassland, 2003-2011, 70/30 strategy.

1445



1450



1455

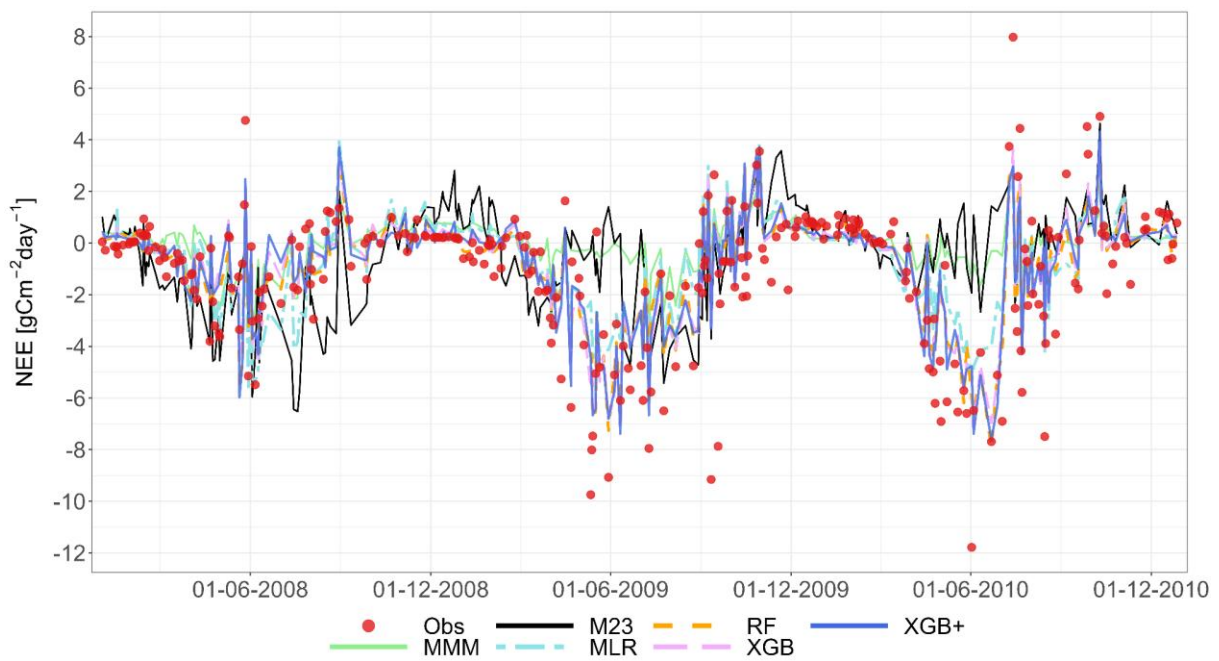
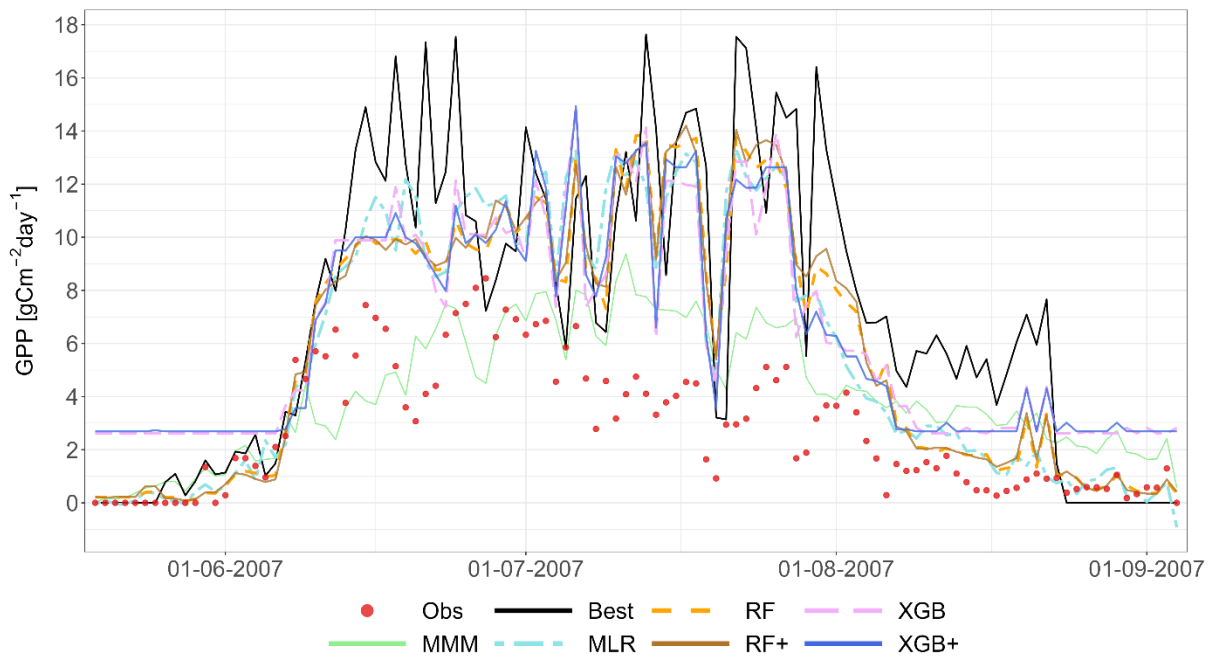


Figure A15: NEE, G4 - Easter Bush (UK), grassland, 70/30 strategy.

1460



1465

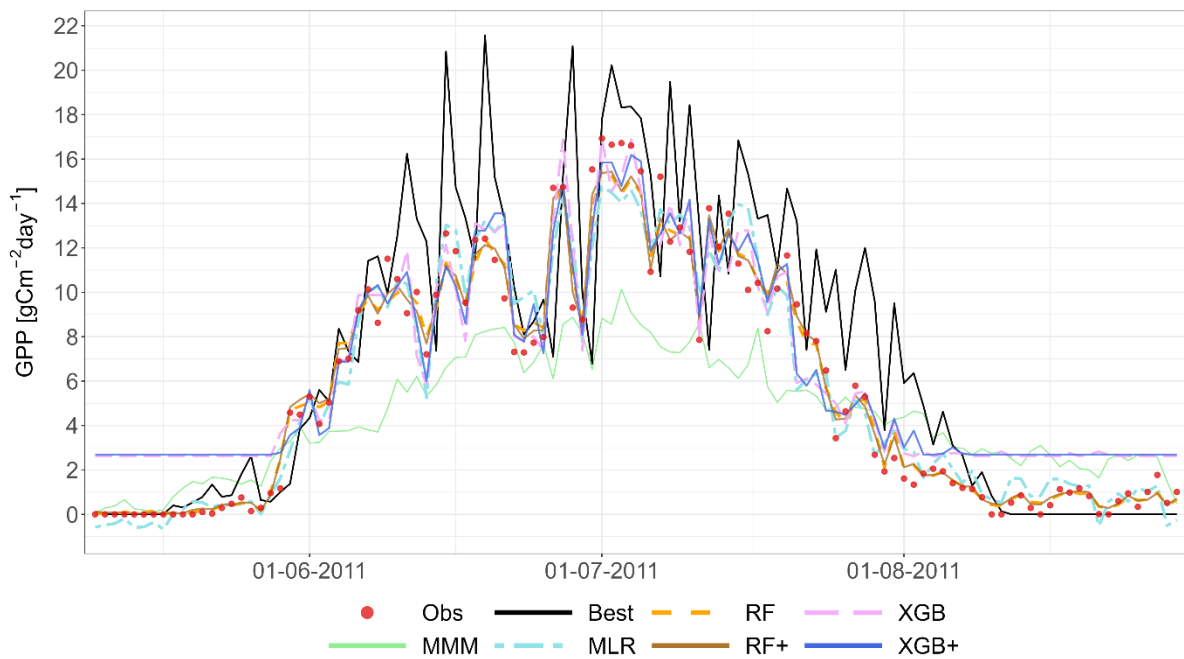
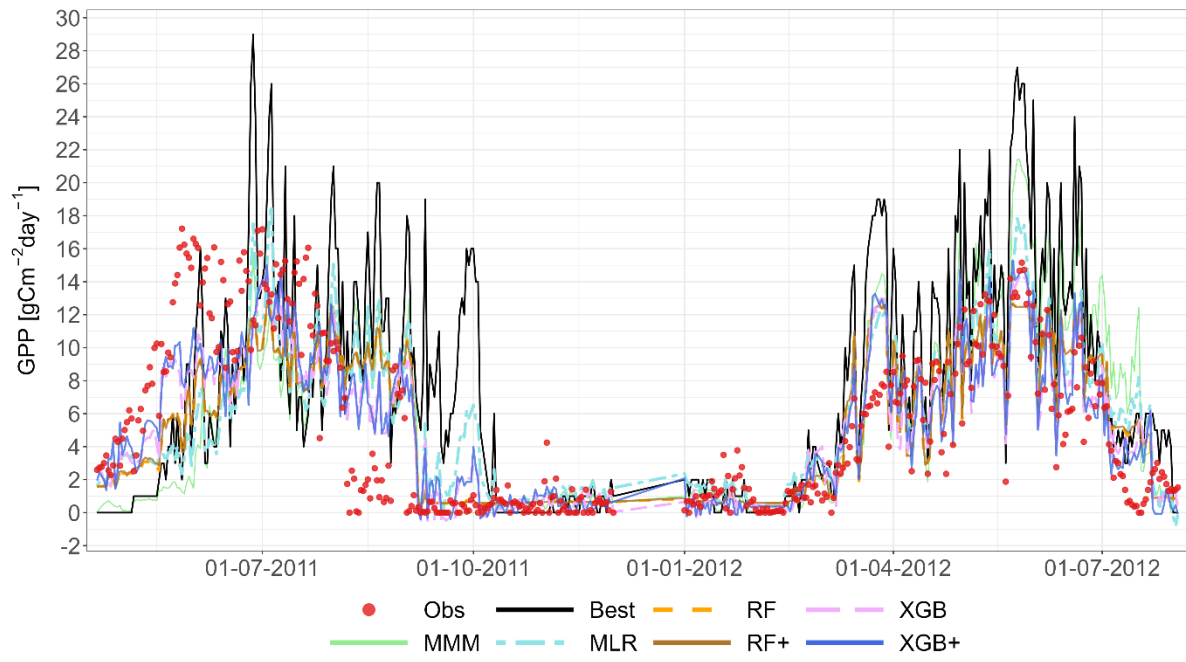


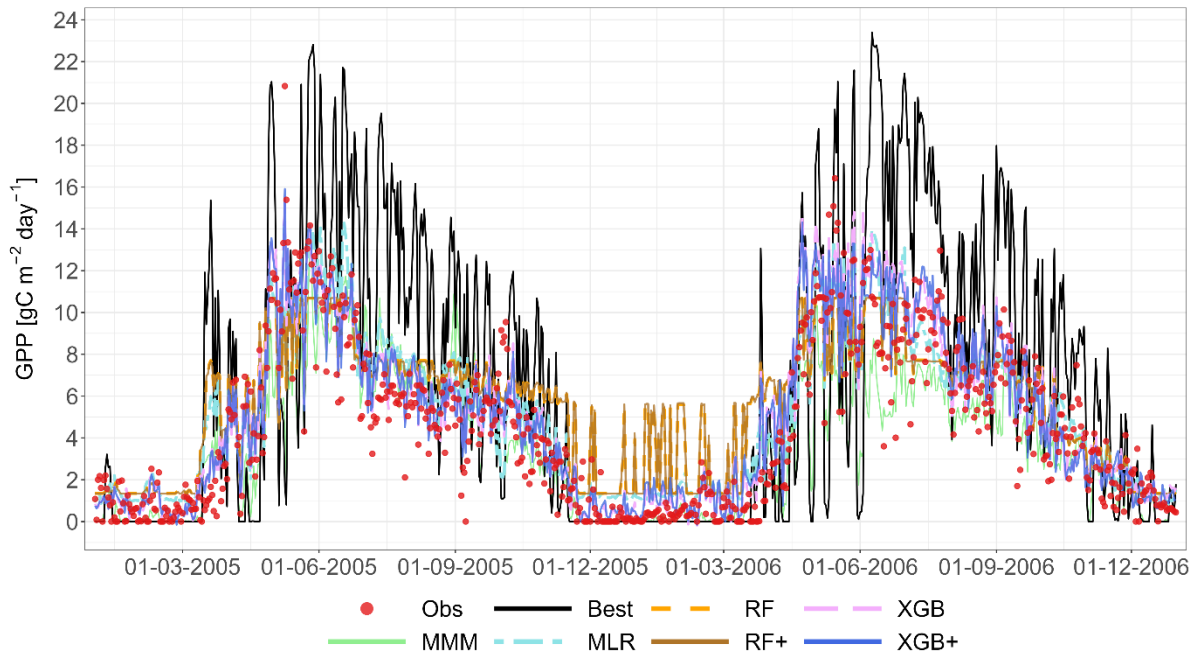
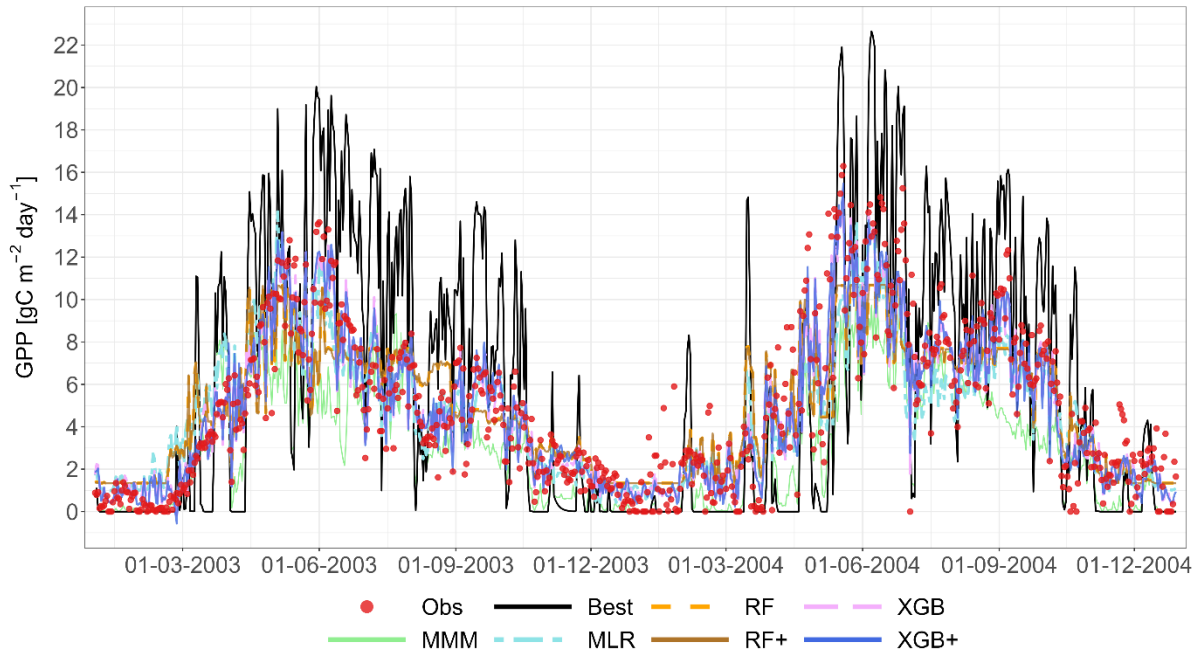
Figure A16: GPP, C1 - Ottawa (CA), cropland, 2007 and 2011, LOYO strategy.

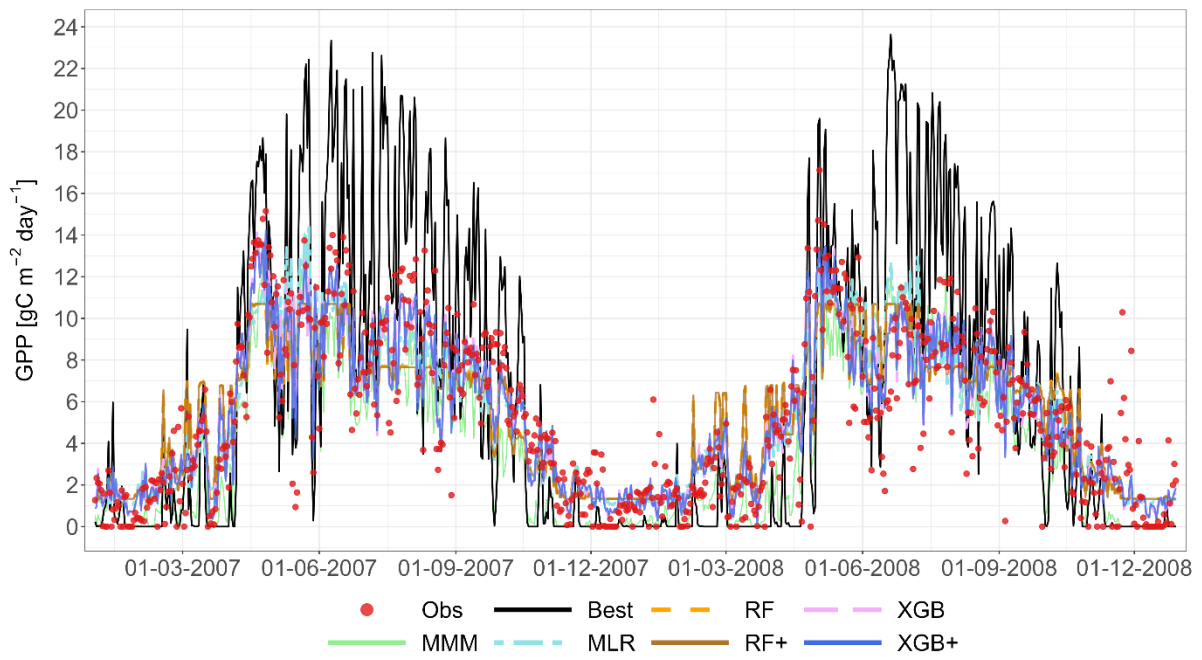


1470

Figure A17: GPP, C2 - Grignon, (FR), cropland, 2011 and 2012, LOYO strategy.

1475





1485

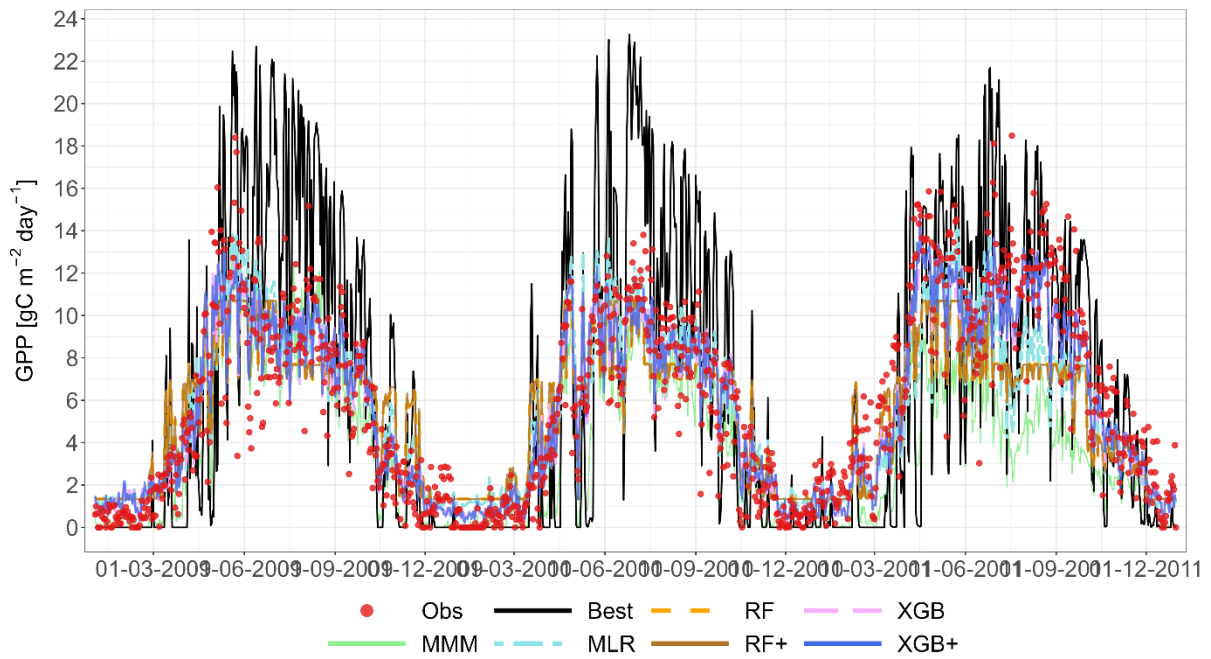
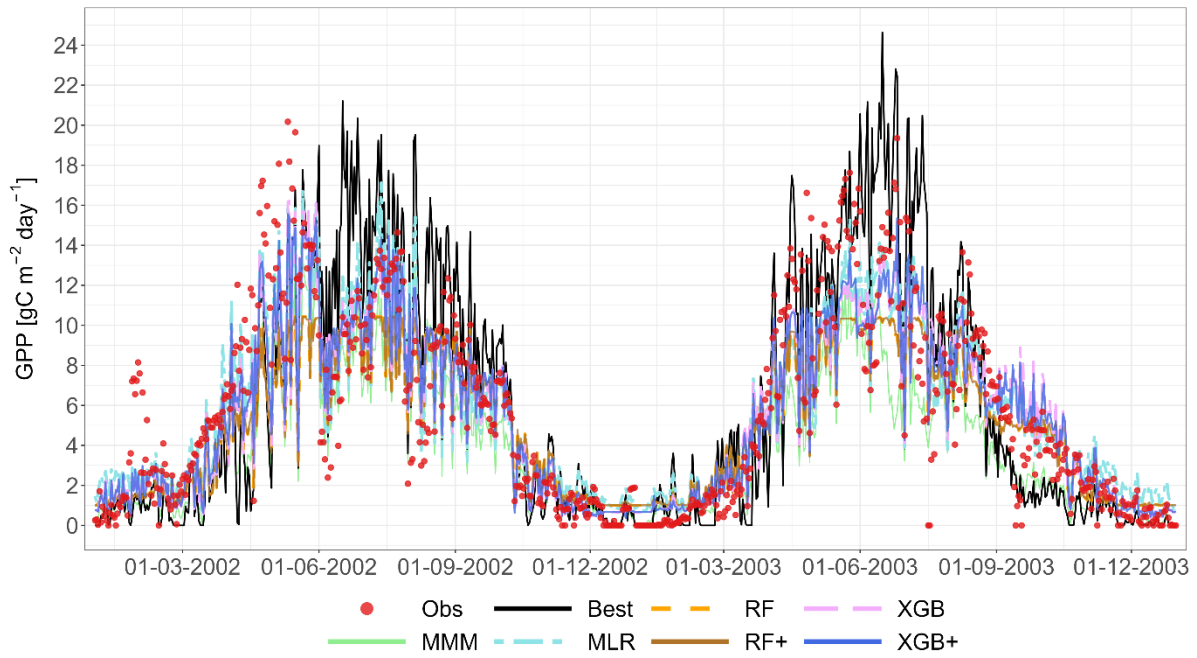


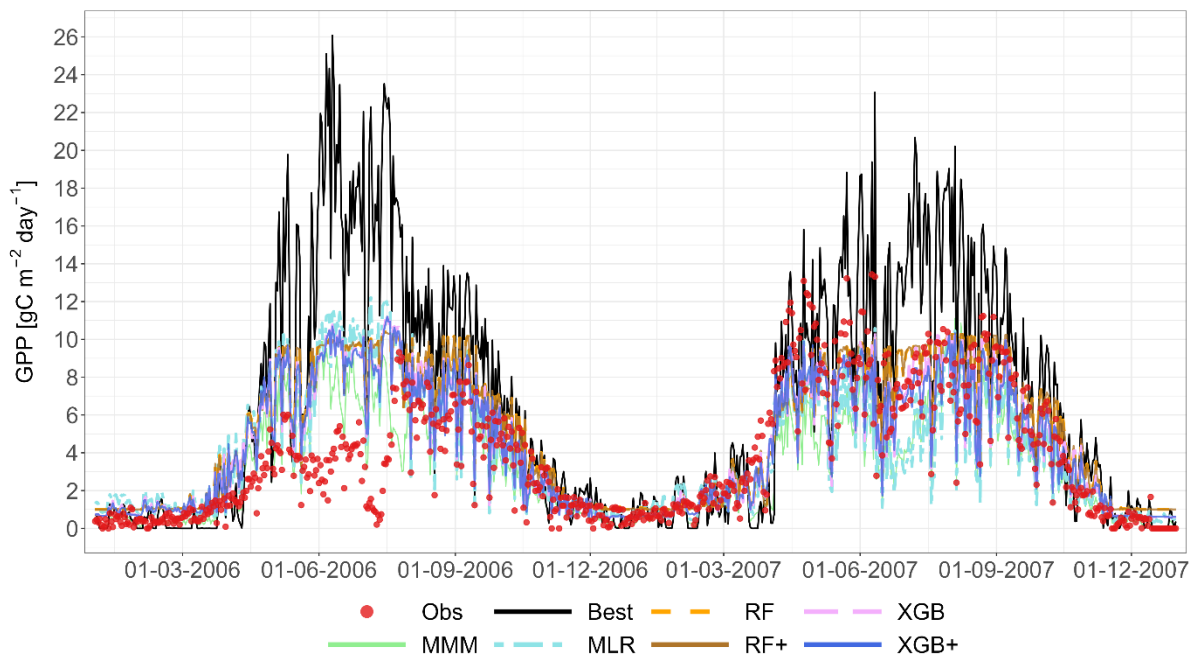
Figure A18: GPP, G3 - Laqueuille (FR), grassland, 2003-2011, LOYO strategy.

1490

1495



1500



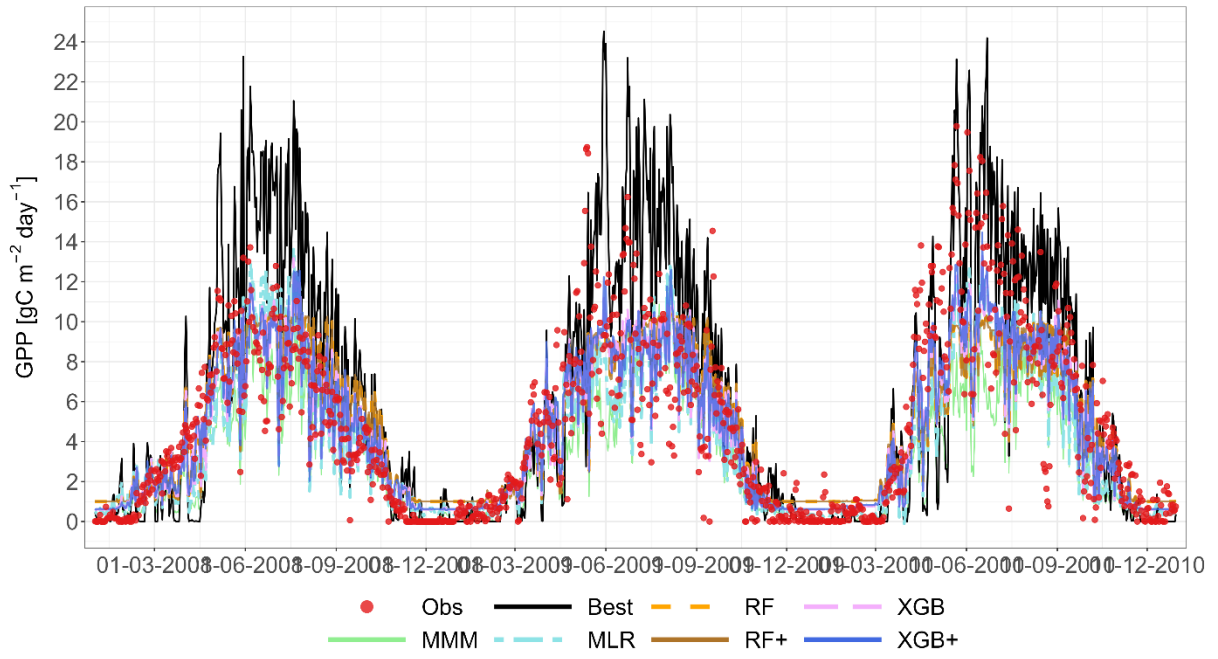
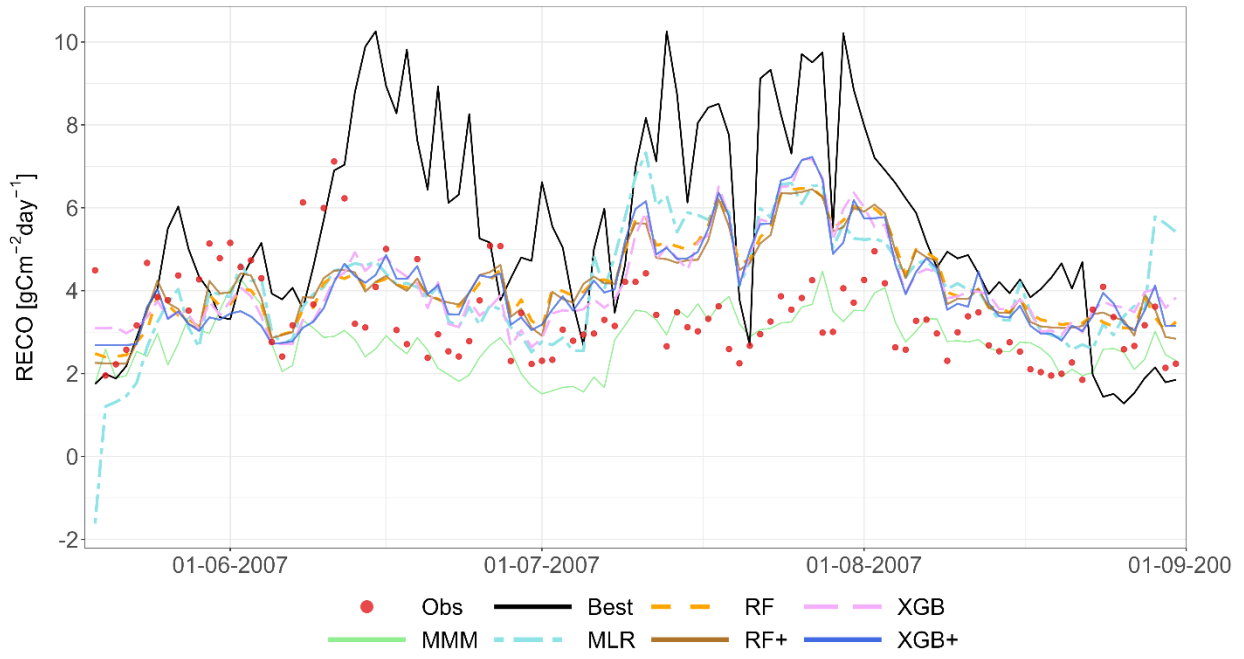


Figure A19: GPP, G4 - Easter Bush (UK), grassland, LOYO strategy.



1510

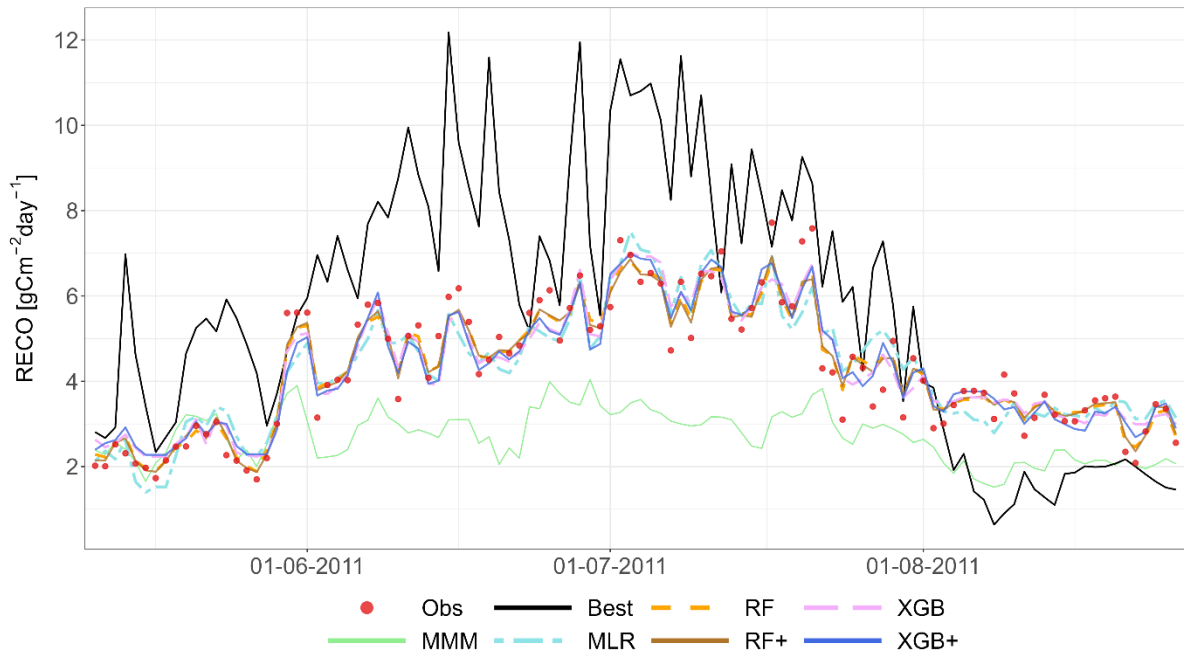
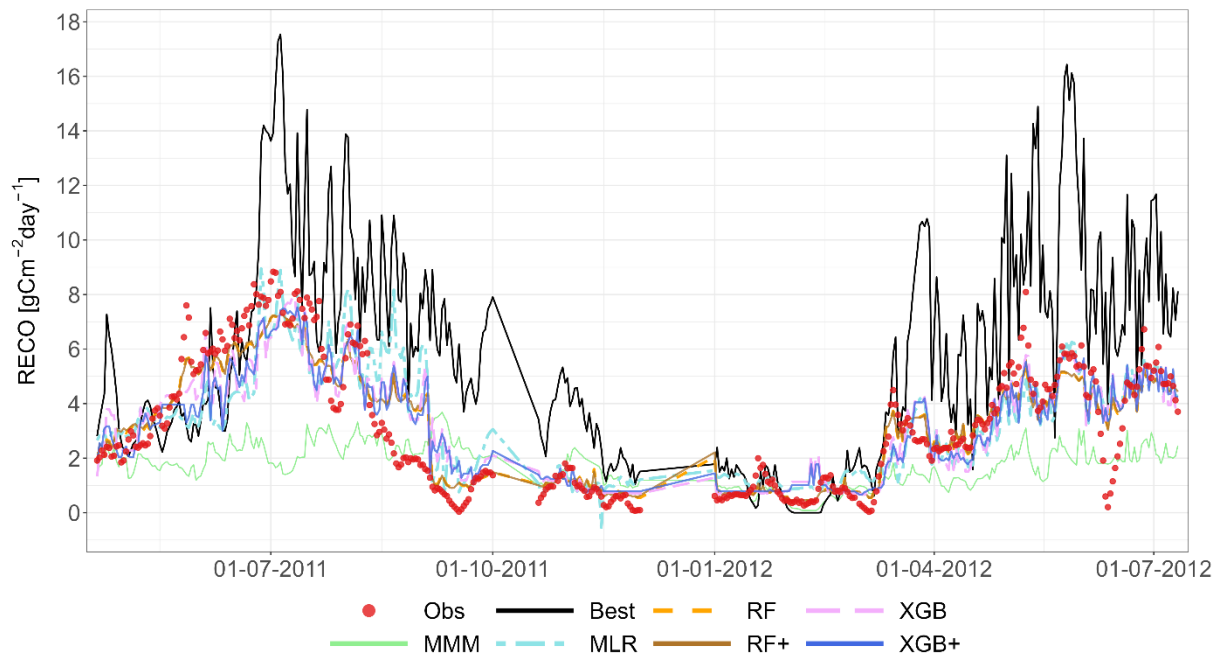


Figure A20: RECO, C1 - Ottawa (CA), cropland, 2007 and 2011, LOYO strategy.

1515



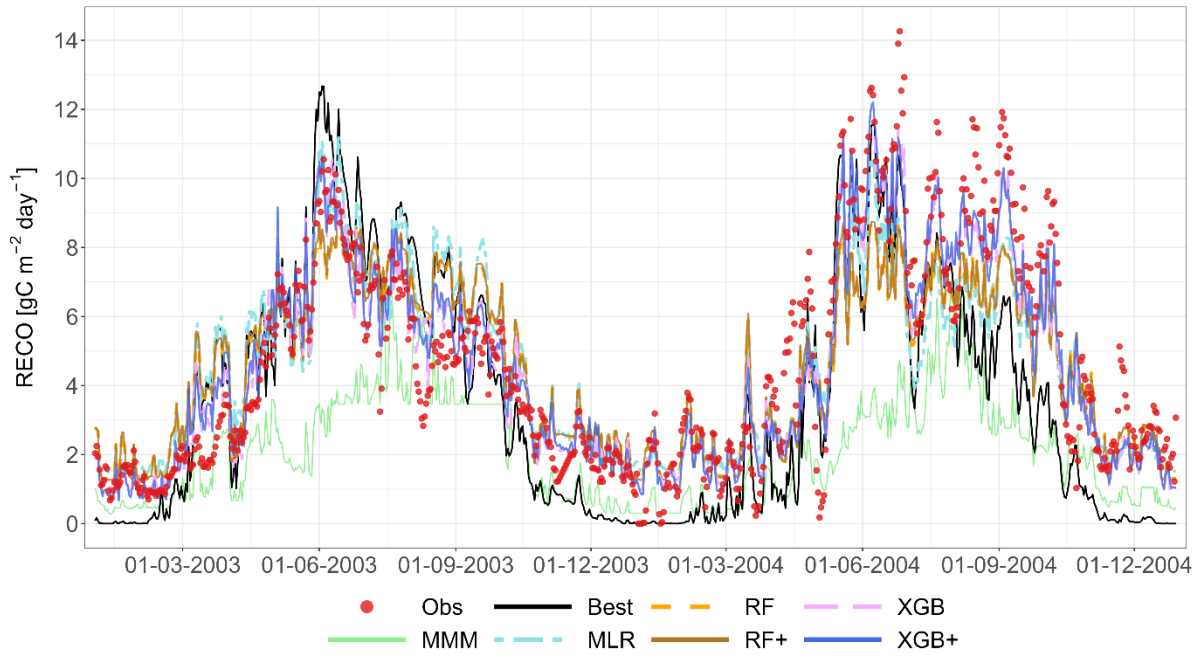
1520

Figure A21: RECO, C2 - Grignon, (FR), cropland, 2011 and 2012, LOYO strategy.

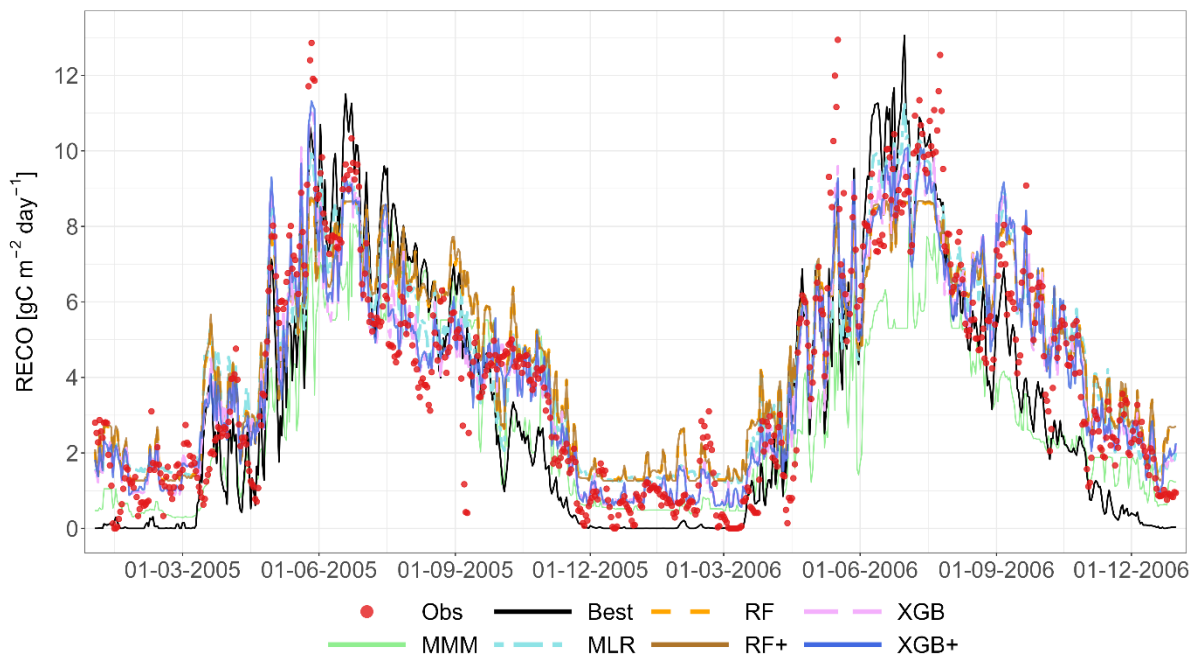
1525

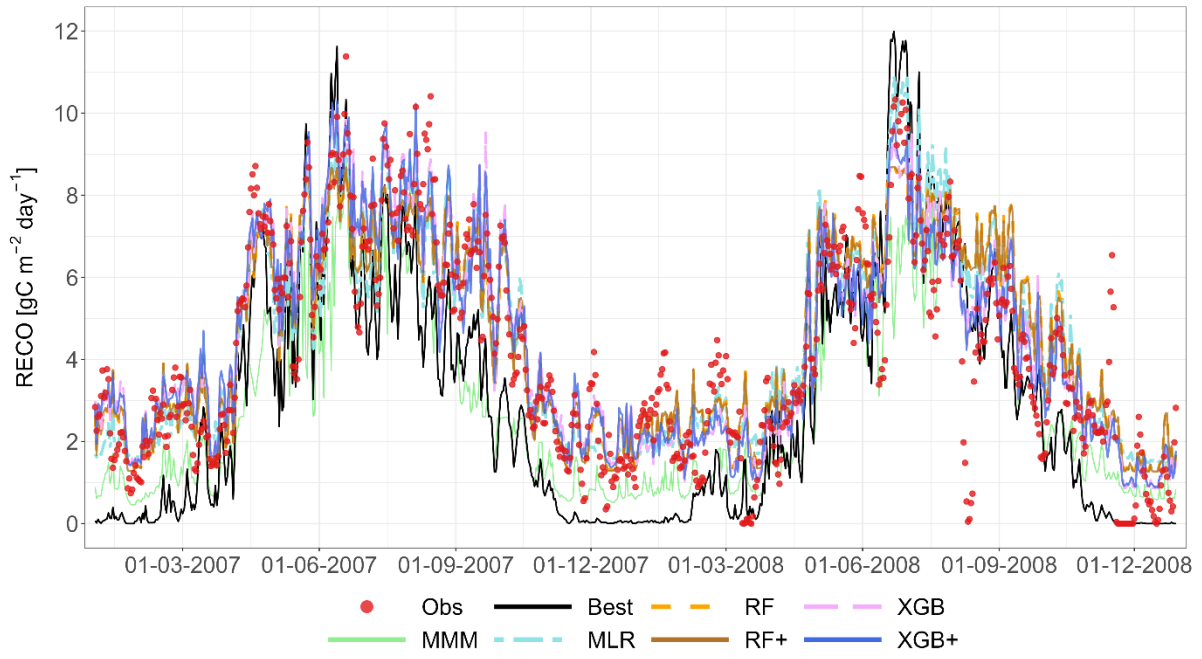
1530

1535



1540





1545

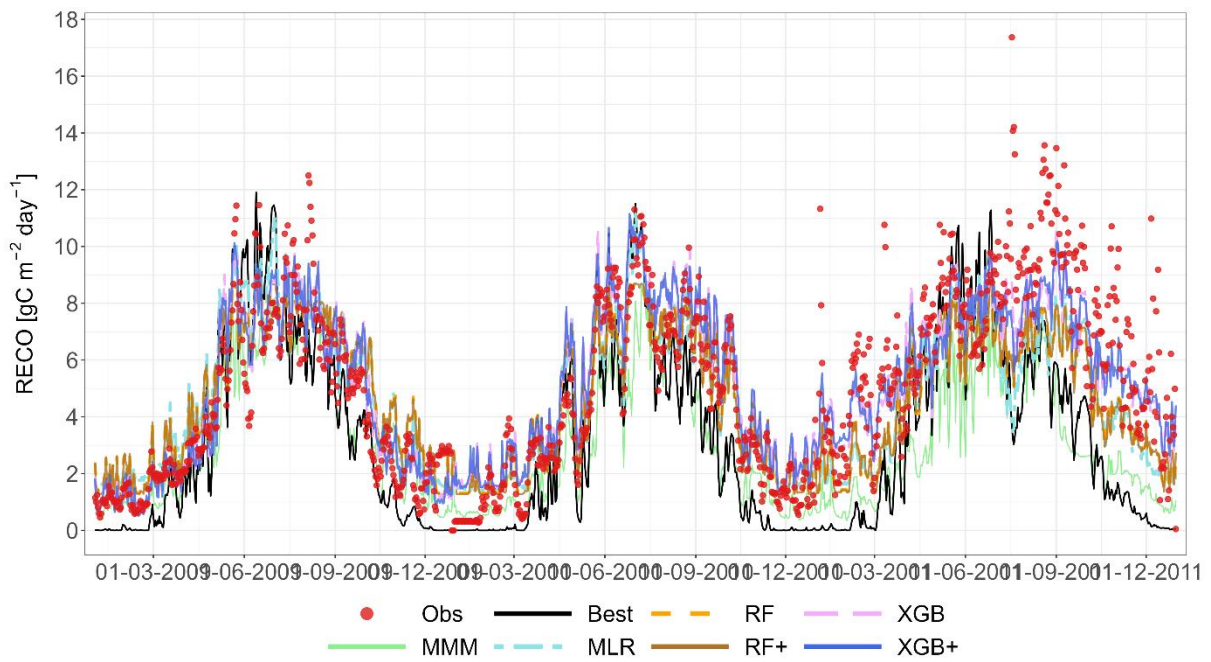
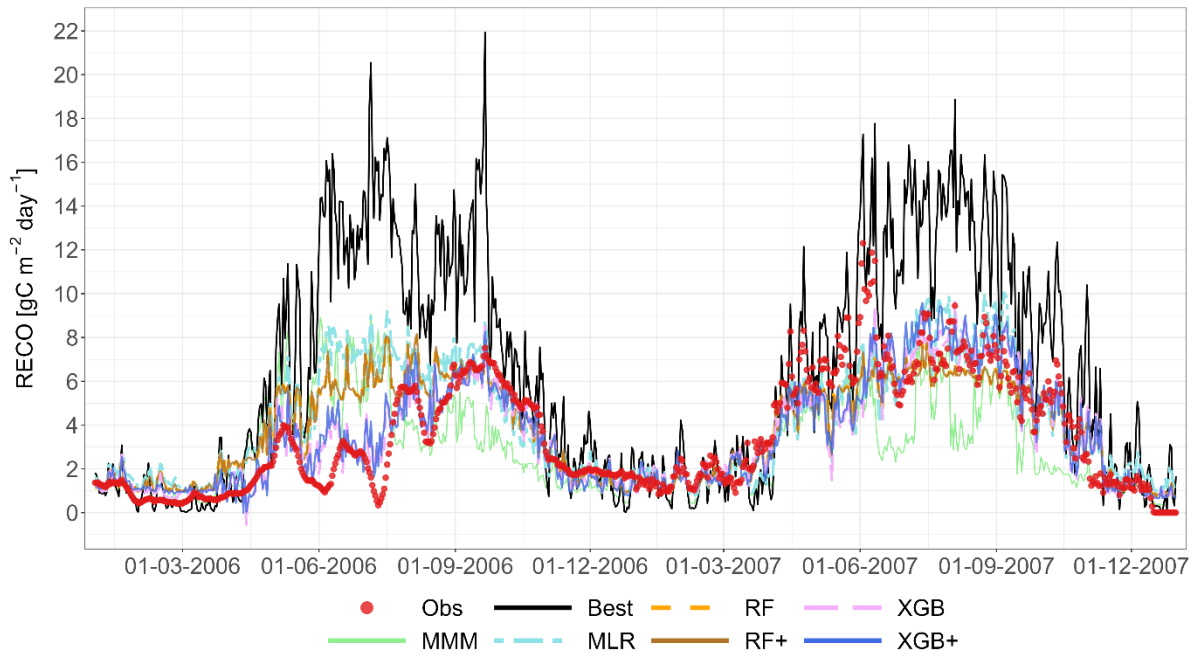
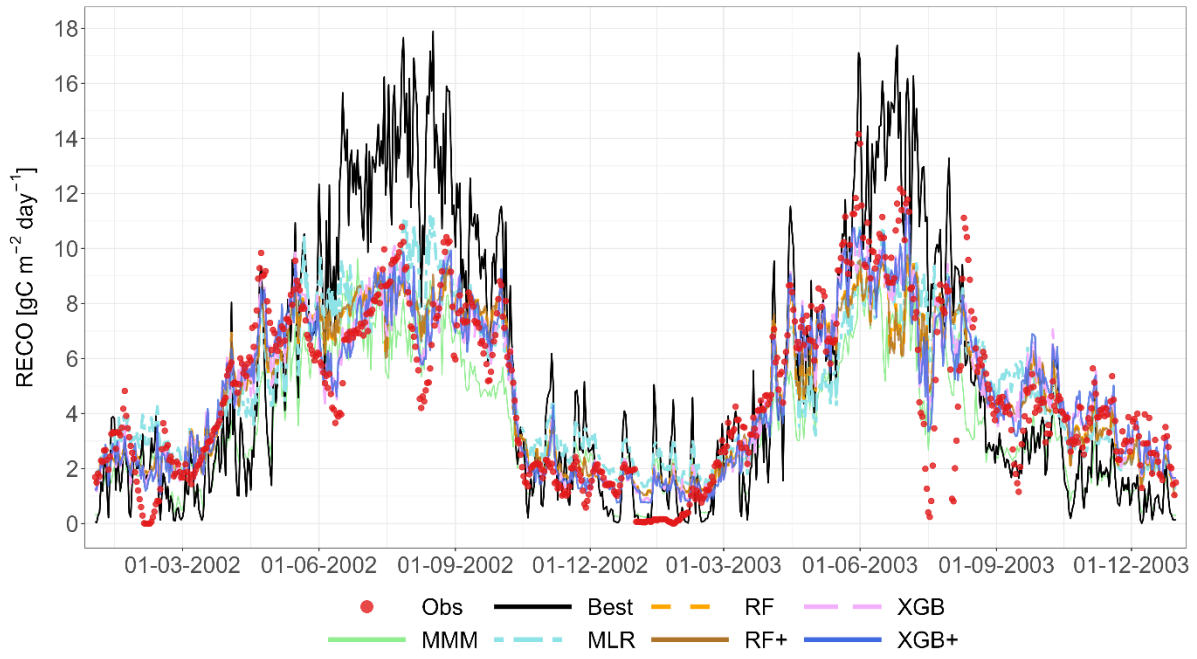


Figure A22: RECO, G3 - Laqueuille (FR), grassland, 2003-2011, LOYO strategy.

1550



1555

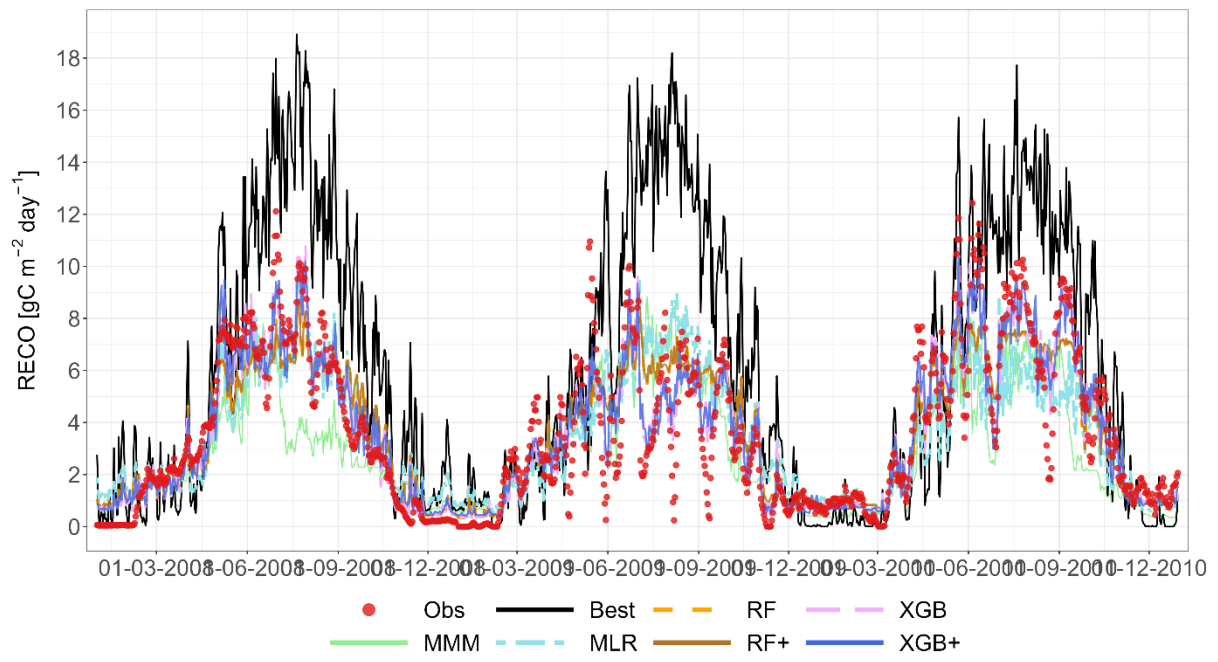


Figure A23: RECO, G4 - Easter Bush (UK), grassland, LOYO strategy.

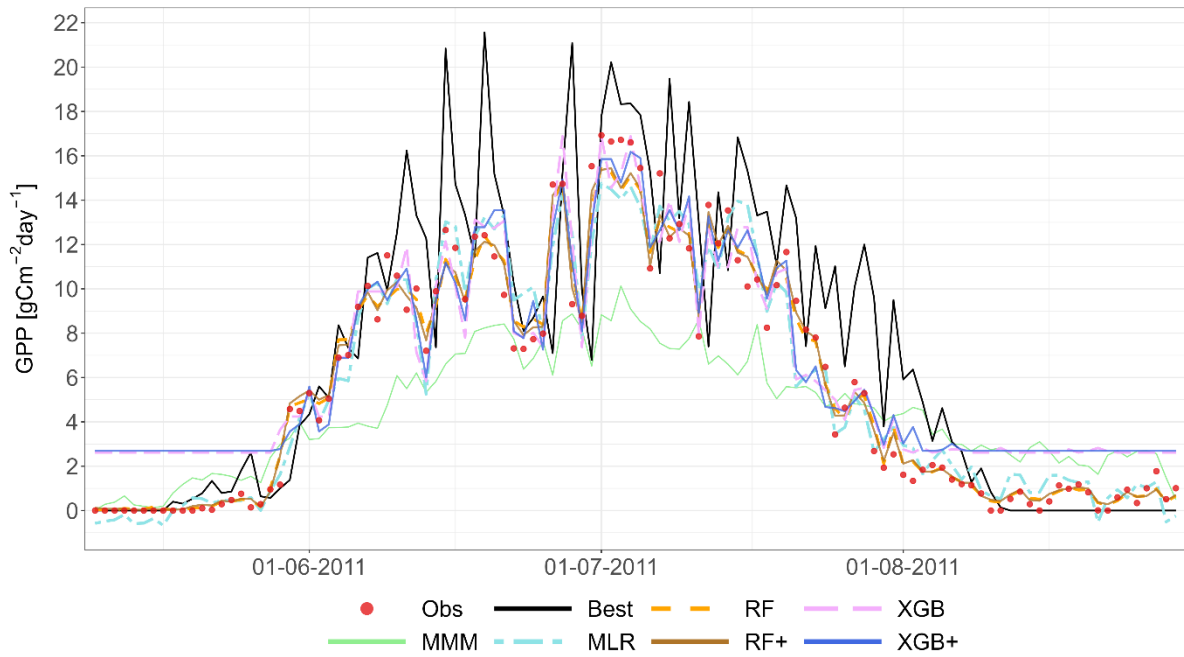
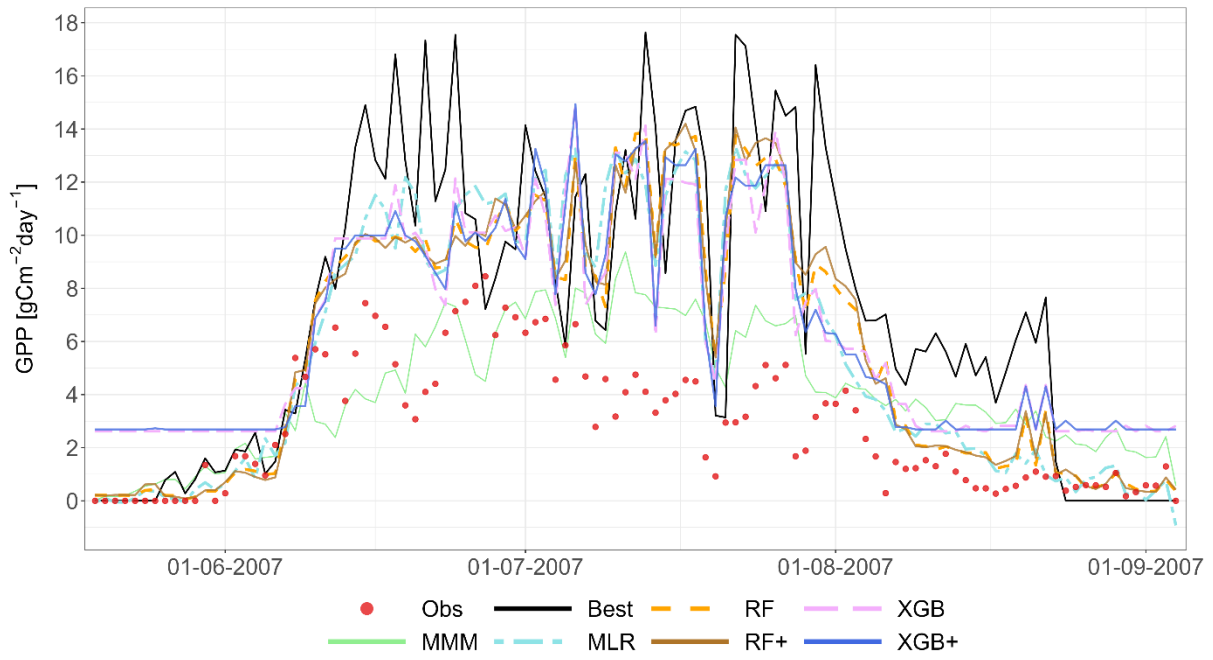


Figure A24: NEE, C1 - Ottawa (CA), cropland, 2007 and 2011, LOYO strategy.

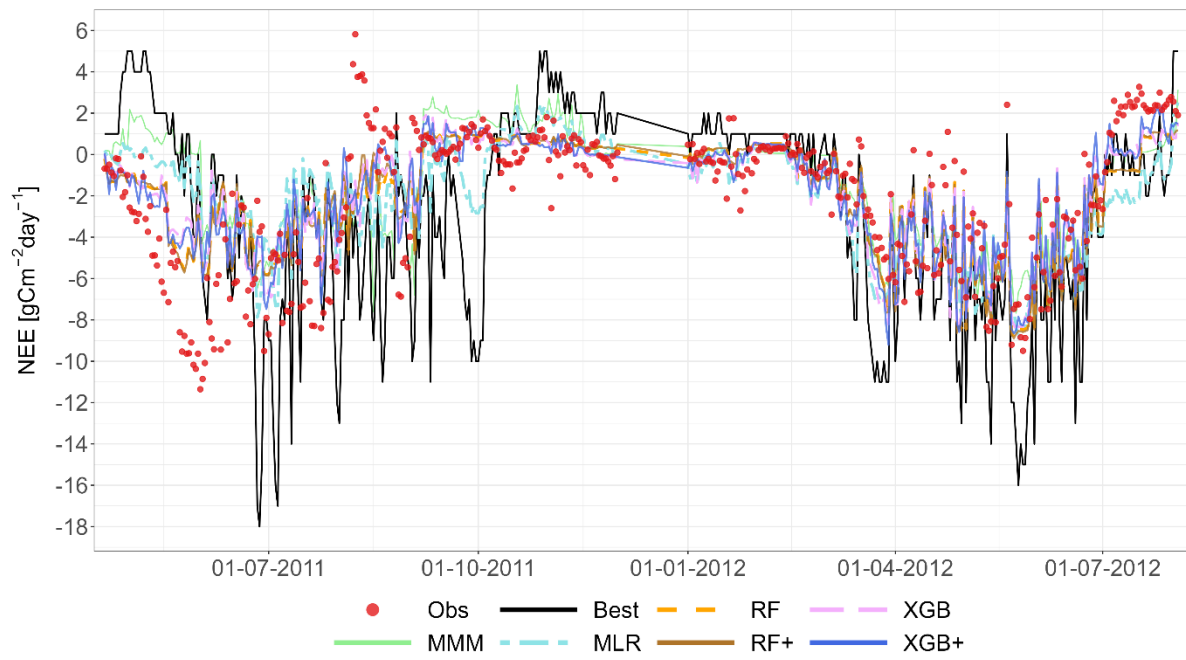
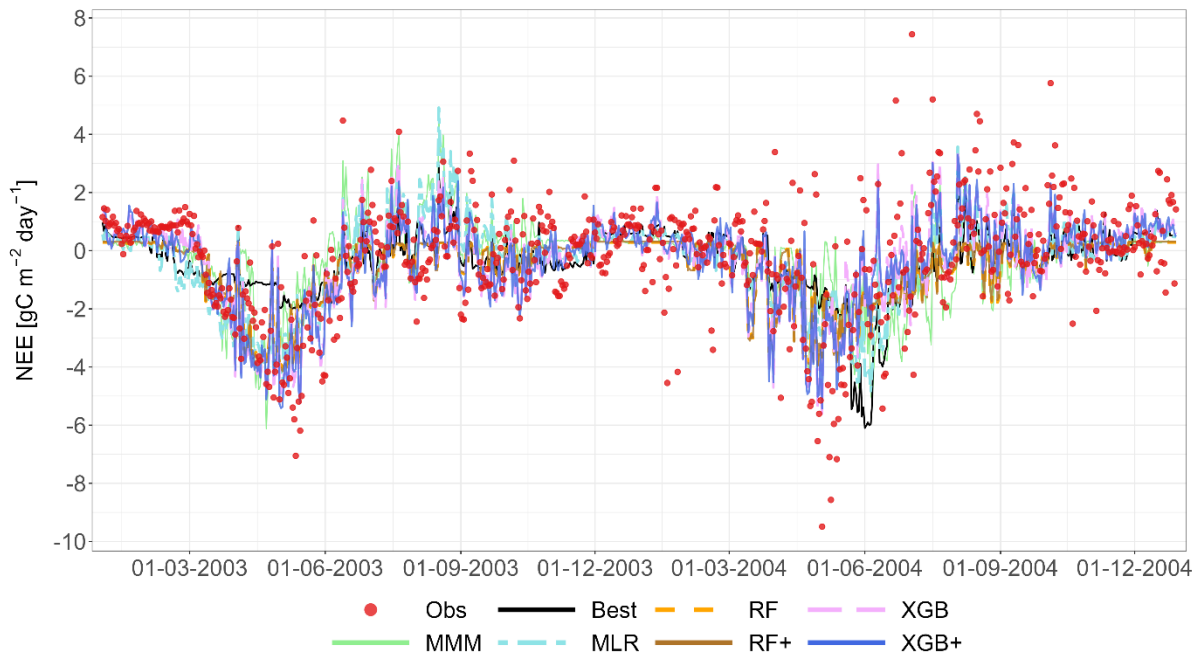
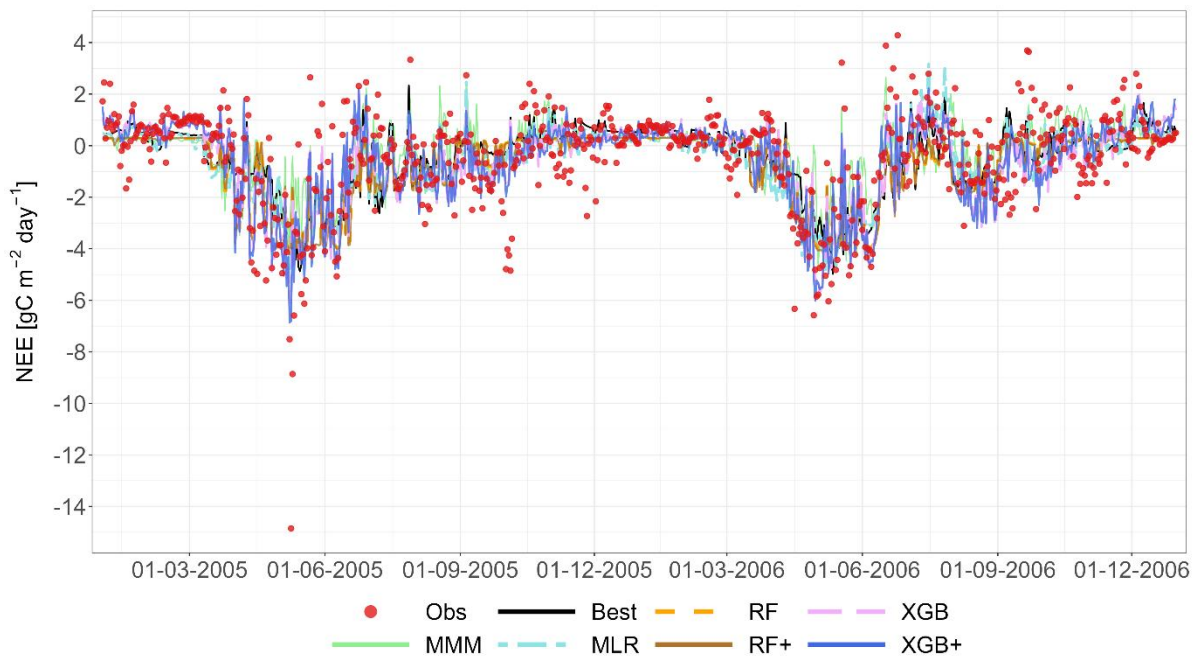


Figure A25: NEE, C2 - Grignon, (FR), cropland, 2011 and 2012, LOYO strategy.



1575



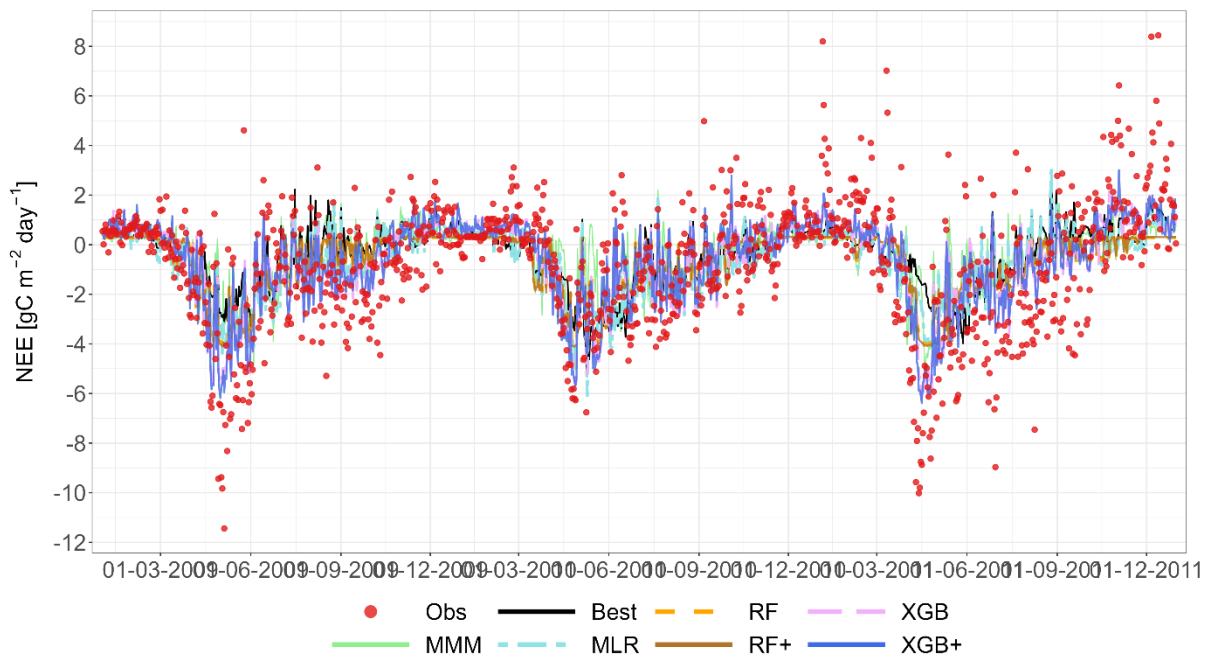
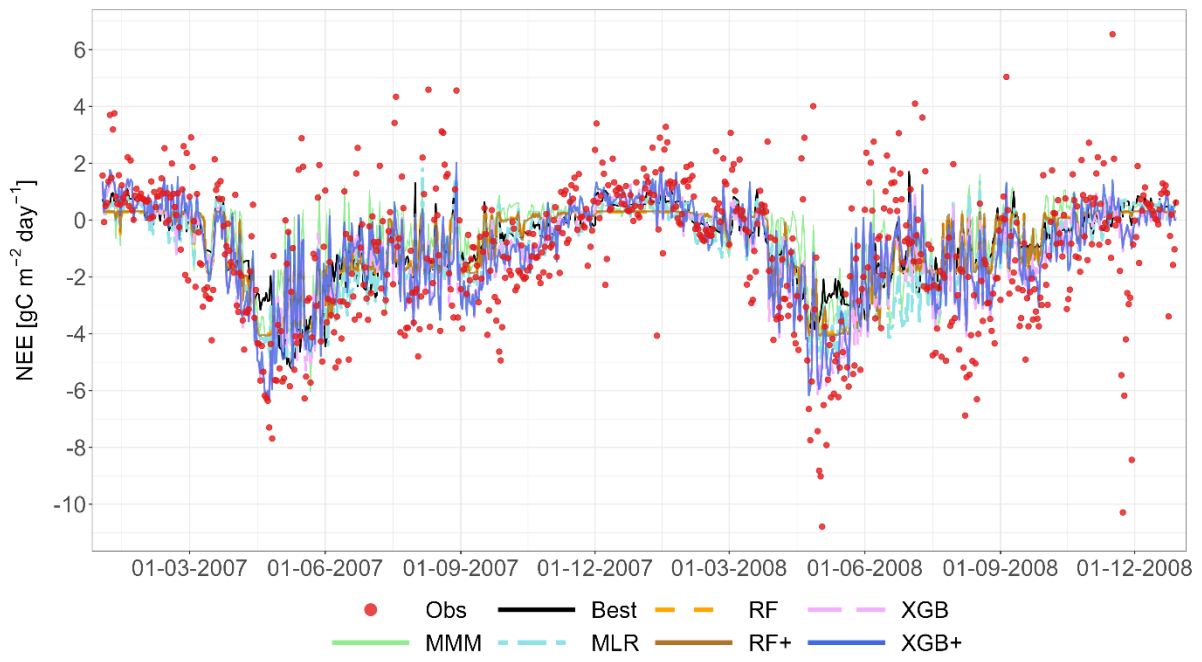
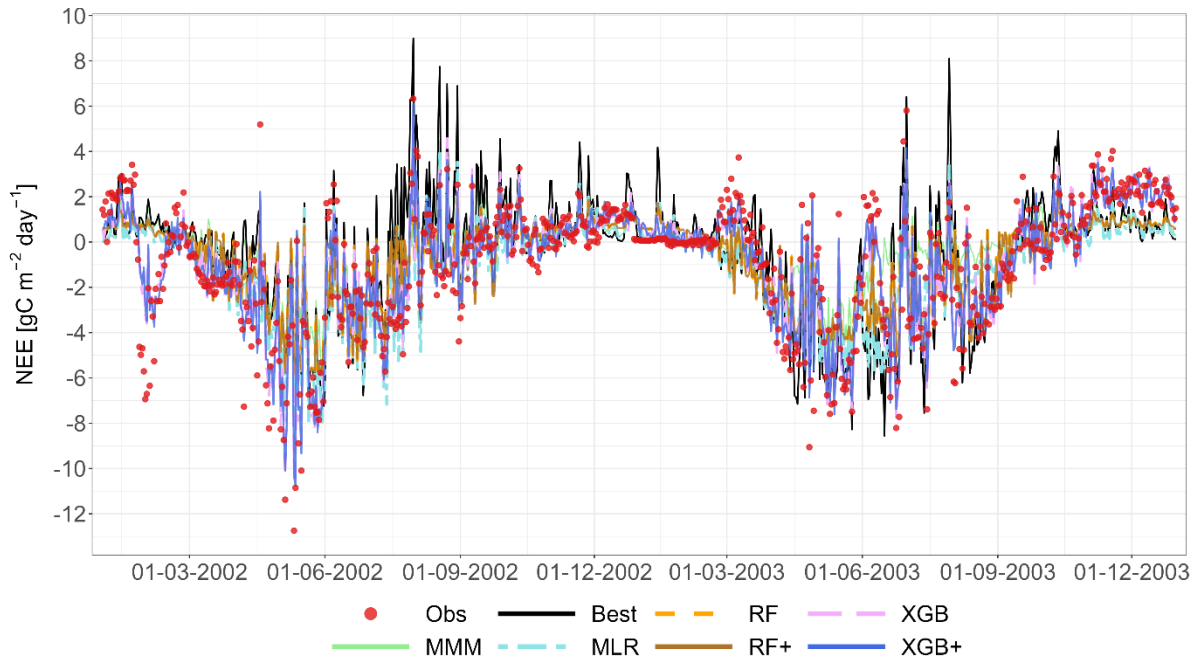
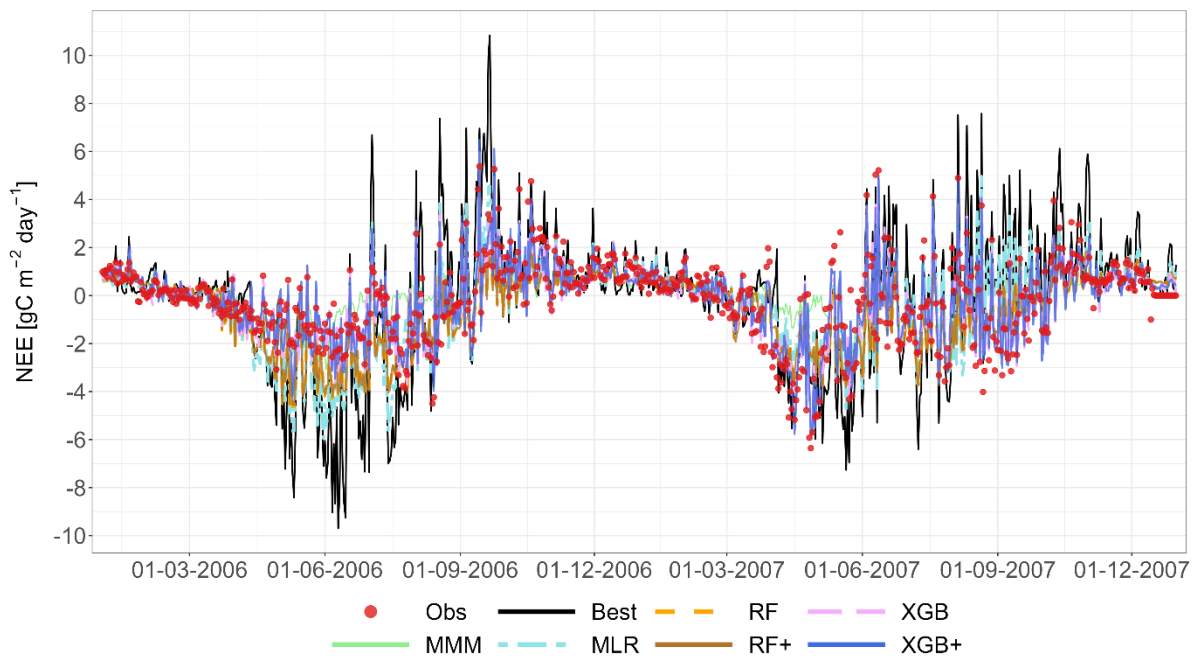


Figure A26: NEE, G3 - Laqueuille (FR), grassland, 2003-2011, LOYO strategy.



1590



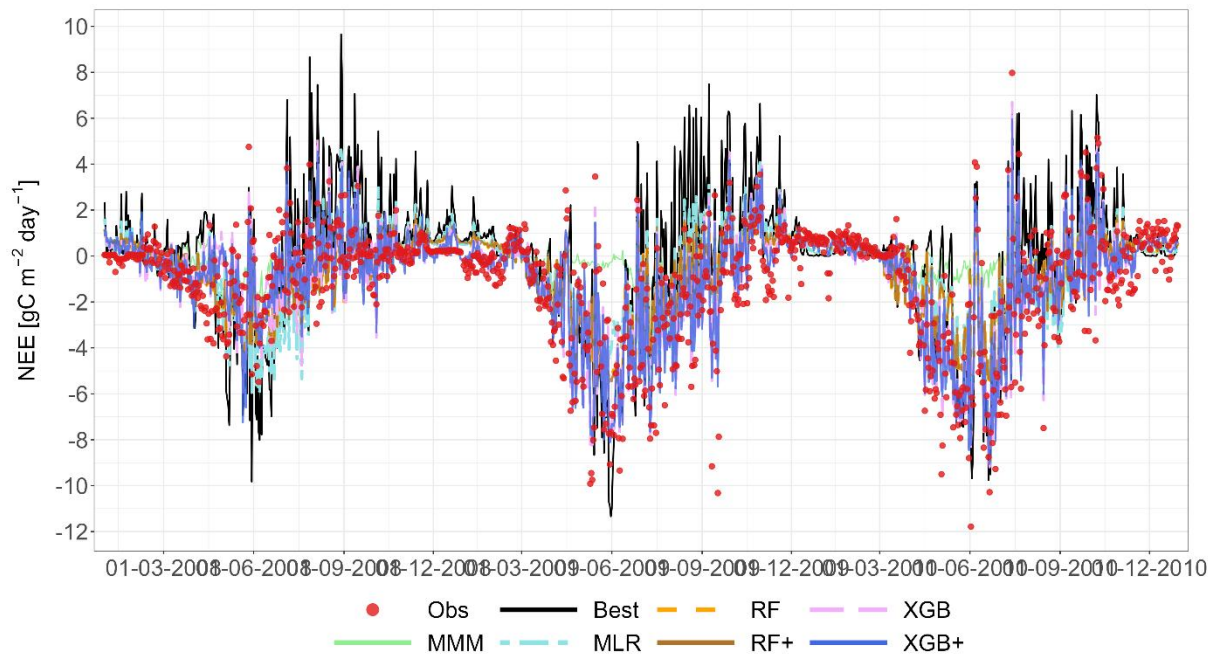


Figure A27: NEE, G4 - Easter Bush (UK), grassland, LOYO strategy.

1595